Dissertation ETH No. 16781

Myomesin family members – implications for the M-band function

A dissertation submitted to the
SWISS FEDERAL INSTITUTE OF TECHNOLOGY, ZURICH

for the degree of
Doctor of sciences ETH Zurich
(Dr. sc. ETH Zürich)

presented by
Roman Schönauer
Dipl. Natw. ETH

born April 10th 1978

citizen of Kirchberg, BE

accepted with the recommendation of
Prof. Dr. U. Boutellier, examiner
Prof. Dr. J.-C. Perriard, co-examiner
Dr. I. Agarkova, co-examiner

Zurich, 2006

1 TABLE OF CONTENTS

2 ZUSAMMENFASSUNG

Das Sarkomer ist die Struktureinheit des quergestreiften Muskels, eine hoch organisierte Maschine der Natur, die chemische Energie in mechanische Kraft umwandelt. Es besteht aus einer regelmäßigen Anordnung von Filamenten der kontraktilen Proteine Aktin und Myosin, die in der Z-Scheibe bzw. in der M-Bande vernetzt sind. Das riesige Protein Titin bildet ein elastisches Filamentsystem, das sich von der Z-Scheibe bis zur M-Bande erstreckt, und hat eine wichtige Funktion in der Entwicklung und Aufrechterhaltung des quergestreiften Muskels. Während die Struktur und Funktion der Z-Scheibe und Titinfilamente intensiv analysiert worden sind, ist bisher relativ wenig über die M-Bande und seine Bestandteile bekannt. Diese Arbeit versucht jene Lücke zu schliessen, indem sie die Funktion und die Expression der Mitglieder der Myomesinfamilie, der strukturellen Bestandteile der M-Bande, untersucht.

Die M-Bande, als bedeutender Teil des Zytoskeletts im Sarkomer, ist ein komplexes Proteinnetzwerk, welches das Gitter der dicken Filamente im Sarkomer während der Kontraktion stabilisiert. Kürzlich wurde gezeigt, dass die konstitutive Komponente der M-Bande in Vertebraten, Myomesin, antiparallele Dimere bilden kann, welche die benachbarten dicken Filamente quervernetzen dürften. Folglich scheint dessen primäre Funktion die Aufrechterhaltung der perfekten Ausrichtung der Myosinfilamente im Sarkomer zu sein. Myomesin ist in allen Typen der quergestreiften Muskulatur exprimiert und besteht aus Immunoglobulin (Ig) und Fibronectin Typ III (Fn) Domänen, aber mehrere Muskeltypen exprimieren die EH-Myomesin Isoform, die durch den Einschluss des einzigartigen EH-Segmentes von etwa 100 Aminosäuren in der Mitte des Moleküls generiert wird.

In dieser Arbeit charakterisieren wir Myomesin auf biophysikalische Art und Weise mit Hilfe von Rasterkraftmikroskopie (atomic force microscopy, AFM), Transmissionselektronen-mikroskopie (TEM) und Zirkulardichroismus(CD)-Spektroskopie. Das Rasterkraftmikroskop identifiziert den „mechanischen Fingerabdruck" der Module, die das Myomesin-Molekül aufbauen. Das Ziehen von homomeren Polyproteinen, konstruiert aus Ig und Fn Domänen von humanem Myomesin, produziert typische Sägezahn-Muster in der Kraft-Ausdehnungskurve, und die Domänen falten leicht zurück nach der Relaxation. Das EH-Segment zeigt keinen Entfaltungs-Peak und ist charakterisiert als entropische Feder. Zusätzlich erscheint es als Lücke innerhalb des Moleküls auf den TEM Bildern, was darauf hinweist, dass es die Konformation einer zufälligen Windung hat ähnlich der PEVK Domäne von Titin. CD Spektroskopie Messungen unterstützen dieses Resultat, indem sie eine

mehrheitlich ungefaltete Konformation des EH-Segmentes zeigen. Dies legt nahe, dass Myomesin eine molekulare Feder ist, deren Elastizität durch alternatives Spleissen moduliert werden kann, während die Ig und Fn Domänen durch sequentielles Entfalten beim Einwirken von extremen Dehnungskräften als reversible „Stossdämpfer" funktioneren dürften.

Zusätzlich wird das Fasertyp-spezifische Expressionsmuster der EH-Myomesin-Isoform im Skelettmuskel der Maus und dessen Korrelation mit M-Protein untersucht. Dabei zeigt sich, dass EH-Myomesin in allen Typ I Fasern und in einem Teil der Typ IIA Fasern während der postnatalen Entwicklung des Skelettmuskels aufreguliert wird. Im Weiteren kann ein komplementäres Expressionsmuster von EH-myomesin und M-protein in histologischen Querschnitten von Mäusehinterbeinen gezeigt werden: Alle M-Banden in schnellen Fasern enthalten M-Protein, während die M-Banden in langsamen Fasern einen signifikanten Anteil an EH-Myomesin enthalten, welches vorher nur im embryonalen Herzen nachgewiesen werden konnte.

Durch die Verwendung von vergleichender Sequenzanalyse haben wir ein neues Gen identifiziert, welches nahe verwandt ist sowohl mit M-Protein als auch Myomesin und welches die gleiche Intron-Exon und Domänenanordnung hat. Wir zeigen, dass dieses neue Mitglied der Myomesinfamilie (Myomesin 3) in verschiedenen Typen der quergestreiften Muskulatur differentiel exprimiert wird, am stärksten in Skelettmuskel von Neugeborenen und in adulten langsam kontrahierenden Muskeln wie Soleus und Diaphragma. Mit Hilfe von Immunhistochemie und konfokaler Mikroskopie beweisen wir, dass Myomesin 3 eine neue Proteinkomponente der sarkomerischen M-Bande ist. Zusätzlich zeigen neonatale Rattenkardiomyozyten, transfektiert mit Konstrukten, welche N-terminale Fragmente von Myomesin 3 kodieren, M-Banden Lokalisierung. Die Expression von Myomesin 3 im Skelettmuskel ist Fasertyp-spezfisch, wobei es in den IIA Fasern der Maus am stärksten exprimiert ist. Interessanterweise ist Myomesin 3 im Mäuseherzen unter normalen Umständen nicht detektierbar, aber im adulten Herzen des Menschen kann es nachgewiesen werden. Im Weiteren können die Expressionslevel der verschiedenen Komponenten der M-Bande wie EH-Myomesin oder Myomesin 3 im Falle von dilatierter Herzmuskelschwäche erhöht sein.

Wir schliessen aus obigen Resultaten, dass jeder Muskel charakterisiert ist durch eine spezifische Zusammensetzung von Proteinen der M-Bande, welche sich an verschiedene physiologische Bedürfnisse in verschiedenen Muskeltypen und Spezies anpassen kann.

3 SUMMARY

The sarcomere is the structural unit of striated muscle, a highly organized natural apparatus that converts chemical energy into mechanical force. It consists of regular arrays of filaments of the contractile proteins actin and myosin that are crosslinked in the Z-disk and M-band, respectively. The giant protein titin forms an elastic filament system, stretching from the Z-disk to the M-band, and has an important function in development and maintenance of striated muscle. Whereas the structure and function of the Z-disk and titin filaments have been intensively studied, relatively little is known about the M-band and its components. This study tries to close this gap by investigating the function and expression of the myomesin family members, the structural components of the M-band.

The M-band, as a prominent part of the sarcomeric cytoskeleteon, is a complex protein network which is believed to stabilize the thick filament lattice in the sarcomere during contraction. It was shown recently that the constitutive vertebrate M-band component myomesin can form antiparallel dimers, which might cross-link the neighboring thick filaments. Consequently, its primary function may be the maintenance of the perfect alignment of the myosin filaments in the sarcomere. Myomesin is expressed in all types of striated muscle and consists of immunoglobulin-like (Ig) and fibronectin type III (Fn) domains, while several muscle types express the EH-myomesin splice isoform, generated by the inclusion of the unique EH-segment of about 100 amino acid residues (aa) in the center of the molecule.

In this study, we biophysically characterize myomesin by using atomic force microscopy (AFM), transmission electron microscopy (TEM) and circular dichroism (CD) spectroscopy. The AFM identifies the "mechanical fingerprints" of the modules constituting the myomesin molecule. Stretching of homomeric polyproteins, constructed of Ig and Fn domains of human myomesin, produces a typical saw-tooth pattern in the force-extension curve and the domains readily refold after relaxation. The EH-segment displays no unfolding peak and is characterized as an entropic spring. In addition, it appears as a gap in the molecule in TEM pictures, indicating a random coil conformation similar to the PEVK region of titin. CD spectroscopy measurements support this result, demonstrating a mostly non-folded conformation for the EH-segment. This suggests that myomesin is a molecular spring, whose elasticity can be modulated by alternative splicing, whereas the Ig and Fn domains might

function as reversible "shock absorbers" by sequential unfolding in the case of extreme stretching forces.

In addition, the fiber-type dependent expression pattern of the EH-myomesin isoform in mouse skeletal muscle and its correlation with M-protein is analyzed, revealing an upregulation of EH-myomesin in all type I and in part of the type IIA fibers during postnatal skeletal muscle development. Furthermore, a complementary expression pattern of EH-myomesin and M-protein can be shown in histological cross-sections of mouse hind limbs: All M-bands in fast fibers contain M-protein while M-bands in slow fibers contain a significant proportion of the EH-myomesin isoform, previously detected only in embryonic heart muscle.

Using comparative sequence analysis we have identified a novel gene, which is closely related to both M-protein and myomesin and shares the same intron-exon and domain arrangement. We show that the new member of the myomesin family (myomesin 3) is differentially expressed in various kinds of striated muscle with the highest level in newborn skeletal and adult slow muscles, like soleus and diaphragm. Using immuno-histochemistry and confocal microscopy we prove that myomesin 3 is a novel protein component of the sarcomeric M-band. Transfections of neonatal rat cardiomyocytes with constructs encoding N-terminal fragments of myomesin 3 show M-band localization as well. The expression of myomesin 3 in skeletal muscle is fiber-type specific with the highest expression level in IIA fibers of mouse. Interestingly, myomesin 3 is absent from the mouse heart under normal conditions, but can be detected in the adult human heart. Besides, the expression level of different M-band components such as EH-myomesin or myomesin 3 can be increased in the case of dilated cardiomyopathy.

We conclude that each muscle type is characterized by its unique M-band protein composition, which is adapted to divergent physiological needs in different muscles and species.

4 ABBREVIATIONS

Ab	antibody
ANF	atrial natriuretic factor
AngII	angiotensin II
APS	ammonium persulfate
ATP	adenosine triphosphate
ADP	adenosine diphosphate
BSA	bovine serum albumin
CCD	charge coupled device
cDNA	complementary deoxyribonucleic acid
Cy3	indocarbocyanine
Cy5	indodicarbocyanine
3D	three-dimensional
Da	dalton
DCM	dilated cardiomyopathy
DMD	Duchenne muscular dystrophy
DMSO	dimethylsulfoxide
DNA	deoxyribonucleic acid
dNTP	deoxynucleoside triphosphate
DRAL	downregulated rhabdosarcoma LIM protein
DTT	dithiothreitol
E. Coli	Escherichia Coli
EH	embryonic heart
EM	electron microscopy
FHC	familial hypertrophic cardiomyopathy
FITC	fluorescein isothiocyanate
Fn	fibronectin type III
GFP	green fluorescent protein
GST	glutathione S-transferase
HA	hemagglutinine epitope tag
HCM	hypertrophic cardiomyopathy
HMM	heavy meromyosin
HRP	horse radish peroxidase
IB	immunoblot
IF	immunofluorescence
Ig	immunoglobulin

IPTG	isopropyl β-D-thiogalactopyranoside
Iso	isoproterenol
1k1c	1-kidney-1-clip
KO	knock-out
LB	Luria-Bertani
LMM	light meromyosin
m	monoclonal
m.	musculus
MetOH	methanol
mo	mouse
mRNA	messenger ribonucleic acid
MHC	myosin heavy chain
MLC	myosin light chain
MLP	muscle LIM protein
MM-CK	muscle isoform of creatine kinase
MMP	matrix metalloproteinases
Murf	muscle RING finger protein
MyBP-C	myosin binding protein C
My	myomesin
NGS	normal goat serum
NRC	neonatal rat cardiomyocytes
PAGE	polyacrylamide gel electrophoresis
PBS	phosphate buffered saline
p.c.	post coitum
PCR	polymerase chain reaction
pers. comm.	personal communication
PFA	paraformaldehyde
p	polyclonal
PONDR	Predictors of Natural Disordered Regions
R	rabbit
RAR	retinoic acid receptor
RNA	ribonucleic acid
Rt	rat
RT	room temperature
RT-PCR	reverse transcriptase polymerase chain reaction
SDS	sodium dodecylsulfate
TAC	trans-aortic constriction

TEMED	N,N,N',N'-tetramethylethylendiamine
TnI	troponin I
TnT	troponin T
Tm	tropomyosin
TOT	tropomodulin overexpressing transgenic
wt	wild type

5 INTRODUCTION

5.1 Muscle types

Muscle is the best-understood system of actin-based motility, derived from the mesodermal layer of the embryo. It was a relatively late development in evolution and is highly specialized compared to more typical animal cells. Although the mechanism of force generation is the same for different types of muscle, their structures are not identical. Two main types of muscles are distinguished in vertebrates: striated and smooth muscle.

The cross-striated skeletal muscles act directly under voluntary control by nerves on bones and therefore cause movement of the skeleton. They are synchronous muscles and generally respond to an electrical stimulus (via motoneurons and acetylcholine) by a single twitch. The long, multinucleated muscle fibers of the skeletal musculature are huge cells, which were formed by fusion of many myoblasts. Single myotubes, lined with the endomysium, are packed together by the perimysium into bundles of myofibers (fascicles), which are then grouped together to form the whole muscle, lined by the epimysium. Sensory muscle spindles are distributed throughout the muscles and provide feedback information on muscle tension to the central nervous system.

Skeletal muscle is further divided into several subtypes such as the type I (slow twitch) and type II (fast twitch) fibers (Pette and Spamer, 1986). The slow and oxidative type I fibers are dense with capillaries and rich in mitochondria and myoglobin, giving the muscle tissue its characteristic red color. There are three major kinds of the fast type II fibers: Type IIA, which are aerobic (like slow mucle), rich in mitochondria and capillaries and also appear red. The second group are the type IIX (IID) fibers, the fastest muscle type in humans. These are less dense in mitochondria and myoglobin, they can contract faster and produce a bigger force than oxidative muscle but they sustain only short anaerobic bursts of activity. The type IIB fibers are anaerobic, glycolytic and build up the so-called "white" muscle, which are even less dense in mitochondria and myoglobin. In small animals (e.g. rodents), this is the major fast muscle type. Various exercises require a predominance of certain muscle fiber utilization. At low exercise intensities (aerobic events such as walking or slow running) type I fibers are selectively utilized because they have the lowest threshold for recruitment. If the pace is suddenly increased to a sprint, the larger fast motor units (type II fibers) will be recruited. In general, as the intensity of exercise increases in any muscle, the contribution of the fast fibers will increase. Interestingly, humans are genetically predisposed with a larger percentage of

one fiber type. Individuals with a greater percentage of type I muscle fibers would theoretically be more adept at endurance events (distance running, cycling), others with a greater percentage of type II fibers would be more likely to excel at anaerobic events (sprint, weight lifting).

Cardiac muscle is also cross-striated, has an autonomous excitatory control system and consists mainly of individual cardiomyocytes, connected to each other by highly specialized cell-cell junctions, the intercalated disks. The heart consists of four chambers, two atria that collect the blood and the two ventricles that pump the blood. The venous blood enters the heart via the right atrium, flows into the right ventricle and is pumped by the right ventricle through the lungs to pick up O_2 and lose CO_2. The oxygenated blood enters the left atrium and delivers O_2 to the tissues by the pumping action of the left ventricle. Alternating contractions (systole) and relaxations (diastole) of the myocardium causes the pumping of the heart; this entire process is called cardiac cycle. There is a pacemaker in the right atrium that generates electrical impulses causing the atria to contract and thereby assisting the ventricles which suck in the blood during dyastole. The rate of the human heart beat is about 70 times per minute at rest, increases during exercise, emotional excitement and fever, and decreases during sleep.

The smooth muscles in the vascular, digestive and reproductive system of vertebrates have no striated appearance. They are involuntary muscles and their contractile behavior (e.g. gut peristalsis) is not regulated primarily by the nervous output from the brain. Striated muscle is often used in short, intense bursts, whereas smooth muscle sustains longer or even near-permanent contractions.

5.2 The contractile apparatus

5.2.1 The sarcomere

Striated muscle is a well-organized machine that converts chemical energy into physical work. These muscles are called "striated" because of their banded structure: alternating I-bands (isotropic bands) and A-bands (anisotropic bands) are seen in the light and electron microscope. Every myofibril consists of a chain of sarcomeres, the minimal building blocks of the force generating apparatus in all kinds of striated muscle. They are highly regular arrays of filaments of the contractile proteins actin and myosin that are crosslinked in the Z-disk (actin) and M-band (myosin) with a typical length of about 2 μm. The A-band of the

sarcomere contains the thick filaments (mostly myosin) and the region of interdigitation between thick and thin filaments (mostly actin), the I-band contains only thin filaments (Figure 5.1). Titin forms an elastic filament system and stretches from the Z-disk to the M-band. The precisely organized sarcomeric complex is linked via proteins such as obscurin, titin and ankyrin to a surrounding web-like structure formed by the sarcoplasmatic reticulum.

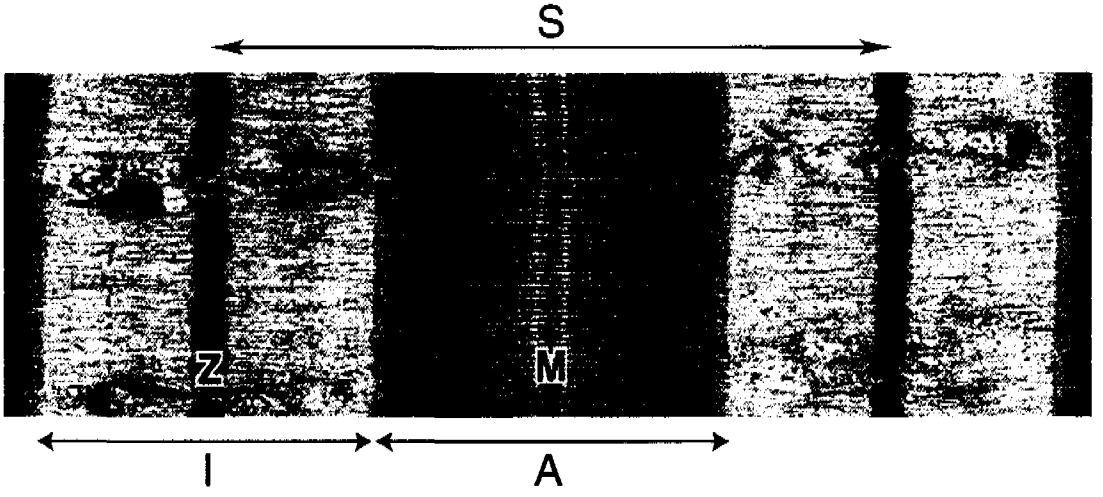

Figure 5.1: *Electron microscopy picture of the sarcomere.* S: sarcomere; I: I-band; A: A-band; Z: Z-disk; M: M-band. The A-band is the region which is occupied by thick filaments and also includes the region of interdigitation between thick and thin filaments. The I-band contains thin but no thick filaments, titin stretches from the Z-disk to the M-band. Note the perfect lateral alignment of the (thick) filaments (Agarkova, 2000).

5.2.2 The sliding filament model

Muscle contraction represents one of the most fascinating biological achievements whose molecular basis was described first by the sliding filament model in 1954 (Huxley and Hanson, 1954). According to this model, the relative sliding of actin and myosin filaments in a sarcomere results in the overall shortening of the whole muscle (for a review see (Cooke, 2004)). The contraction mechanism involves a cyclic binding/unbinding of myosin heads, to the thin actin filaments, which is controlled by calcium and ATP. It starts with a relaxed state characterized by a low cytosolic calcium concentration. In this state myosin binds either ADP or ATP with high affinity. ATP is hydrolyzed by the S1 portion of myosin, accompanied by conformational changes in the myosin molecule. The products ADP and Pi remain bound in an intermediate complex with myosin. In this state myosin binds weakly to actin and the myosin heads are oriented nearly perpendicular to the thin filaments. This binding strongly accelerates the process of izomerisation of the myosin-ADP-Pi intermediate and the following

release of the products of the ATPase reaction from the active site. First, the initially bound Pi is released from the myosin heads, concomitantly with the tight binding of the head to actin. This release triggers the power stroke, a conformational change facilitated by the flexible hinges in the myosin molecules, with the neck region (light-chain domain) of the myosin head acting as a lever arm. During this power stroke, the head regains its original conformation and loses its bound ADP. The S1 moves back to an angle of about 45°, pulling the thin filament towards the center of the sarcomere. By the subsequent binding of ATP the interaction of the myosin heads with the actin filament weakens and they return to the perpendicular orientation.

5.3 Contractile proteins

5.3.1 Myosin

Myosin is one of the most abundant proteins in muscle and can also be found in nonmuscle cells. All myosin types represent a superfamily of more than 100 proteins, which are very diverse both in their structure and functions in cells. On the basis of phylogenetic analysis, all myosins are subdivided into 17 classes (Hodge and Cope, 2000). They have one or two heads containing in the "neck" region from one to six binding sites for light chains or calmodulin. The C-terminal regions (tails) are very diverse in size and sequence among different myosins, dictating the specificity of individual myosin functions in the cell (Sellers *et al.*, 1996). Unlike the C-terminal parts, the globular N-terminal parts are highly conserved for all myosins.
"Conventional" myosin (myosin II) is an asymmetric, hexameric protein consisting of four light chains of about 20 kDa and two heavy chain of about 200 kDa (Lowey and Steiner, 1972). The two myosin heavy chains (MHC) intertwine at the carboxyl terminus forming a α-helical coil (the rod), while the amino terminus of each heavy chain forms the globular head region containing two heads connected by the neck regions to the rod. Myosin II has three important properties: it is an enzyme with ATPase activity, it has the ability to bind actin and it aggregates to form thick filaments. The first two properties are associated with the globular head and are important for muscle contraction and a number of various motility mechanisms in eukaryotic cells. The aggregating activity is due to its tail and is responsible for the formation the characteristic thick filaments of about 1.6 μm length (Huxley, 1963). The C-terminal part of MHC also harbours binding sites for titin, the M-band proteins myomesin and

M-protein, and accessory proteins like myosin binding protein C (MyBP-C; (Bennett *et al.*, 1986)). Four light chains are associated with the neck region of each heavy chain and modulate the speed of contraction (Figure 5.2).

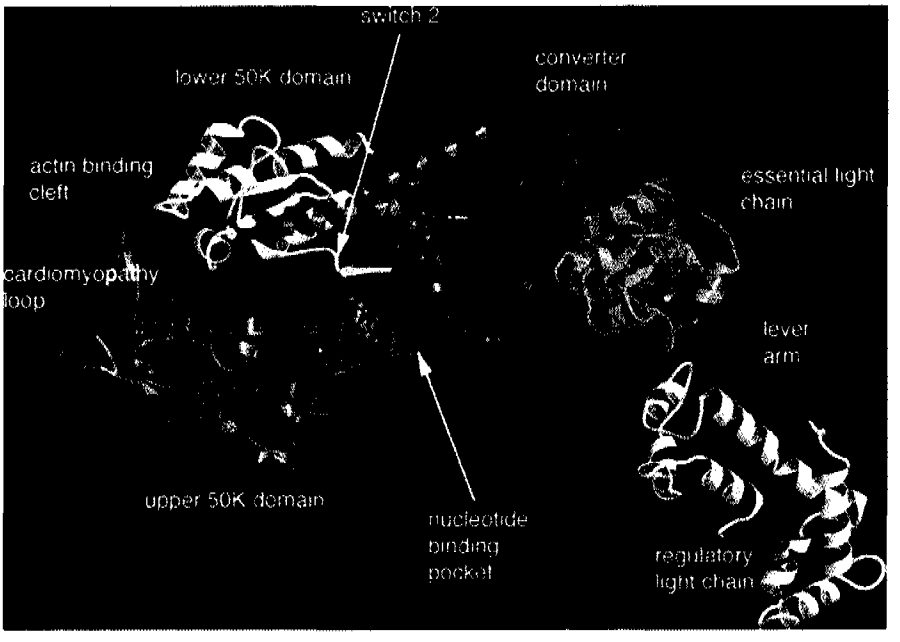

Figure 5.2: *Structure of the head region of myosin.* The catalytic domain is shown on the left. The upper 50K, lower 50K, nucleotide binding, and converter domains are colored red, white, green, and blue, respectively. The relay helix is colored blue with its distal end connected to the actin binding side in the lower 50K domain by a blue strand, shown at the top of he molecule (Rayment *et al.*, 1993).

By limited proteolysis of the myosin molecule with trypsin, chymotrypsin or papain, different fragments can be obtained: myosin subfragment 1 (S1, isolated myosin head); myosin rod; myosin subfragment 2 (S2, N-terminal part of the rod); light meromyosin (LMM, C-terminal part of the rod); heavy meromyosin (HMM, consisting of two heads attached to S2). It has been shown that isolated myosin heads (S1) are capable of moving actin filaments in vitro (Toyoshima *et al.*, 1987) and in this way are sufficient to perform the motile functions without the myosin rod.

Myosin exists in multiple isoforms whose major functional differences reside in the heavy chain portion of the myosin molecule (Weiss *et al.*, 1999). A good example is the ATPase activity, which is associated with the globular head region of the myosin heavy chain (MHC). The heavy chains are encoded by a multigene family (Leinwand *et al.*, 1983). To date, a total

of 11 MHC isoforms have been identified. Some of these isoforms appear to be expressed in a muscle-specific manner (MHC-II_m, MHC_{eom}, MHC-I_{ton}, MHC-Iα, MHC-Ia, MHC_{emb}, MHC_{neo}), others are more widely distributed in different skeletal muscles (MHC-Iβ, MHC-IIa, MHC-IId, MHC-IIb), (Table 5.1). In addition, species differences exist in the expression of some of these isoforms. For example, body size appears to correlate with the relative concentrations of MHC-Iβ, MHC-IIa, MHC-IId, and MHC-IIb (Aigner *et al.*, 1993, Hamalainen and Pette, 1995).

Designation	Nomenclature	Muscle/fiber location
Fast-twitch	MHC-IIb	Fiber types IIB, IIBD
Fast-twitch	MHC-IId	Fiber types IID, IIBD, IIDA
Fast-twitch	MHC-IIa	Fiber types IIA, IIDA, I/IIA
Fast-twitch	MHC_{eom}	Extraocular and laryngeal muscles
Fast-twitch	MHC-II_m	Masticatory muscles
Slow-twitch	MHC-Iβ	Heart, fiber types I, I/IIA
Slow-twitch	MHC-Iα	Heart, extraocular, diaphragm, masseter muscles, fast-to-slow transforming fibers
Slow-twitch	MHC-Ia	Plantaris, soleus, slow-to-fast transforming fibers
Slow-tonic	MHC-I_{ton}	Extraocular, laryngeal, tensor tympani muscles
Embryonic	MHC_{emb}	Skeletal muscle development, extraocular muscles
Neonatal	MHC_{neo}	Skeletal muscle development, extraocular, masseter muscles

Table 5.1: *Myosin heavy chain isoforms in mammalian muscles* (adapted from (Pette and Staron, 2000)).

Skeletal muscle is an extremely heterogeneous tissue composed of a variety of fast and slow fiber types. These muscle fibers are capable of adjusting their phenotypic properties in response to altered functional demands. They differ in their composition of myosin light chain (MLC) and heavy chain isoforms. MHC isoforms appear to represent the most appropriate markers for fiber type characterization. Pure fiber types are characterized by the expression of a single MHC isoform, whereas hybrid fiber types express two or more MHC isoforms. Under certain conditions, changes can be induced in MHC isoform expression in the direction of either fast-to-slow or slow-to-fast. Increased neuromuscular activity and hypothyroidism are conditions that induce fast-to-slow transitions, whereas reduced neuromuscular activity and

hyperthyroidism cause transitions in the slow-to-fast direction (Schiaffino and Reggiani, 1996).

5.3.2 Actin

Actin is one of the most conserved proteins in nature and plays an essential role in maintaining the cell shape, cell motility, phagocytosis, cytokinesis and muscle contraction. It has a globular structure with a single polypeptide chain of about 375 amino acids and a molecular weight close to 42 kD. The molecule consists of two half-domains with a deep cleft between, which is responsible for harboring the nucleotide (ATP or ADP) and the divalent ion (Mg^{2+} or Ca^{2+}) binding site (Kabsch *et al.*, 1990). Under physiological conditions it associates into a double-stranded spiral polymer (F-actin), whereas in low salt buffer, actin is a monomeric globular protein (G-actin) (Pollard, 1990). The polymerization is regulated by the hydrolysis of a tightly bound nucleotide, whereby each monomer in F-actin contacts its neighbors above and below it and those from the opposite strand. Since the actin monomer is asymmetric, the actin filament has a polarity. The association kinetics of monomers is different at actin polymer ends, which are called barbed (fast growing) and pointed (slow growing) ends based on their appearance after decoration with myosin S1 fragments containing the heads. The major reason for many forms of activity is the ability of actin to polymerize-depolymerize reversibly.

An important evolutionary development is its participation in muscle contraction, the basis of which is the sliding of myosin along the actin filament (Huxley and Hanson, 1954). The length of the thin filaments in striated muscles is precisely regulated by its interaction with a group of associated actin-binding proteins. Nebulin was suggested to be the main element of this controlling mechanism for thin filament length in skeletal muscles (Trinick, 1994). Tropomyosin and troponin are responsible for the regulation of the Ca^{2+} triggered muscle contraction and are tightly associated with the thin filaments (Farah and Reinach, 1995). Tropomodulin is supposed to play an important role in the regulation of the thin filament length in developing muscle by capping the actin filament pointed end (Gregorio *et al.*, 1995). Depending on their isoelectric point (from acidic to basic), all actins fall into three classes: α-, β-, and γ-actins (Garrels and Gibson, 1976). These isoforms have been additionally sub-divided into muscle and cytoplasmic actins, according to their tissue distribution and amino acid sequence (Vandekerckhove and Weber, 1981). The muscle group consists of skeletal α-,

cardiac α-, and smooth muscle α-actin. Enteric γ-actin also belongs to the muscle actins and is accumulated in stomach, intestine and blood vessels. The cytoplasmatic group consists of β- and γ-actins, which are major cytoskeletal proteins in non-muscle cells.

5.4 Other sarcomeric components

5.4.1 Titin (connectin)

In order to stabilize thin and thick filaments in the positions that are optimized for their interaction, the sarcomeres possess a third filament system, an elastic lattice that is built from the giant protein titin. This protein was originally identified as a high molecular weight component of striated muscle (Wang *et al.*, 1979) and is considered to be not only the biggest protein in vertebrate striated muscle, but also one of the most abundant (for recent reviews see: (Tskhovrebova and Trinick, 2003, Granzier and Labeit, 2005). Sequencing of human cardiac titin revealed a protein with a molecular mass of about 3000 kDa (Labeit and Kolmerer, 1995). The titin molecule is about 1 μm long and consists mainly of immunoglobulin-like (Ig) and fibronectin type III (Fn) domains, which are interspersed with unique sequences. Titin filaments stretch from the Z-disk to the M-band and may serve as a template for sarcomeric assembly (Figure 5.3; (Trinick, 1994, Young *et al.*, 1998, Ehler *et al.*, 1999)).

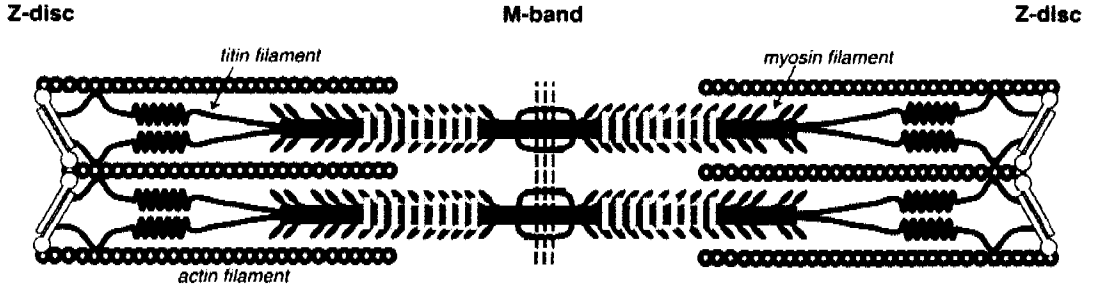

***Figure 5.3**: The elastic lattice of Titin.* Titin (blue) stabilizes the actin and myosin filaments in the optimal position for interaction and serves as template for sarcomeric assembly (Agarkova, 2000).

An important function of titin is to bring the A-band as a whole back to the central position during muscle relaxation (Horowits and Podolsky, 1987). Titin filaments are needed to

maintain tension during the contraction cycle and seem to be the main player responsible for passive elasticity of striated muscle (Maruyama, 1994, Trinick, 1994, Trinick, 1996, Gregorio *et al.*, 1999). Many distinct isoforms of titin are generated by alternative splicing in the Z-disk, I-band and M-band region (Kolmerer *et al.*, 1996), but only a single copy of the gene has been identified in the vertebrate genome. The I-band part of titin functions as a molecular spring and is involved in controlling the elastic properties of different muscle types by altering the length of unique sequence insertions and clusters of Ig-domains in a tissue- and development-specific manner (Lahmers *et al.*, 2004, Opitz *et al.*, 2004). One of these unique sequences is the PEVK region (rich in P, E, V, and K), which belongs to the intrinsically unstructured proteins (IUP) and may function as a major elastic spring element in titin. Two other unique peptide regions are the N2A as well as the cardiac specific N2B-region.

Titin molecules form a continuous filament system within myofibrils by overlapping in the Z-disks (Gregorio *et al.*, 1998) and M-bands (Obermann *et al.*, 1996) and offer a multitude of spatially distinct binding sites for the major structural components of the sarcomere: α-actinin, actin, myosin, myosin binding protein-C (MyBPC), myomesin and M-protein (Tskhovrebova and Trinick, 2003, Granzier and Labeit, 2005). In addition, several scaffolding and signalling proteins such as DRAL (Lange *et al.*, 2002) or the Murf proteins (Centner *et al.*, 2001) are associated with titin. The single kinase domain of titin (close to the C-terminus) is implicated in the regulation of sarcomeric development, myofibrillar assembly and sarcomeric remodelling (Mayans *et al.*, 1998, Amodeo *et al.*, 2001) and may serve as a link between different signalling pathways and mechanical strain (Grater *et al.*, 2005). Telethonin, a binding partner of the N-terminal titin domains Z1/Z2, was found to be a major phosphorylation substrate for the kinase domain of titin (Mayans *et al.*, 1998, Gregorio *et al.*, 1998, Zou *et al.*, 2006, Pinotsis *et al.*, 2006). In addition, obscurin was identified as a binding partner of Z-disk titin (domains Z8Z9; (Young *et al.*, 2001)). Characterized protein-protein interactions in the I-band region are the cardiac specific association of actin filaments to the PEVK and the N2B region (Kulke *et al.*, 2001) as well as the interactions of MARP, myopalladin and calpain-3 to the N2A region of titin (Kinbara *et al.*, 1997, Miller *et al.*, 2003). A-band titin interacts with myosin binding protein-C (MyBP-C) and the tail region of myosin. In this region, identical clusters of fibronectin and immunoglobulin-like domains can be found, which may harbour binding sites for myosin and MyBP-C (Freiburg and Gautel, 1996).

5.4.2 α - actinin and the structure of the Z-disk

The barbed ends of the actin filaments are anchored to the Z-disk, where each actin filament overlaps with four filaments from the opposite sarcomere, forming a square lattice. These filaments are crosslinked via antiparallel α-actinin dimers (subunit mass of about 100 kDa) whose modular structure of the central rod part is based on a triple-stranded α-helix as repeating unit. The number of α-actinin dimers and therefore the thickness of Z-disks vary in different muscle types, but is tightly regulated within a given myofibril (Squire, 1981). In this way, α-actinin provides the tetragonal lattice of the Z-disk as its major structural component. Nebulin and titin are the candidates organizing the Z-disk assembly (for review see: (Trinick, 1994). A model of the molecular structure of the Z-disk is based on the analysis of protein interactions between the main Z-disk components (Young *et al.*, 1998). Titin participates in the central region of the Z-disk and defines the number and positions of the α-actinin cross-links, while nebulin /nebulette may determine the end of Z-disk structure and the transition to the I-band (Millevoi *et al.*, 1998). Furthermore, non-sarcomeric α-actinin links actin to several integral membrane proteins, such as cadherins and catenins (Knudsen *et al.*, 1995, Nieset *et al.*, 1997), which can be found at the intercalated disk.

5.4.3 Ultrastructure and function of the M-band

The M-band is proposed to be essential for the regular packing of the thick myosin filaments (Knappeis and Carlsen, 1968) in the center of the sarcomere and seems to participate in the maintenance of the A-band lattice (Luther *et al.*, 1981). These passive structural forces can control excessive deformation of the lattice in relaxed muscle, saveguarding the optimal distance between thick and thin filaments at the beginning of contraction. Furthermore, M-bridges contribute to the distribution of mechanical stress across the lattice in active muscle. In addition, the M-band might play an important organizational role during myofibrillogenesis, when the nascent thick filaments have to assemble (Wang *et al.*, 1998, Ehler *et al.*, 1999). The main structural M-band proteins are the C-terminal portion of titin (Labeit and Kolmerer, 1995), myomesin (Grove *et al.*, 1984) and M-protein (Masaki and Takaiti, 1974).

The M-band is located in the central light (bare) zone of the A-band, where no myosin crossbridges are present and appears as a dark line of about 100 nm width in the electron

microscope. The detailed analysis of electron micrographs revealed five prominent lines, which are about 22 nm apart from each other: M1, M4/M4', M6/M6' (Sjostrom and Squire, 1977). 3-dimensional reconstruction of negatively stained longitudinal and transverse cryosections resulted in the conventional M-band model (Figure 5.4).

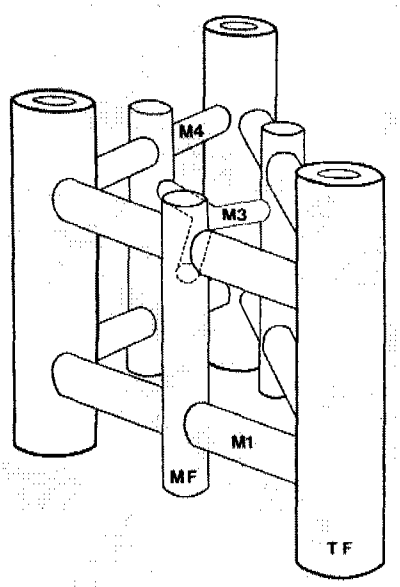

Figure 5.4: *3-dimensional model of the M-band region deduced from EM data.* The relationship among these bridges, the M-filaments (MF), the thick filaments (TF), and the M-bridge lines M4 and M1 are indicated. In a three-line M-band, the structure as visualized here would be mirrored in the M1 plane to yield the whole M-band assembly. The longitudinal M-filaments run in parallel to the thick filaments. The Y-shaped secondary M-bridges crosslink the M-filaments around the M3 line. (Knappeis and Carlsen, 1968, Luther and Squire, 1978).

The M4/M4' lines are present in all muscles, while the density of M1 and M6/M6' lines correlates with the physiological performance of different muscle types. The fastest fibers have 3-lines in their M-bands (M6/M6' lines missing), the slowest fibers have 4-lines (M1 line missing), and fibers of intermediate speed have variations on a 5-line pattern (Sjostrom and Squire, 1977, Thornell *et al.*, 1987, Edman *et al.*, 1988). In addition, the M1 line disappears during the first four weeks from the differentiating slow fibers (Carlsson and Thornell, 1987) and the M-band appearance correlates well with the beating rate in the heart of different species (Pask *et al.*, 1994). All these observations indicate that the M-band structure reflects the contractile characteristics of the myofibrils. In addition, some types of striated muscle (embryonic heart and extraocular muscle) do not display an electron-dense M-band on EM pictures (Smolich, 1995, Andrade *et al.*, 2003).

Recently, it was suggested, that the M-band limits the longitudinal misalignments of thick filaments in the activated myofibril (Agarkova *et al.*, 2003). In the relaxed state, thick filaments are kept in the sarcomere center by titin, but during contraction, a force imbalance between two filament halves might lead to the displacement of the thick filaments from the center and consequently to an increase in the force acting in the same direction. It was

suggested, that the M-band filaments appreciably help titin to counteract such force imbalances by linking individual thick filaments together, which leads to an averaging effect of the M-band web and an improved stability of the A-band in the activated sarcomere (Figure 5.5).

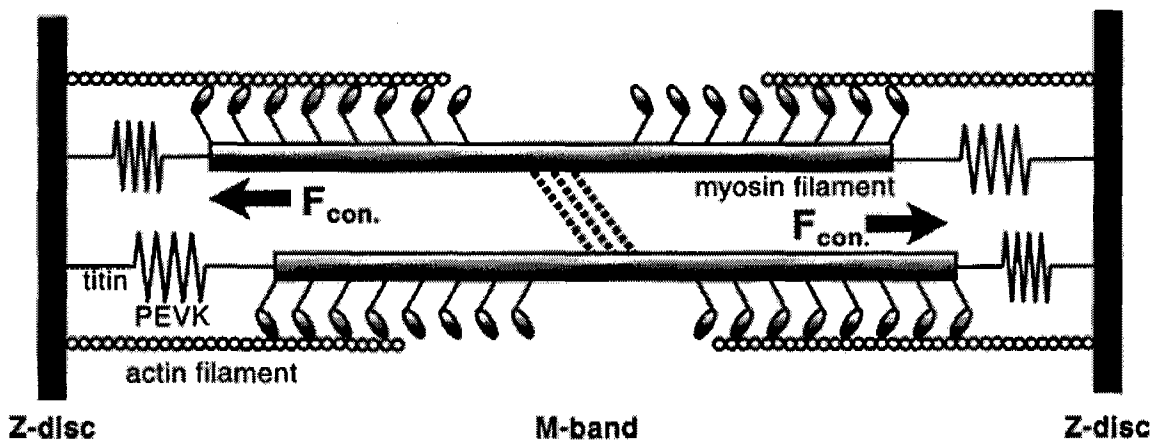

Figure 5.5: *Elastic titin filaments and the M-band play different roles in the activated sarcomere.* During sarcomere activation the thick filaments try to escape into different directions, according to differences in the amount of activated cross-bridges on both halves. The M-band filaments equilibrate these imbalances in force through all thick filaments in the half-sarcomere ensuring therefore a symmetrical shortening of the sarcomeric unit. The titin filaments are responsible for the centering of the A-band unit as a whole (Agarkova *et al.*, 2003).

The approximate positions of titin, myomesin and M-protein in the sarcomere were determined by biochemical assays and EM epitope localization. These results were summarized in the (two-dimensional) molecular model of the M-band, where M-protein bridges the myosin filaments at the level of the M1 line (Obermann *et al.*, 1996, Obermann *et al.*, 1997). But this model could not explain, how the connection between the myosin filaments is established in muscles which lack M-protein. This puzzle could be recently clarified by biochemical and biophysical approaches that focused on the properties of the prominent M-band component myomesin. These studies resulted in a 3-dimensional model of the myomesin incorporation into the M-band, where antiparallel dimers of myomesin link two myosin filaments (Figure 5.6).

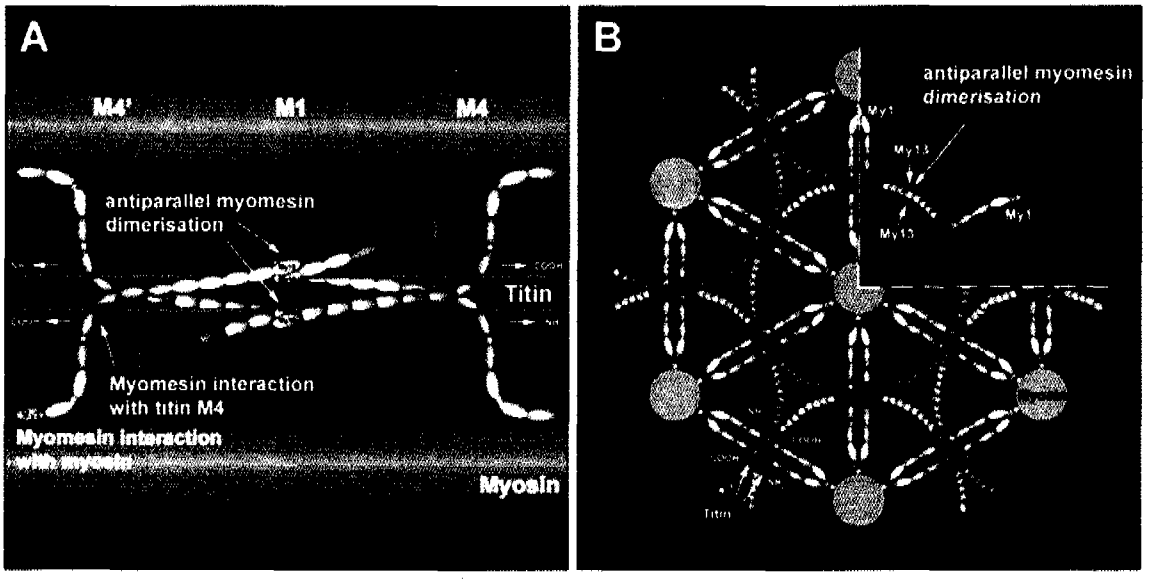

Figure 5.6. *3-dimensional model of myomesin incorporation into the M-band based on molecular interactions.* Myomesin is depicted in yellow, titin and myosin in grey; immunoglobulin domains in myomesin are presented in a lighter shade, fibronectin type-3 domains in a darker shade. Titin and myosin are represented only schematically, with the exception of the titin m4 domain, the binding site to myomesin. A) Longitudinal view showing two myosin filaments, their associated titin strands at this section plane and the connecting myomesin molecules. B) Projection of the molecular interactions between myomesin, titin and myosin in a cross-section. The position of a myomesin dimer is highlighted in the top right corner (Lange *et al.*, 2005b).

5.4.4 Members of the myomesin family

Myomesin (Myomesin 1) and M-protein (Myomesin 2) belong both to the myomesin protein family but are produced from two separate genes. Comparative sequence analysis revealed that both proteins share the same intron-exon arrangement and are composed of a unique head domain followed by 12 immunoglobulin-like (Ig) and fibronectin type III (Fn) domains (Figure 5.7). The main difference between the two proteins is in the sequence of their N-terminal domains: the N-terminal domain of myomesin is much larger than the N-terminal domain of M-protein.

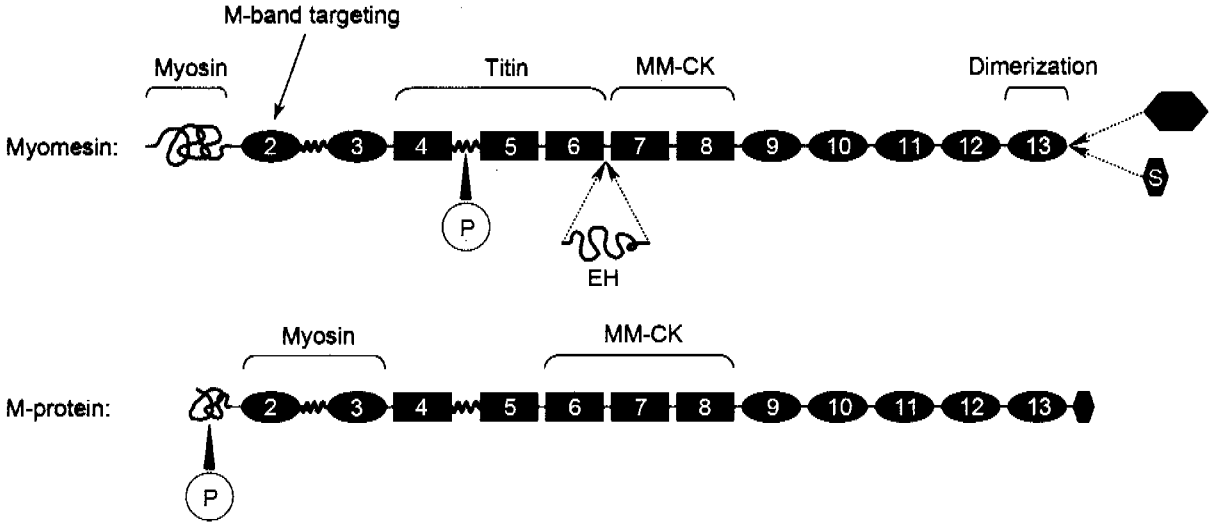

Figure 5.7: *Schematic representation of the myomesin family members.* The main part of myomesin and M-protein consists of identically arranged tandem repeats of Ig (ellipses) and Fn (rectangles) domains. The N-terminal parts as well as the alternatively spliced EH-segment are predicted to be in an intrinsically disordered state. Myomesin has two sites of alternative splicing. The one at the C-terminus is specific for birds and leads to the expression of H (heart) and S (skeletal) myomesin isoforms. Mammalian muscles express the shorter S-myomesin in all muscle types. The EH-myomesin isoform is generated by the inclusion of the EH-segment in the central part of the molecule. Phosphorylation sites (P, blue circles) (Obermann *et al.*, 1997, Obermann *et al.*, 1998) and interacting partners (identified above brackets) (Obermann *et al.*, 1997, Obermann *et al.*, 1998, Hornemann *et al.*, 2003, Lange *et al.*, 2005b) are indicated (adapted from (Agarkova and Perriard, 2005)).

5.4.4.1 Myomesin

Myomesin has a molecular mass of about 185 kDa and is an integral component of the M-band. It is expressed in all types of striated muscle (Agarkova *et al.*, 2004 and chapter 6.2) and at all stages of development (Grove *et al.*, 1989). Studies on myofibrillogenesis have shown that myomesin becomes localized in its characteristic pattern simultaneously with the appearance of the first sarcomeres (Ehler *et al.*, 1999). Biochemical assays showed the binding of fragment My4-6 of myomesin to titin domain M4, which is regulated by phosphorylation (Obermann *et al.*, 1997). Two different domains seem to mediate the interaction with myosin: My2 (Ig domain) is sufficient for the localization to the M-band (Auerbach *et al.*, 1999) whereas the N-terminal domain My1 was shown to interact with light meromyosin (LMM) in vitro (Obermann *et al.*, 1997). In addition, myomesin has the ability to form antiparallel dimers via its C-terminal domain (Lange *et al.*, 2005b). These findings were integrated into the novel three-dimensional model of the sarcomeric M-band in which myomesin is considered to be the principal thick filament cross-linking protein analogous to α-actinin in the Z-disk (Lange *et al.*, 2005b). Besides, myomesin was shown to interact with

the mucle isoform of creatine kinase (Hornemann *et al.*, 2003) and with MR-1, a myofibrillogenesis regulatory factor (Li *et al.*, 2004).

Myomesin can be expressed in different isoforms generated by alternative splicing (Bantle *et al.*, 1996, Agarkova *et al.*, 2000). In embryonic heart of birds and mammals, alternative splicing in the central part of the molecule (between domains My6 and My7) gives rise to the EH-myomesin isoform, previously known as a separate protein called skelemin (Price and Gomer, 1993, Steiner *et al.*, 1999). It represents the major myomesin isoform at early embryonic stages of heart but is rapidly downregulated around birth (Agarkova *et al.*, 2000). To a lower extent it is also expressed in slow twitch skeletal muscle and extraocular muscle of mouse (Agarkova *et al.*, 2004 and chapter 6.2). Interestingly, the alternatively spliced EH-segment, which has a high variability in its sequence between different species (Agarkova *et al.*, 2000), has a disordered conformation. In chicken, two alternative splicing events give rise to four myomesin isoforms contrary to only one splicing event (EH-segment) with two possible isoforms in mice (Agarkova *et al.*, 2000). A splicing event at the C terminus results in two splice variants termed H-myomesin and S-myomesin, which represent the major myomesin species in heart and skeletal muscle of avian species, respectively. The smaller skeletal muscle isoform is homologous to mammalian myomesin.

5.4.4.2 M-protein

M-protein (myomesin 2) has a molecular weight of 165 kDa and shares with myomesin its domain pattern as well as comparable interaction sites with other sarcomeric components as myosin (Obermann *et al.*, 1998), titin (Nave *et al.*, 1989) or MM-CK (Hornemann *et al.*, 2003). This indicates that both proteins are closely related and have a common ancestor in evolution (Kenny *et al.*, 1999). Although myomesin and M-protein may fulfill closely related functions, their tissue-specific expression pattern is different: M-protein is transiently expressed in the M-bands of all muscle fibers late in embryonic development, but is restricted to fast skeletal fibers and cardiac muscle in the adult animals (Grove *et al.*, 1989). In this way, M-protein is expressed in a reciprocal fashion compared to EH-myomesin (Agarkova *et al.*, 2004 and chapter 6.2) but in contrast to myomesin, no alternatively spliced isoform could be detected for M-protein.

5.4.5 Myosin binding protein-C (MyBP-C, C-Protein)

Myosin binding protein-C belongs (like myomesin and titin) to the class of sarcomeric proteins characterized by its moduar Ig and Fn domain composition (Bennett *et al.*, 1999). There are three isoforms of this protein: slow skeletal (X-Protein), fast skeletal and cardiac MyBP-C, which has an additional N-terminal Ig domain (C0) and an additional loop in domain C5. The C-terminus of MyBP-C was reported to bind to light meromyosin (LMM) and to titin, while the N-terminus interacts with the S2 fragment of myosin. There are indications that domains C5 and C8 permit the formation of homodimers. Besides its structural role to cross-link myosin and titin, MyBP-C was also suggested to be involved in the thick filament assembly and regulation of contractility (Flashman *et al.*, 2004). Several mutations in MyBP-C have been linked to cardiomyopathies (Bonne *et al.*, 1995).

5.4.6 The muscle isoform of creatine kinase (MM-CK) and M-band appearance in EM

The creatine kinase is important for the energy supply in skeletal and cardiac muscle (Wallimann *et al.*, 1992), catalyzing the reaction of ADP and phosphocreatine to creatine and ATP. Two M-CK subunits with a molecular weight of about 43 kDa combine to form the enzymatically functional dimer MM-CK. In fully differentiated skeletal muscle, MM-CK is the predominant creatine kinase isoform (Perriard and Eppenberger, 1978). A significant but small amount of the cytosolic MM-CK (~5% of total) is localized in the M-band in some muscle types (Stolz *et al.*, 1998), which could be an advantage for muscle metabolism and ATP regeneration during contraction (Wallimann *et al.*, 1984). The MM-CK seems to be the major component responsible for the M-band appearance in electron microscopic pictures (Strehler *et al.*, 1983, Hornemann *et al.*, 2003). The prominent M4'/M4 lines might result from the attachment of MM-CK to myomesin, while the varying M1 line is due to its binding to M-protein. All muscle types where M-bands appear indistinct (diffuse) contain a high proportion of the EH-myomesin isoform and lack M-protein (Agarkova *et al.*, 2003). In addition to its interaction with proteins of the myomesin family (Hornemann *et al.*, 2003), MM-CK was also shown to bind to DRAL (Lange, 2005). Astonishingly, MM-CK deficient mice are viable and show no pathological changes in cardiac or skeletal muscle with the exception of a reduced maximal power output in fast skeletal muscle. Consequently, an essential structural role of this protein can be excluded (van Deursen *et al.*, 1993).

5.4.7 Muscle LIM protein (MLP)

MLP (CRP3) belongs to the family of the LIM domain proteins, is composed of two tandemly arranged LIM and glycine-rich modules and interacts with proteins such as α-actinin, β-spectrin, telethonin and N-RAP (Arber and Caroni, 1996, Flick and Konieczny, 2000). Depending on the developmental status of the cell, it can be localized in the nucleus as well as in the cytoplasm, where it is preferentially associated with actin filaments and with the Z-disk region of muscle cells (Arber and Caroni, 1996). MLP was found to play an important role in cardiac development, since the MLP KO mouse shows a dilated cardiomyopathy (DCM) phenotype with a disorganized contractile apparatus and defects in costameres as well as in the intercalated disk (Arber *et al.*, 1994, Arber *et al.*, 1997, Ehler *et al.*, 2001). Various mutations in MLP have been associated with the development of hypertrophic or dilated cardiomyopathies. In addition, MLP is highly expressed during differentiation of all kinds of striated muscle, but its expression in the adult is restricted to cardiac and slow twitch fibers of skeletal muscle (Arber *et al.*, 1994, Schneider *et al.*, 1999). It is dramatically upregulated in fast-to-slow fiber type transformation and after eccentric contraction (EC)-induced muscle injury (Chen *et al.*, 2002). Furthermore, MLP (together with T-cap) was suggested to be a key component of the stretch sensor machinery in the Z-disk (Knöll *et al.*, 2002).

5.5 Cardiomyopathy and heart failure

5.5.1 Hypertrophic cardiomyopathy

Hypertrophic cardiomyopathy (HCM) is a relatively common primary cardiac disorder defined as the presence of hypertrophied, non-dilated left ventricle in the absence of other diagnosed etiology. The clinical phenotype is diverse, ranging from minimal cardiovascular symptoms to chest pain, dyspnoea, impaired conciousness and finally severe heart failure (diastolic dysfunction, outflow tract obstruction and ischaemia) and sudden death can occur often due to arrythmias. While most of the patients exhibit a normal lifespan, some individuals show significant morbidity and early sudden cardiac death. The histopathological changes are characterized by myocyte "disarray", myocellular hypertrophy and fibrosis. Many cases are familial in origin and transmitted in an autosomal dominant manner, which was first shown for a severe form of HCM, mapped to a mutation in β-MHC (Geisterfer-Lowrance *et*

al., 1990). Until now, more than 200 independent mutations (mostly amino acid substitutions) in sarcomeric proteins have been linked to Familial Hypertrophic Cardiomyopathy (FHC), and several transgenic models expressing these mutant forms have been studied: β-MHC (approximately 50%), cardiac troponin T (cTnT), cardiac troponin I (cTnI), tropomyosin (Tm), MyBP-C, regulatory myosin light chain (MLC-1), essential myosin light chain (MLC-2), actin and titin. Recently, MLP mutations have been identified as a rare cause of HCM (Geier *et al.*, 2003). These mutant proteins can act either via a dominant negative mechanism, or they lead to haploinsufficiency by inactivation of one allele.

Most of the β-MHC mutations are missense mutations occurring in the HMM region but also mutations in the COOH-terminal portion of LMM were identified (Blair *et al.*, 2002), generally resulting in early onset of the HCM disease (Anan *et al.*, 1994). The observed phenotypic variability seems to be determined by alterations in the biophysical properties of the molecule: Several studies showed a decrease in V_{max} of the ATPase, and increased association for actin and a decrease in the actin sliding speed in vitro (Sweeney *et al.*, 1998, Roopnarine and Leinwand, 1998). These results suggest that the severe hypertrophy in some patients was due to a variable decrease in the motor function of myosin and a compensatory hypertrophic response. The first murine model for FHC was based on the R403Q human mutation (Geisterfer-Lowrance *et al.*, 1996) and was generated in α-MHC. Heterozygous animals have similar problems compared to human patients, such as impaired relaxation and chamber filling, increase in Ca^{2+} sensitivity, myocyte disarray, progressive fibrosis and left atrial enlargement. Confusingly, a newer study showed that the actin-dependent ATPase activity, *in vitro* sliding speed and force production were increased in these mice (Tyska *et al.*, 2000), which could result in an increase of energy cost and inefficient ATP utilization. Thin filament mutations comprise about 25% of FHC, developing a complex cardiomyopathy with varying degrees of ventricular hypertrophy and a high frequency of arrhythmias and sudden cardiac death (Moolman *et al.*, 1997). Cardiac TnT and Tm –related FHC mutations tend to cluster in several functional domains, having profound effects on protein flexibility, Ca^{2+} sensitivity, sliding speed, force generation and Tm binding. An increase in Ca^{2+} sensitivity of tension development and in basal levels of myofilament activation is thought to be a central component of the pathogenic mechanism.

Furthermore, patients carrying mutations in cardiac MyBP-C include about 25% of all FHC cases. Phenotype-genotype association studies revealed that patients with such mutations form a distinct subtype characterized by a relatively positive prognosis (late onset) and less marked symptoms (Charron *et al.*, 1998). While mutations in β-MHC and thin filament proteins are

largely missense substitutions, most MyBP-C mutations result in truncated proteins. One central question is, whether these incorporate into the sarcomeres or are excluded and degraded, leading to haploinsufficiency. Surprisingly, the MyBP-C KO mouse displays a normal cardiac ultrastructure but develops cardiac hypertrophy, impaired systolic and diastolic function and depressed myocyte contractility (Harris *et al.*, 2002). In addition, an increase in unloaded shortening velocity could be showed in myocytes lacking MyBP-C suggesting that this protein normally provides a viscous load during contraction.

5.5.2 Dilated cardiomyopathy

Dilated cardiomyopathy (DCM) is characterized by dilatation and impaired contraction of the left ventricle. The causes of DCM can be idiopathic, viral, toxic, due to association with other cardiovascular diseases or familial. It affects about 37 out of 100'000 people, of which 25-30% are familial (Kamisago *et al.*, 2000). They are strongly associated with mutations in proteins of the sarcomere, cytoskeleton and sarcolemma such as: β-MHC, MyBP-C, actin, Tm, TnT, TnI, TnC, titin, T-cap, desmin, vinculin and MLP. The strong correlation between the disease and mutations in proteins of sarcomere and cytoskeleton suggests a converging pathway for all associated mutations. It was suggested that the cardiomyocyte possess a kind of "stretch sensor" which can detect changes in contractility caused by the mutations and initiates long term morphological and functional compensatory mechanisms.

Most of the DCM mutations can be linked to the β-MHC gene and are grouped in those which are found in S1, those found in the tail region, and those with transition from HCM to DCM. Mutations found in S1 have been implicated in the disruption of myosin-actin interaction (Daehmlow *et al.*, 2002), thereby causing contractile dysfunction. The mutations found in the tail occur in highly conserved residues, whose substitution may affect the structure of the molecule. Furthermore, DCM related mutations have been found in all three subunits of Tn, of which TnT mutations are the most frequent ones. All of these display functional characteristics distinct from those caused by HCM associated mutations and are associated with slightly decreased Ca^{2+} sensitivities and decreased actomyosin ATPase rates (Venkatraman *et al.*, 2005, Gomes and Potter, 2004). In addition, several familial mutations in titin have been associated with DCM: These are located mainly in the α-actinin or T-cap binding domains of the Z-disk region or they can be found in the cardiac specific N2B region. Interestingly, titin displays an isoform switching towards longer isoforms in the case of DCM

(Makarenko *et al.*, 2004). The identification of DCM associated mutations in titin emphasizes its importance in the maintenance of cardiac function. It was suggested, that the various mutations found in patients suffering from DCM suggest a common pathway for progression from mutation to the diseased state. Candidates for the transmission of contractile changes to signaling pathways are several proteins of the Z-disk, such as MLP, T-cap or even titin. In addition, members of the matrix metalloproteinases (MMP) have been identified to play a role in DCM disease remodelling processes (Spinale *et al.*, 2000).

One of the first genetically manipulated mouse with a cardiac DCM phenotype was the MLP-deficient mouse (Arber *et al.*, 1997), which displays the typical symptoms of dilated cardiomyopathy (DCM). These are enlargement of cardiac chambers with ventricular wall thinning, severe systolic and diastolic ventricular dysfunctions, defects in calcium cycling, increases in wall stress, elongated action potential duration and desensitization of β-adrenergic receptor. Interestingly, several genes involved in the regulation of Ca^{2+} cycling have been associated with the phenotype of dilated cardiomyopathy, such as phospholamban (Schmitt *et al.*, 2003) or FKBP12 (Shou *et al.*, 1998).

Phospholamban (PLN), a highly conserved 52-amino acid peptide, whose expression is restricted to heart and slow skeletal muscle, is an endogenous inhibitor and regulator of SERCA2 in the heart. Besides, it is a substrate of protein kinase A, protein kinase C and CaMKII (Tada *et al.*, 1998) and is hypophosphorylated in many settings of heart failure (Sande *et al.*, 2002). Interestingly, in double knockout mice (MLP KO/PLN KO), the PLN ablation prevented the appearance of heart failure found in MLP KO mice (Minamisawa *et al.*, 1999). Beneficial effects of phospholamban ablation was also noted in two other cardiomyopathy models (calsequestrin- and α-MHC (R403Q) overexpressing mice (Sato *et al.*, 2001, Freeman *et al.*, 2001)).

Other studies have linked cytoskeletal proteins to DCM such as the Z disk proteins ALP (Hoshijima *et al.*, 2002) and ZASP/cypher (Zhou *et al.*, 2001), membrane cytoskeletal proteins dystrophin (Megeney *et al.*, 1999) and sarcoglycans (Durbeej and Campbell, 2002), and the intermediate filament component desmin (Milner *et al.*, 1996).

Although most of the genetic defects in the myofilament proteins have been linked to hypertrophic phenotypes (Frey and Olson, 2003), several mice with mutations in myofilament proteins display signs of DCM: A homozygous mutation of α-MHC (Fatkin *et al.*, 1999), the homozygous truncated mutant of MyBP-C (McConnell *et al.*, 1999) and the overexpression of tropomodulin in the heart (Sussman *et al.*, 1998) cause aggressive forms of DCM. In addition, overexpression of several nuclear signaling molecules has been shown to cause DCM: The

membrane GTP-binding protein Gαq (D'Angelo *et al.*, 1997), the artificial Gi-coupling receptor Ro1 (Redfern *et al.*, 2000), the dominant-negative form of CREB (Fentzke *et al.*, 1998), the δB nuclear form of CaMKII (Zhang *et al.*, 2002) and the rhoA oncogene (Sah *et al.*, 1999) were overexpressed in the mouse heart and dilated cardiomyopathy was observed. Recently, cardiac transgenic mice overexpressing a constitutively active protein kinase A were documented to develop dilated cardiomyopathy (Antos *et al.*, 2001).

5.6 Single-molecule mechanics

5.6.1 Atomic force microscopy

The AFM consists of a microscale cantilever with a sharp tip at its end that is used to scan the specimen surface. When the tip of the cantilever, which is typically made of silicon or silicon nitrite, is brought into proximity of a sample surface, forces between the tip and the sample lead to a deflection of the cantilever. Typically, the deflection is measured using a laser spot reflected from the top of the cantilever into a photodiode. In most cases a feedback mechanism is employed to adjust the tip-to-sample distance to maintain a constant force between the tip and the sample. Traditionally, the sample is mounted on a piezoelectric tube, that can move the sample in the z direction for maintaining a constant force, and the x and y directions for scanning the sample, resulting in a three-dimensional surface profile. Samples viewed by AFM do not require any special treatments (such as metal/carbon coatings like in EM) that would irreversibly change or damage the sample. Most AFM modes can work perfectly well in air or a liquid environment, which makes them perfectly suited to study biological macromolecules and even living organisms.

The AFM can be operated in several modes, which are divided into static (contact) modes and dynamic modes. In contact mode, the force between the tip and the surface is kept constant during scanning whereas in the dynamic mode, the cantilever is externally oscillated close to its resonance frequency. Because of this, keeping the probe tip close enough to the sample for short-range forces to become detectable while preventing the tip from sticking to the surface presents a major hurdle for the non-contact dynamic mode. Dynamic contact mode (also called tapping mode) was developed to bypass this problem. In this mode, the cantilever is oscillated such that it comes in contact with the sample with each cycle, and then enough restoring force is provided by the cantilever spring to detach the tip from the sample.

Single-molecule atomic force microscopy (AFM; Figure 5.8) has become a powerful tool to examine the conformation of proteins under a stretching force, because this technique is capable of measuring the forces required to unfold protein domains with piconewton (pN) sensitivity and the length changes with angstrom resolution (Rief *et al.*, 1997, Carrion-Vazquez *et al.*, 1999a).

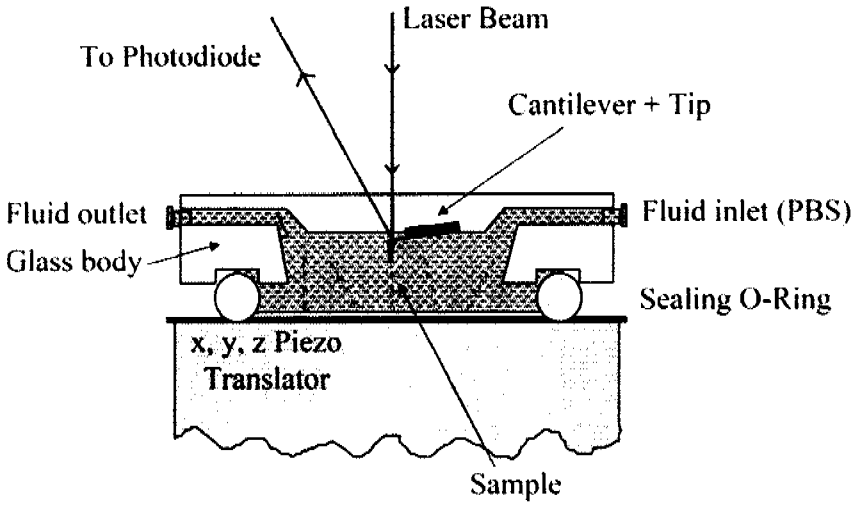

Figure 5.8: *Single-molecule measurements by atomic force microscopy.* First, the protein sample is bound to the gold surface, preferentially by cysteine residues. Then, the tip of the cantilever approaches the surface by moving up of the piezo translator and can pick up a molecule by unspecific adhesion. Finally, the piezo translator moves down again resulting in the pulling of the molecule, which changes the angle of the cantilever. This can be measured by the change in deflection of the laser beam and allows to calculate the applied force (adapted from Bertoncini, P.).

In a typical experiment (Figure 5.9), the tip of the cantilever is brought into contact with a layer of protein attached to the substrate, then the piezoelectric positioner retracts. When a portion of a single protein is picked up at random by the tip through adsorption, the retraction of the positioner stretches the suspended segment of the protein. Extension of the molecule reduces its entropy producing a restoring force that results in bending of the cantilever. This changes the angle of a laser beam, reflected by the surface of the cantilever, and can be measured by a photodiode (Figure 5.8). Using the spring constant of the cantilever, the relationship between deflection and force can be calibrated and the force calculated. The force-extension curves generated by such measurements provide a characteristic sawtooth pattern that serves as a fingerprint of single molecules in experiments of mechanical unfolding and refolding of proteins containing tandem modules such as titin (Rief *et al.*, 1997).

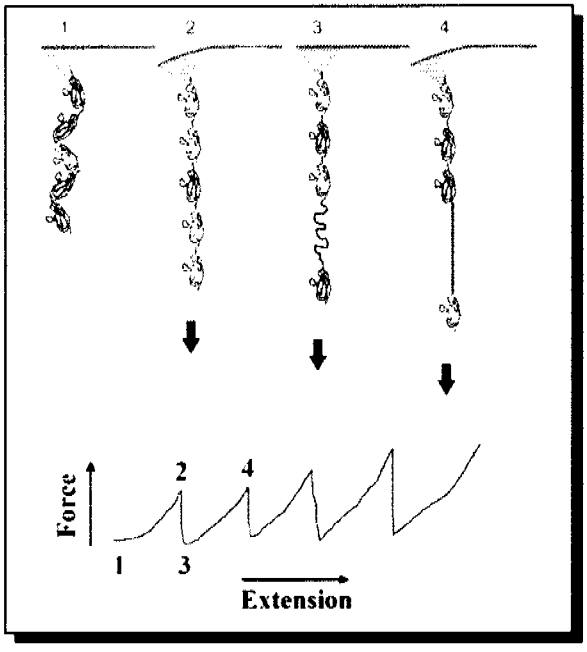

Figure 5.9: *Unfolding kinetics of multidomain proteins.* 1) The polyprotein, picked up by the tip of the cantilever, is in relaxed state. 2) Stretching the protein to its folded contour length requires a force measured as a deflection of the cantilever. 3) The applied force triggers the unfolding of a domain, relaxing the cantilever back to its resting position. 4) Further stretching removes the slack and brings the protein to its new contour length (adapted from (Carrion-Vazquez *et al.*, 1999a)).

5.6.2 Intrinsically unstructured proteins (IUP)

Intrinsically unstructured/disordered proteins (IUP) are defined as proteins or regions of proteins that lack a defined tertiary structure under physiological conditions (Tompa, 2002). Because they differ in amino acid composition from typical globular proteins, several computational methods have been developed to use this tendency to predict whether a given protein sequence is characterized by a high flexibility and consequently likely to be disordered. An example of such a method is PONDR (Predictors of Natural Disordered Regions, Molecular Kinetics, La Pas Trail, IN, USA), which is a series of predictors that use amino acid sequence data to predict disorder in a given region. IUP are rather common in eukaryotic proteins and appear to be involved in a variety of functions, including target recognition and modulation of specificity/affinity of protein interactions (Dunker *et al.*, 2002). A subclass of the IUP includes entropic springs, which produce restoring forces in response to any attempt to change their conformation.

5.6.3 Entropic elasticity

In the absence of an external force, polymers in solution have a coiled conformation which maximizes their entropy. But if such polymers are extended or compressed, they generate an elastic restoring force due to the reduction of entropy. This force is weak during a small elongation (or compression) and grows exponentially when approaching the contour length of the molecule. The advantage of such random coils is that they can be mechanically extended and relaxed without heat dissipation, driven entirely by their entropic elasticity, which is well characterized by the worm-like-chain (WLC) model of polymer elasticity (Bustamante *et al.*, 1994, Marko and Siggia, 1995). This model predicts that the force F(x) needed to extend the ends of a polymer chain to a distance x is of the form

$$F(x) = \frac{kT}{p} f\left(\frac{x}{L_c}\right)$$

where k is the Boltzmann's constant, T the temperature in Kelvin, p the persistence length of the polymer and Lc the contour length. In this way, the mechanical properties of polymers can be described by their persistence length, which is a measure of flexibility: Rigid polymers have a long persistence length (relative to their contour length) and their straightening requires little external force, while the opposite is true for more flexible polymers.

Largely disordered amino acid sequences, such as the PEVK domain of titin, which strongly contributes to the passive elasticity in muscle, behave like random coils and are also called entropic springs. In addition, elastomeric proteins consisting of tandem repeats of Ig or Fn domains (e.g. titin, myomesin or fibronectin) are also predicted to function similarly by straightening of the Fn/Ig domains chain and which partially determines the elasticity of various tissues. Consequently, the giant elastic titin molecule can be modelled as a series of entropic springs with variable elasticity (Tskhovrebova *et al.*, 1997, Li *et al.*, 2002). It has to be added, that the Ig or Fn modules themselves in titin or myomesin are viscous elements, because during unfolding the enthalpy changes and the whole process shows hysteresis during refolding. Therefore, such modular proteins have complex visco-elastic properties resulting from elastic (entropic springs) and viscous (Ig/Fn domains) units.

5.7 Sequence analysis

5.7.1 Choosing a peptide for generation of antibodies

When examining a protein sequence for potential antigenic epitopes, it is important to choose sequences that are hydrophilic, surface oriented, and flexible, because antibodies normally bind to hydrophilic residues located on the surface of a protein. The N- and C-termini of proteins are often exposed and have a high degree of flexibility, often making these regions a good choice for generating antibodies directed against the intact protein. In addition, the antigenicity of polypeptide sequences can be determined by using sequence analysis programs such as Protean (DNASTAR, Madison, WI, USA). This software is able to calculate the antigenic index, surface probability and hydrophilicity of a specific amino acid sequence, which facilitates the search for a suitable peptide. In addition, other factors have to be taken into account: First, the risk of a possible cross-reaction with related proteins should be minimized by choosing a peptide, which is as distinct as possible between these proteins. Secondly, a specific reaction with the same protein in different species may be promoted by chosing sequences that are conserved between species. Thirdly, the peptide length also should be considered when designing a peptide antigen. The typical length for generating anti-peptide antibodies is in the range of 10 to 20 residues. Peptide sequences of this length minimize synthesis problems, are reasonably soluble in aqueous solution and may have some degree of secondary structure.

5.7.2 Blast searches and sequence alignments

At present, many tools (internet servers and programs) are available which facilitate the detailed analysis and comparision of protein or nucleotide sequences. A lot of sequence data are freely accessible on the internet on databases such as Pubmed (www.ncbi.nlm.nih.gov) or Ensembl (www.ensembl.org) and blast searches help to find recent sequence data (cDNA sequences) of previously unknown proteins (in our case myomesin 3) and to compare it with already known sequences of related proteins. At present, the genome of several species has already been sequenced and their number grows almost exponentially.
In addition, the conserved domain database (www.ncbi.nlm.nih.gov) can be used to predict the structure and borders of protein domains, which have not been crystallized yet. This

database is able to find the 3D-structure of the most related protein domain, which makes it a powerful tool for planning and analyzing experiments basing on the structure of single domains (e.g. single-molecule measurements, crystallization studies). Sequence alignments of related proteins can be performed by programs such as Megalign (DNASTAR, Madison, WI, USA) or LALIGN (www.expasy.com), which assist to find which parts of the sequence show a high degree of conservation. Such analyses lead to new insights in the possible function of the analyzed proteins and its domains. Phylogenetic studies (using algorithms such as ClustalW) can complement such studies by predicting evolutionary relationships between the sequences.

5.8 Aim of this study

The sarcomere of striated muscle is a natural apparatus that transforms chemical energy into mechanical work. It is cruicial that all its contractile and structural elements are precisely coordinated to optimize the efficiency of contraction. The M-band in the center of the sarcomere, as important element of the sarcomeric cytoskeleton, has the task to maintain the thick filament lattice. To achieve this goal, it must endure mechanical stress during sarcomeric contraction to counteract possible misalignments of thick filaments. To understand the principle of the M-band function, one needs to analyze the expression pattern and properties of its components and their interactions.

The investigation of the M-band has a long history in the Institute of Cell Biology (Turner *et al.*, 1974, Strehler *et al.*, 1980, Eppenberger *et al.*, 1981). One of the most evident successes of this study was the discovery of myomesin (Grove *et al.*, 1984). Following investigations have shown that this essential sarcomeric component might be expressed in different isoforms (Grove *et al.*, 1985). This was later confirmed by the identification of two different myomesin mRNA transcripts in chicken striated muscle (Bantle *et al.*, 1996), revealing the differential expression in chicken heart and skeletal muscles.

In order to examine the appearance and distribution of these isoforms at the protein level, isoform-specific antibodies have been produced and the expression pattern of myomesin isoforms has been analyzed in chicken (Agarkova *et al.*, 2000), showing that one of the splice variants (EH-myomesin) seems to be expressed only in embryonic heart. Sequence analysis showed that the alternatively spliced EH-segments of mouse and chicken are rather divergent with only 36% of identity. Therefore it was necessary to generate antibodies against the EH-

segment of mouse, to be able to further analyze the expression pattern of EH-myomesin in this animal. In my diploma work (Schoenauer, 2002), I did a first characterization of the new antibodies against mouse EH-myomesin.

The main goal of my dissertation was to further analyze the function of the EH-myomesin isoform in respect to the sarcomeric M-band structure. To achieve this we first analyzed the expression pattern of EH-myomesin in different muscle types of mouse, revealing that this isoform is expressed not only in the embryonic heart, but also in slow skeletal muscle ((Agarkova *et al.*, 2004) and chapter 6.2). In the second part of my dissertation, the main goal was to measure the mechanical properties of myomesin using single-molecule measurements (atomic force microscopy) and in this way underline its important function for sarcomeric stability. This study showed that myomesin is a molecular spring with complex visco-elastic properties which can be modulated by alternative splicing of the elastic EH-segment ((Schoenauer *et al.*, 2005) and chapter 6.1). In the end of 2004, we were surprised to find in a blast search a third gene (myomesin 3) which belongs to the myomesin protein family. This was the starting point for the third part of my doctoral thesis, during which I analyzed the expression pattern of this gene on the RNA and protein level (chapter 6.3). This study showed that myomesin 3 is a novel component of the sarcomeric M-band and is expressed mainly in type IIA fibers of skeletal muscle in mouse.

5.9 Organization of the manuscript

The results and discussion parts are structured as three sections, which can be read individually and were integrated into different publications. In addition, the third section includes the most recent and consequently unpublished data. Nevertheless, all three chapters illuminate myomesin function from different points of view and complement each other nicely.

6 RESULTS

6.1 Biophysical characterization of myomesin

6.1.1 Introduction

Vertebrate striated muscle sarcomeres contain in addition to thick and thin filaments a complex network of cytoskeletal proteins. These proteins form two transverse structures, which are essential for the regular arrangement of the contractile filaments: the Z-disk, which anchors the actin filaments and the M-band, which is thought to cross-link the myosin filaments. The elastic longitudinal connection between them is provided by titin (Trinick *et al.*, 1984), which spans the space from the Z-disk (N-terminus) to the M-band (C-terminus) (Fürst *et al.*, 1988). Titin is tightly bound to the thick filaments in the A-band, while its I-band portion, consisting of serially connected Ig-domain chains and unique PEVK and N2B regions, is extensible. The molecular basis for the elasticity of titin is quite well understood due to the recent progress in single-molecule analysis techniques such as optical tweezers and atomic force microscopy (for recent review see (Tskhovrebova and Trinick, 2003, Granzier and Labeit, 2004)). There are two main sources of elasticity in the extensible I-band portion of this protein: one deriving from the straightening of the Ig domains chain, the other from the extension of the largely non-folded PEVK and N2B regions (Tskhovrebova *et al.*, 1997). Upon stretching sarcomeres, first the Ig segments straighten while their individual Ig domains remain folded. When the sarcomeres are further stretched (beyond 2.7 μm), the PEVK extension becomes dominant (Trombitas *et al.*, 1998). Recent analyses revealed that the unique PEVK region not only acts as an entropic spring, but also has actin-binding properties and was therefore suggested to produce a viscous force component opposing filament sliding (Linke *et al.*, 2002). Strong stretching forces can exhaust the elasticity of the titin molecule and lead to the sequential unfolding of the modular domains (Tskhovrebova *et al.*, 1997). Single-molecule manipulations by AFM of recombinant fragments of titin have shown a characteristic saw-tooth pattern in the force-extension relationship, with each peak corresponding to the unfolding of a single domain (Rief *et al.*, 1997). The unfolding force of individual Ig-domains ranged from 150 to 300 pN and the modules readily refold upon release of tension (Rief *et al.*, 1997). Ig-domains located in different portions of the extensible part of I-band titin demonstrate a hierarchy of mechanical stability, with the weakest Ig-domains

(unfolding force ~150 pN) located adjacent to the Z-disk (Li *et al.*, 2002). The differentially expressed domains in the central portion of I-band titin show intermediate stability (~180 pN), while the mostly stable domains (~220 pN) constitute the C-terminal portion of the titin I-band region, near the tip of the thick filament(Watanabe *et al.*, 2002a). Further investigations revealed that the Fn domains have in general lower unfolding forces (100-200 pN) than the Ig domains (150-300 pN) (Rief *et al.*, 1998, Tskhovrebova and Trinick, 2004). It has been discussed that some parts of titin may participate in accommodating changes in sarcomere length through reversible unfolding and refolding (Kellermayer *et al.*, 1998). Thus, the single-molecule measurements of the individual titin domains allowed reconstruction of the mechanical characteristics of the whole molecule (Li *et al.*, 2002) and to clarify the mechanical function of titin in the sarcomere (for review see (Tskhovrebova and Trinick, 2003, Granzier and Labeit, 2004)).

The sliding filament model of muscle contraction implies that the central position of the thick filament in the sarcomere is intrinsically unstable in the activated sarcomere. Due to differences in the number or extent of cross bridge activation or due to slight variations in the overlap with actin filaments, the forces generated on two halves of activated thick filaments can not be identical. Any initial imbalance of forces will be further enhanced during contraction due to the progressive displacement of thick filaments from the center. A-bands, moved towards one of the Z-disks, were indeed observed in EM pictures of activated skeletal muscle (Page and Huxley, 1963, Bergman, 1983). However, the stability of sarcomeric contraction requires the proper centering of the thick filaments at the end of each contraction cycle. It is believed that elastic titin filaments, connecting the thick filaments with the Z-disks, accomplish this important job (Horowits and Podolsky, 1987, Horowits and Podolsky, 1988, Horowits *et al.*, 1989). However, as suggested recently, an important contribution comes from the M-band bridges, cross-linking the thick filaments (Agarkova *et al.*, 2003). Due to this connection the random initial imbalance of the cross-bridge forces gets averaged through all thick filaments present in one sarcomere; this significantly facilitates the efforts of titin to maintain the status quo. This model implies that the M-band filaments are stretched during the contraction cycle, due to force differences between neighboring thick filaments (Figure 6.1 a). Unfortunately, no information is presently available on the mechanical properties of structural M-band proteins at the molecular level.

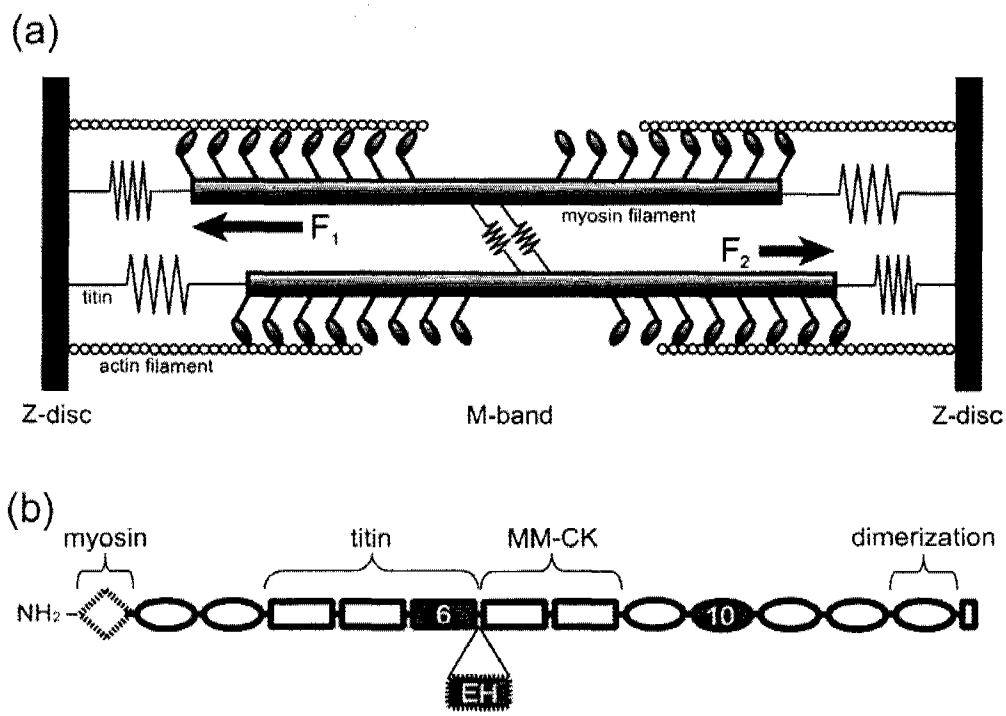

Figure 6.1: *(a) Schematic representation, demonstrating the role of the M-band in the contracting sarcomere.* The cross-bridge forces acting on both halves (F_1, F_2) are not equal, leading to progressive deviations of the thick filaments from the center during contraction. This is partially compensated by the M-band filaments, which equilibrate these force imbalances over all thick filaments present in one sarcomere. Adapted from (Agarkova *et al.*, 2003). *(b) Schematic representation of myomesin.* Myomesin is mainly composed of immunoglobulin-like (ellipses) and fibronectin type III domains (rectangles). The EH-isoform has an additional EH-segment (EH, in grey) inserted in the center of the molecule. Myomesin domain My1 interacts with myosin, My4-6 is the titin binding region, My7-8 interacts with MM-CK and My13 mediates an antiparallel dimerization. In addition to the EH-segment, domains My6 (6, in grey) and My10 (10, in grey) have been selected for the cloning of polyproteins (Schoenauer *et al.*, 2005).

The main candidates for the role of M-bridges, connecting the myosin filaments in the M-band (Obermann *et al.*, 1996) are two closely related proteins of the Ig-superfamily, myomesin and M-protein (Nave *et al.*, 1989). These are modular proteins, consisting of a unique N-terminal domain followed by a conserved sequence of twelve immunoglobulin-like (Ig) and fibronectin type III (Fn) domains (Bantle *et al.*, 1996, Vinkemeier *et al.*, 1993) (Figure 6.1 b). In contrast to M-protein, which has a muscle-type specific expression pattern (Grove *et al.*, 1987), myomesin is expressed in all types of vertebrate striated muscles (Agarkova *et al.*, 2000) and localizes to the M-band already in the first nascent sarcomeres in embryonic heart (Ehler *et al.*, 1999).

The N-terminus of myomesin is involved in the interaction with myosin (Obermann *et al.*, 1995, Obermann *et al.*, 1997, Auerbach *et al.*, 1999), the central part interacts with the titin m4 domain (Obermann *et al.*, 1997) and muscle-type creatine kinase (MM-CK) (Hornemann

et al., 2003) while the C-terminal domain 13 of myomesin was recently shown to form antiparallel dimers (Lange *et al.*, 2005b). In the central part of the molecule, an alternative splicing event can take place (Agarkova *et al.*, 2000, Steiner *et al.*, 1999) leading to the insertion of the additional EH-segment (96 aa in the human sequence) between domains My6 and My7 (Figure 6.1 b). This generates the EH-isoform, which is the main myomesin species in the embryonic heart of all higher vertebrates (Agarkova *et al.*, 2000) and shows a fiber-type dependent expression pattern in adult mouse skeletal muscle (Agarkova *et al.*, 2004). Interestingly, this unique EH-segment is rather heterogeneous in sequence between different species (Agarkova *et al.*, 2000) and its structure seems to be in an intrinsically disordered state (Schoenauer et al., 2005) according to computer simulations such as PONDR (Predictors of Natural Disordered Regions, Molecular Kinetics, La Pas Trail, IN, USA). The recently published three-dimensional model of the M-band (Lange *et al.*, 2005b) suggests that anti-parallel dimers of myomesin cross-link myosin filaments in the M-band, playing a role analogous to that of α-actinin, which cross-links actin filaments in the Z-disk. Therefore, the myomesin molecule may be stretched during sarcomere contraction due to small deviations in the register of neighboring thick filaments (Agarkova *et al.*, 2003).

To characterize the mechanical properties of myomesin and to elucidate its function in the M-band, we performed single-molecule measurements on different myomesin domains. The stretching of polyproteins, constructed of My6 (Fn domain), My10 (Ig domain) and the unique EH-segment by atomic force microscopy reveals new insights into the mechanics of the M-band and is complemented by transmission electron microscopy (TEM) and circular dichroism (CD) measurements

6.1.2 The mechanical stability of My6 and My10

In order to measure the mechanical properties of individual myomesin domains, we used atomic force microscopy. This technique was designed specifically to study the force-extension characteristics of single molecules with high precision. First, we constructed homomeric polyproteins containing identical repeats of myomesin domains My6 (Fn) or My10 (Ig), as illustrated by the schematic representation in Figure 6.2. Because the exact three-dimensional structures of My6 and My10 are not identified yet, we determined their boundaries by comparison to the known X-ray structure of similar domains (see Materials and Methods).

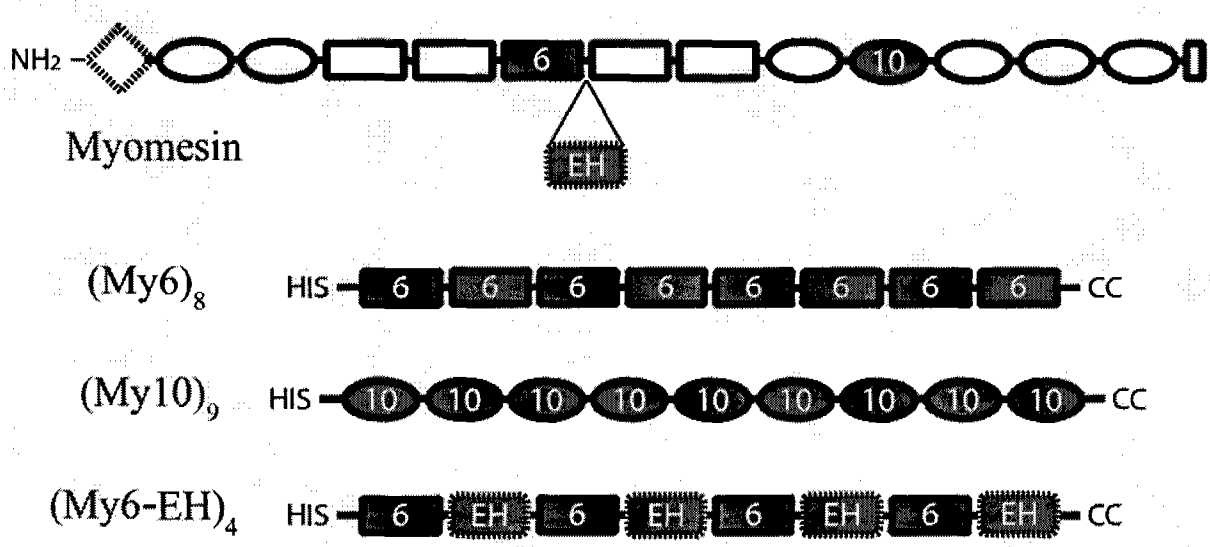

Figure 6.2: *Schematic representation of myomesin and constructed polyproteins used for AFM measurements.* Myomesin is mainly composed of immunoglobulin-like (ellipses) and fibronectin type III domains (rectangles), with an alternatively spliced EH-segment (EH) in the center of the molecule. Domains (My6, EH, My10) and the individual multimodular polyproteins $(My6)_8$, $(My10)_9$ and $(My6\text{-}EH)_4$ used for the AFM measurements are shown in grey (adapted from Schoenauer et al., 2005).

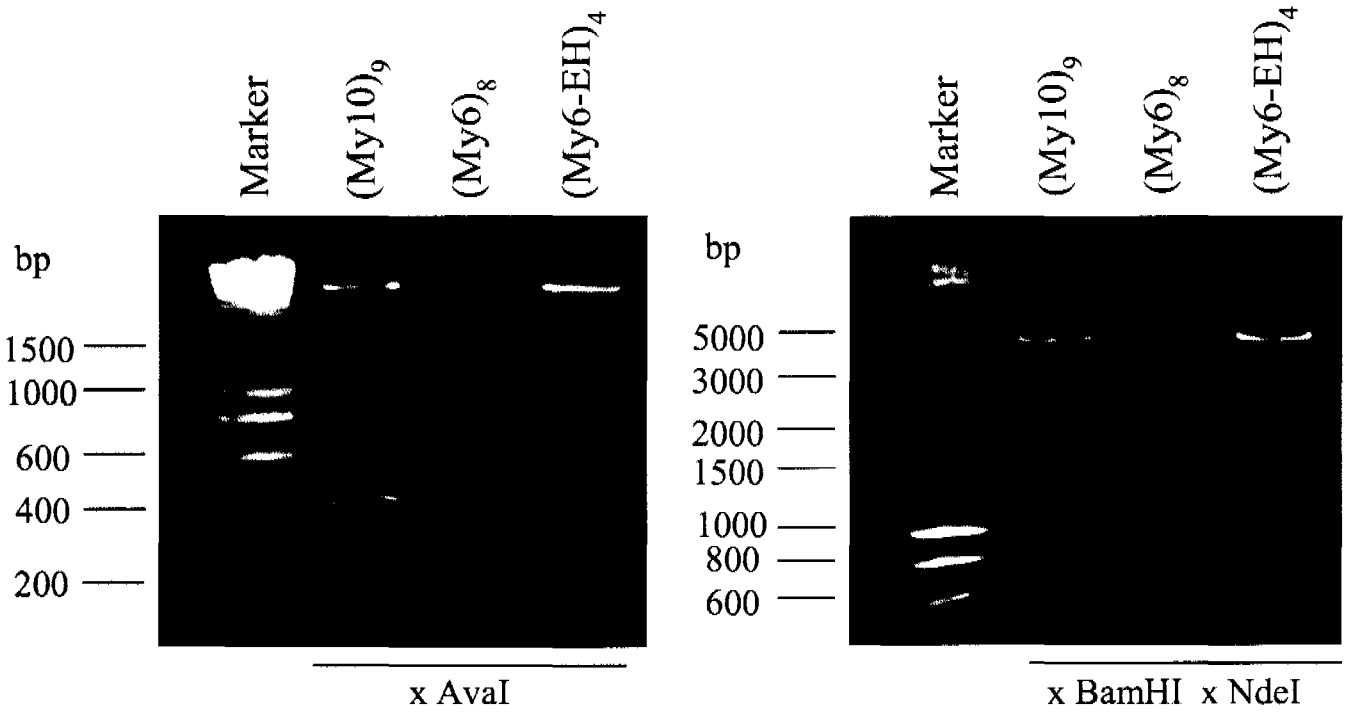

Figure 6.3: *Control digests of myomesin polyprotein constructs.* Repeats of a single myomesin domain (My6, My10) or repeats of two neighboring domains (My6-EH) were produced by directional DNA concatemerization (via the AvaI site) of myomesin fragments generated by PCR from human cDNA. These concatemers were then ligated into the bacterial expression vector pETAvaI and the generated clones were further analyzed. A restriction digest with AvaI (left picture) confirms the correct size of all myomesin repeats (about 300 bp (My6), 400 bp (My10) or 600 bp (My6EH)) whereas the double digest with BamHI and NdeI shows the size of the whole insert allowing to calculate the number of repeats: $(My10)_9$, $(My6)_8$, $(My6\text{-}EH)_4$.

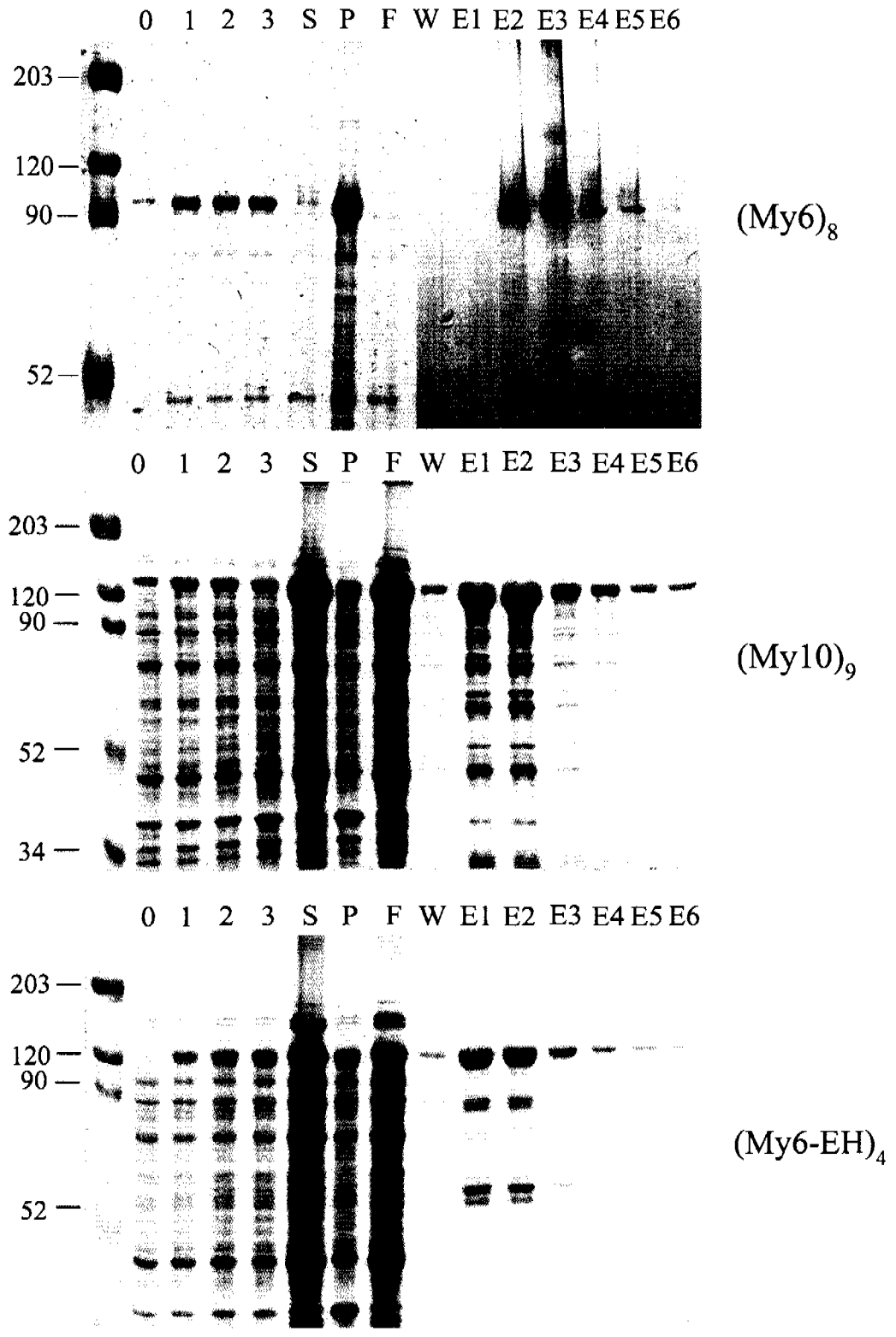

Figure 6.4: *Expression and purification of human myomesin polyproteins from E. coli.* The $(My6)_8$, $(My10)_9$ and $(My6\text{-}EH)_4$ polyproteins were expressed in E.coli strain BLR as His-tagged proteins. Bacterial extracts were prepared after IPTG induction for the indicated period of time (0, 1, 2 and 3 hours). Insoluble components of the bacterial lysates (P = pellet) were separated and removed from the soluble fraction by centrifugation. The supernatant (S) was applied directly for Ni^{2+} affinity chromatography with the non-binding proteins remaining in the flowthrough (F). After a washing step (W) the purifed proteins were eluted using Imidazol (eluates E1, E2, E3,...). The integrity of the polyproteins was analyzed by 8% SDS-PAGE followed by Coomassie staining. Molecular markers are indicated in kDa.

These constructs were generated using directional DNA concatemerization by self-ligation of the myomesin fragments via the flanking Ava I sites (control digests in Figure 6.3). The His-tagged polyproteins were finally expressed in *E.coli* and purified by Ni^{2+} affinity chromatography as illustrated in Figure 6.4 (details see Materials and Methods). Interestingly, the $(My6)_8$ polyprotein was less soluble compared to $(My6\text{-}EH)_4$ or $(My10)_9$, possibly because of some tendency of aggregation. Consequently, most of the $(My6)_8$ protein was lost during centrifugation (lane P), leading to a smaller amount of protein and to the presence of some high molecular aggregates in the eluates (lanes E2 – E6 of gel $(My6)_8$). In addition, the $(My6\text{-}EH)_4$ and $(My10)_9$ polyproteins are partially fragmented (see eluates in $My6\text{-}EH)_4$ and $(My10)_9$ gels), maybe because the longer linkers are more sensitive to proteases.

The stretching of $(My6)_8$ polyproteins at a pulling speed of 1000 nm/s results in force-extension curves with the expected saw-tooth patterns (Figure 6.5 a) revealing unfolding forces of around 190 pN (190(±41) pN, n = 299; Figure 6.5 b). This value is comparable to the already published data of Fn domains of titin (A-band titin: 180 pN, I-band titin: 200 pN(Rief *et al.*, 1998)) and fibronectin (75 – 220 pN (Oberhauser *et al.*, 2002)). A fit of the worm-like chain (WLC) model of polymer elasticity (Bouchiat *et al.*, 1999) to the force extension curve of $(My6)_8$ (Figure 6.5 a), dashed line and dotted lines) shows an increase in contour length of ~26.3 nm per force peak, which is consistent with the length of an unfolded domain calculated as the predicted number of amino acids between the first and last β-sheet (88 aa x 0.3 nm/aa = 26.4 nm).

If the height of each individual force-peak is plotted as a function of its position in the saw-tooth pattern, a hierarchical relationship is observed. There is a tendency for the domains unfolded first to have slightly lower unfolding forces than the subsequent domains, which can be predicted from theoretical studies (Zhang and Evans, 2001). An average increase in force of 7.4 pN (Figure 6.5 c) was determined from one peak to the next, which may result from the decrease in unfolding probability, as more domains are unfolded. Because the AFM tip picks up the molecule at random locations in the polyproteins, the number of peaks observed serves as a count of the number of modules contained in the segment that was picked up. The linker extension of a polyprotein can be determined by fitting the worm-like chain (WLC) model to the initial part of the force-extension curve, before any unfolding is observed (L_0, dashed line; Figure 6.5 a). It depends on the number of modules picked up by the AFM tip and represents the length of the fully stretched chain before any unfolding occurs. A plot of L_0 versus the number of My6 modules shows a slope of 3.7 nm/module, which is close to the predicted linker length (15 aa x 0.3 nm/aa = 4.5 nm; Figure 6.5 d).

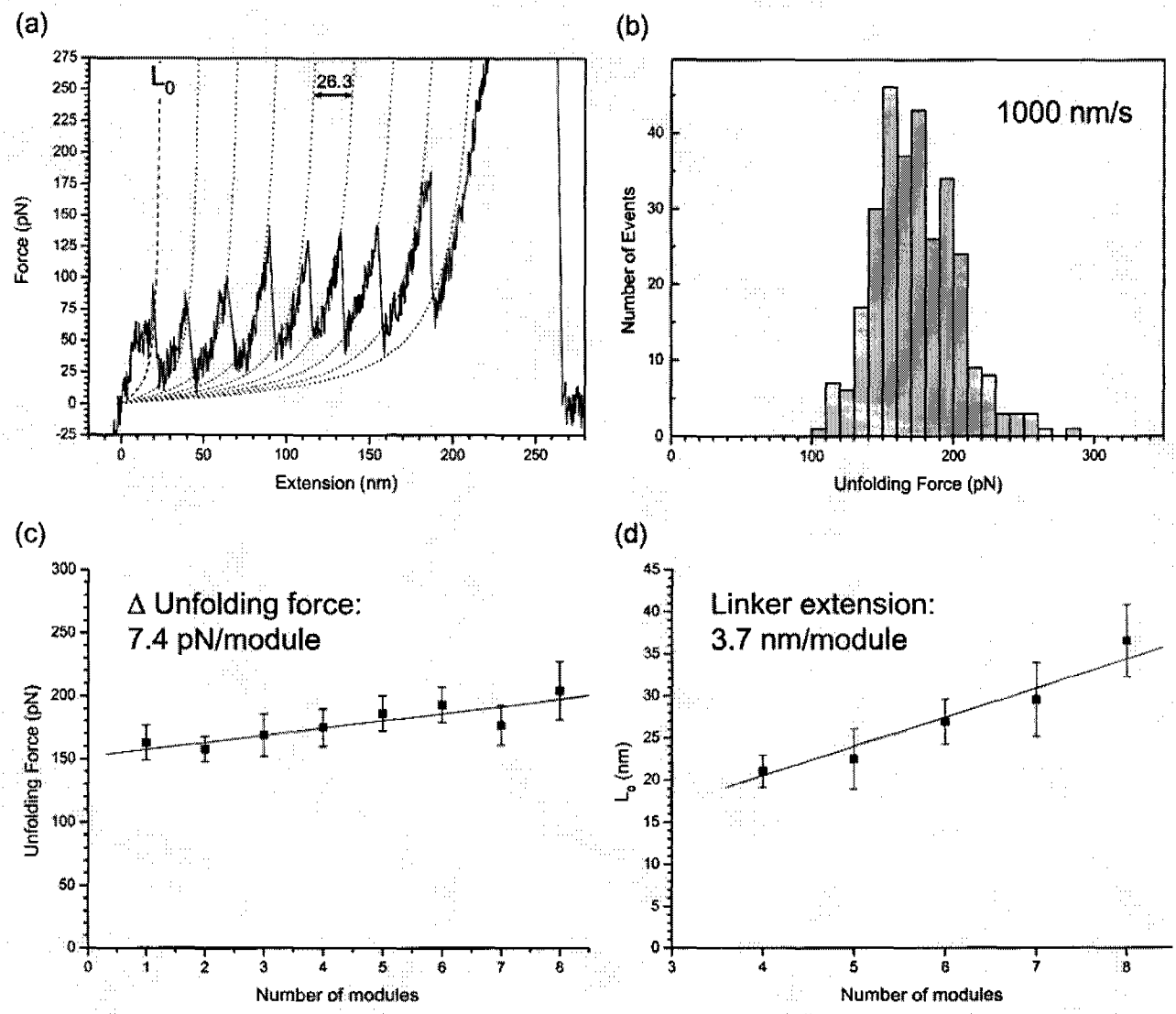

Figure 6.5: *The mechanical properties of myomesin domain My6 (Fn).* (a) Stretching of $(My6)_8$ polyproteins at a pulling speed of 1000 nm/s results in force-extension curves with the typical saw-tooth pattern. The curves show an increase in contour length of 26.3(±1.3) nm per unfolded domain. The dashed line (L_0 = linker extension) and the dotted lines show a fit of the WLC model of polymer elasticity. (b) Probability distribution of the unfolding force of My6 revealing a mean value of 190(±41) pN (n = 299) with a pulling speed of 1000 nm/s. (c) Relationship between the unfolding force and the force-peak position in the saw-tooth pattern obtained from $(My6)_8$ polyproteins. The slope of the line corresponds to an increase of 7.4 pN/peak. (d) The linker extension L_0 also shows a linear dependence on the number of modules picked up by the AFM tip with a slope of 3.7 nm/module. The error bars in (c) and (d) correspond to the standard deviation (Schoenauer et al., 2005).

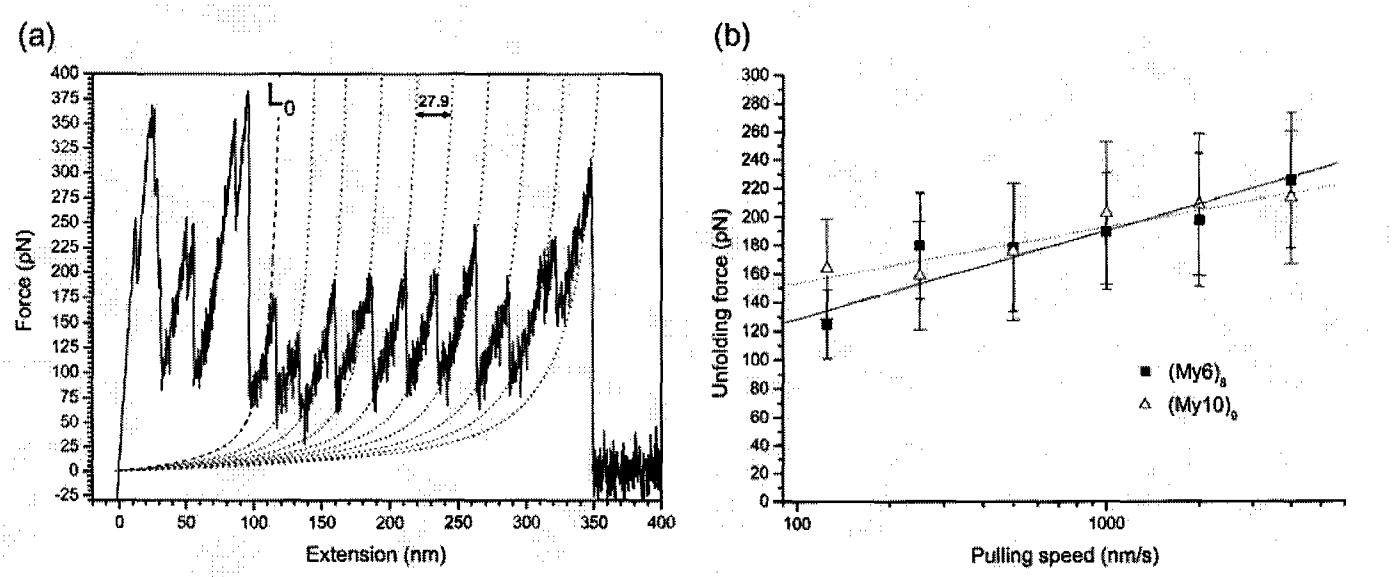

Figure 6.6: *The mechanical stability of myomesin domain My10 (Ig).* (a) Stretching of $(My10)_9$ polyproteins at a pulling speed of 1000 nm/s results in force-extension curves showing a mean unfolding force of 203(±50) pN and an increase in contour length of 27.9(±1.5) nm per unfolded domain. After an initial unspecific interaction possibly due to a second molecule adhering to the tip or due to short range interactions, the individual My10 (Ig) domains are unfolded unit by unit. The dashed line (L_0 = linker extension) and the dotted lines show the fit of the WLC model. (b) Comparison of velocity dependence of the mean unfolding force on the pulling speed for the My6 (Fn, black squares) and My10 (Ig, white triangles) domains of myomesin. The unfolding kinetics of both domains is very similar and shows the typical linear dependence on the logarithm of the pulling speed (lines correspond to linear fit). The error bars correspond to the standard deviation. Pulling speed: 125-4000 nm/s (Schoenauer et al., 2005).

To compare the mechanical characteristics of the Fn and Ig domains of myomesin, we constructed a second homomeric polyprotein consisting of a sequence of 9 Ig domains My10. Figure 6.6 a) shows a force-extension curve obtained from the $(My10)_9$ polyprotein including the fit of the WLC model (dashed line and dotted lines). The average unfolding force of the My10 domain is ~200 pN (203(±50) pN) at a pulling speed of 1000 nm/s. This value is slightly higher compared to the My6 (Fn) domain, but the difference is not significant. The contour length of $(My10)_9$ is higher (~27.9 nm per domain), corresponding to the bigger predicted length of an unfolded My10 domain (95 aa) compared to the My6 domain (88 aa). The initial peaks probably stem from short range unspecific interactions whereas the first peak used for fitting exhibits the right length (L_0, dashed line) for an individual My10 polyprotein being present within the tip and the substrate interface. These measurements suggest that the mechanical stability of domain My10 is rather similar to the Ig segments of the differentially spliced (I65-70) regions of titin but significantly lower than that of the constitutive (I91-98) regions (Watanabe *et al.*, 2002a). Furthermore, the Ig domain I27 of titin shows comparable characteristics (unfolding force ~200 pN, extension of contour length: 28.1 nm/module (89 aa), Carrion-Vazquez *et al.*, 1999a).

6.1.3 The rate dependency of mechanical unfolding

During muscle contraction, the domains of structural muscle proteins such as titin and myomesin may be stretched with a wide range of speeds. Since the mechanical characteristics may not be the same at different pulling speeds, as shown for titin (Rief *et al.*, 1998, Carrion-Vazquez *et al.*, 1999b), we also studied the rate-dependency of the stability of myomesin domains.

Figure 6.6 b) shows the dependence of the unfolding forces of myomesin domains My6 (Fn) and My10 (Ig) on the pulling speed. For both domains, the average unfolding force shows a linear dependency with the logarithm of the pulling speed. With an increase of pulling speed from 125 nm/s to 4000 nm/s, the unfolding force of My6 rises from 125 to 226 pN, whereas My10 shows values from 164 to 214 pN. These data are similar to the already published unfolding forces of titin Ig and Fn domains (Rief *et al.*, 1998). Although the unfolding force of domain My10 shows a slightly weaker dependence on the pulling speed compared to My6, the difference is not significant. For My10, the unfolding kinetics are strikingly similar to the differentially spliced (I65-70) Ig segment of titin (Watanabe *et al.*, 2002a). Furthermore, the

mechanical properties of My6 are comparable to individual Fn domains of fibronectin (Oberhauser *et al.*, 2002).

6.1.4 Myomesin domains can refold after unfolding

Titin Ig domains are believed to fold spontaneously (Politou *et al.*, 1995) and it is speculated that reversible folding may play a physiological role under overstretch conditions (Soteriou *et al.*, 1993). In order to test if myomesin domains also are able to refold after mechanical unfolding, we used a two-pulse stretching protocol to repeatedly stretch and relax the $(My6)_8$ and $(My10)_9$ polyproteins while limiting the total extension of the molecule to prevent its detachment from the AFM tip. Subsequent extension traces of the same molecule were recorded and after each extension, the polyprotein was allowed to relax completely and remained attached to the AFM tip (up to 20 cycles). After a variable relaxing time (1.5, 5 or 10 seconds) the protein was stretched again and the number of force peaks was counted. The number of extended domains was typically less than the maximum since the polyprotein is picked at a random length and the total extension of the protein is limited by detachment. Statistical analysis for the My6 (Fn) domain shows a refolding rate of 74 % (1.5 s relaxing time), 85 % (5 s) and 100 % (10 s), which is comparable to the Fn domains of fibronectin (Oberhauser *et al.*, 2002). These data reveal that most of the unfolded My6 domains refold spontaneously upon relaxation and that the refolding rate is dependent on the relaxing time. For illustration, 24 unfolding traces of the unfolding-refolding cycles and three complete unfolding and refolding cycles obtained when stretching a $(My6)_8$ protein (1.5 s relaxing time) can be seen in Figure 6.7 a) and b), respectively. The force curves in these plots are shifted vertically for clarity, so they do not share a common zero force level. In addition, domain My10 (Ig) also has the ability to refold after mechanical unfolding with a refolding rate of ~50 % (relaxing time: 1.5 s). These results show that a big fraction of myomesin domains refolds in less than 1.5 seconds if the protein is fully relaxed. The observation that myomesin domains can be unfolded in a reversible manner raises the possibility that this mechanism is of physiological importance in case of extremely high or extremely long lasting stretching forces.

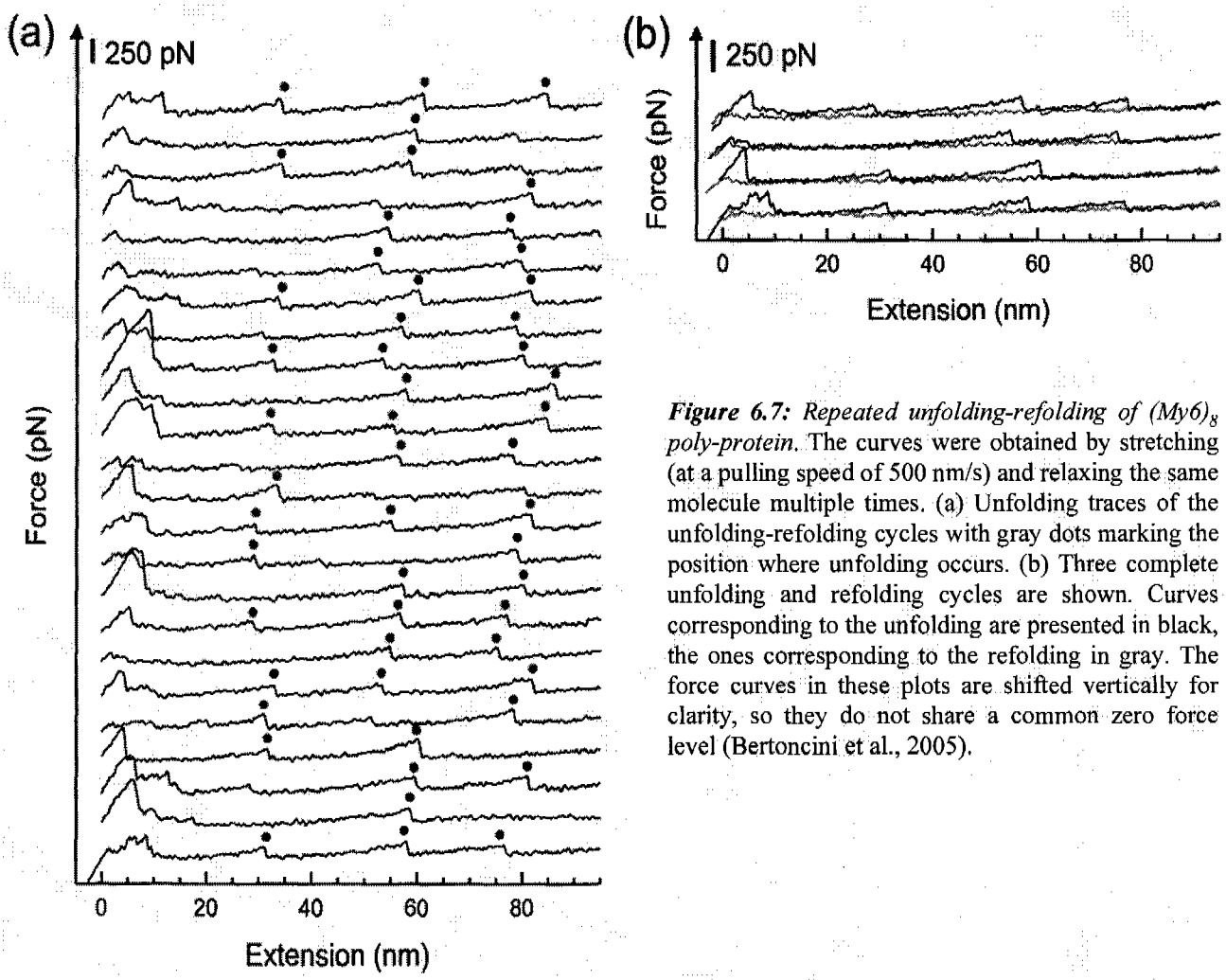

Figure 6.7: *Repeated unfolding-refolding of* $(My6)_8$ *poly-protein.* The curves were obtained by stretching (at a pulling speed of 500 nm/s) and relaxing the same molecule multiple times. (a) Unfolding traces of the unfolding-refolding cycles with gray dots marking the position where unfolding occurs. (b) Three complete unfolding and refolding cycles are shown. Curves corresponding to the unfolding are presented in black, the ones corresponding to the refolding in gray. The force curves in these plots are shifted vertically for clarity, so they do not share a common zero force level (Bertoncini et al., 2005).

6.1.5 Mechanical properties of the EH-segment

We further used the AFM technique to investigate the mechanical properties of the EH-segment of myomesin. Although it seems obvious to engineer a poly-EH protein for single-molecule AFM, stretching a random coil would give a featureless force-extension curve that would be difficult to distinguish from that observed for a denatured protein fragment. Hence, we used the My6 module, whose molecular "fingerprint" was identified in the previous experiment, as an easily recognizable marker for the construct. Figure 6.8 a) shows several force-extension curves for the $(My6\text{-}EH)_4$ polyprotein at a pulling speed of 500 nm/s. The characteristic fingerprint of the integrated My6 module shows that it unfolds at around 180 pN, extending the contour length of the protein by 26.3 nm. Four types of recordings are shown with one (curve 1), two (curves 2 and 4), three (curve 3), and four (curve 5) My6 unfolding events, excluding the last peak (detachment of the molecule from the AFM tip).
In contrast to the My6 polyproteins, the stretching of a $(My6\text{-}EH)_4$ polyprotein produces a saw-tooth pattern only after an initial spacer L0, ranging from ~20 nm to ~120 nm, corresponding to the stretching of one (curve 1), two (curves 2 and 3), or three (curves 4 and 5) EH-segments. Because the polyprotein is constructed of alternating My6 and EH domains, if four (three) My6 unfolding peaks are observed, at least three (two) EH-segments must have been stretched. If we observe two My6 unfolding peaks, at least one EH-segment has been extended. In this way we can be sure that the EH-segments are stretched and that the mechanical properties of EH are represented by the initial part of the force-extension curves, revealing its elastic properties. In Figure 6.8 b) a frequency histogram of the initial length L_0 is shown. It shows three distinct peaks centered at about 39 nm, 71 nm and 105 nm. Hence, the length distribution can be explained by assuming that the initial length L_0 occurs as approximately integer multiples of about 35 nm. This is consistent with the predicted contour length (L_C) of the human EH-segment (plus linkers), which is 34.8 nm (116 aa x 0.3 nm/aa). These results suggest that the elastic properties of the initial plateau in the force-extension curves (Figure 6.8 a) correspond to the extension of EH-segments of the $(My6\text{-}EH)_4$ polyprotein. The persistence length of this segment was calculated by the WLC model of polymer elasticity (Figure 6.8 a), dotted lines), which describes the nonlinear increase in force quite accurately. A histogram of calculated persistence lengths (Figure 6.8 (c)) shows a distribution from ~0.1 nm to ~0.6 nm with a clear peak at ~0.3 nm, which is comparable to the length of one amino acid. This result indicates that the EH-segment behaves like a fully

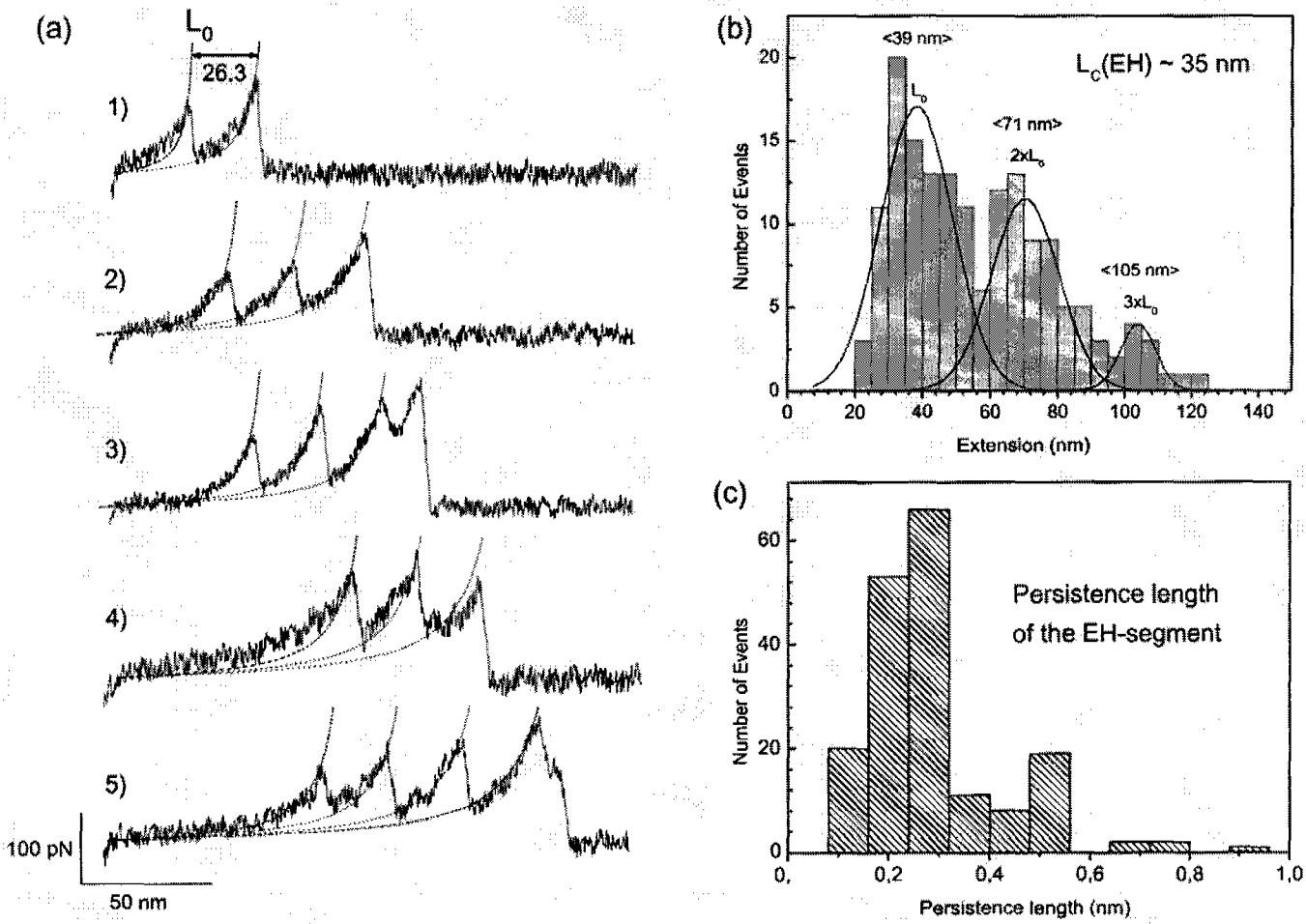

Figure 6.8: *The EH-segment of myomesin has elastic properties.* (a) Stretching a (My6-EH)4 polyprotein with the AFM produces a saw-tooth pattern only after an initial spacer (~20–120 nm), illustrating the elasticity contributed by the EH-domain. The saw-tooth peaks are typical for the My6 domain unfolding because they occur at around 180 pN, extend by about 26.3 nm and the recordings show one (curve 1), two (curves 2 and 4), three (curve 3), and four (curve 5) My6 unfolding events. Three discrete values of L_0 can be measured, which result from stretching one (curve 1), two (curves 2 and 3) or three (curves 4 and 5) EH-segments before any My6 unfolding occurs. Pulling speed: 500 nm/s. (b) Statistical analysis of the elasticity measurements of the EH-segment. A frequency histogram of the initial length L_0 shows three clearly separated peaks at 39, 71, and 105 nm. This length distribution can be explained by assuming that the initial length L_0 occurs as integer multiples of about 35 nm, i.e. the contour length (L_c) of the EH-segment. (c) Histogram of the persistence length distribution of the EH-domain extracted from measurements on single $(My6\text{-}EH)_4$ polyproteins showing a clear peak at ~0.3 nm (Schoenauer et al., 2005).

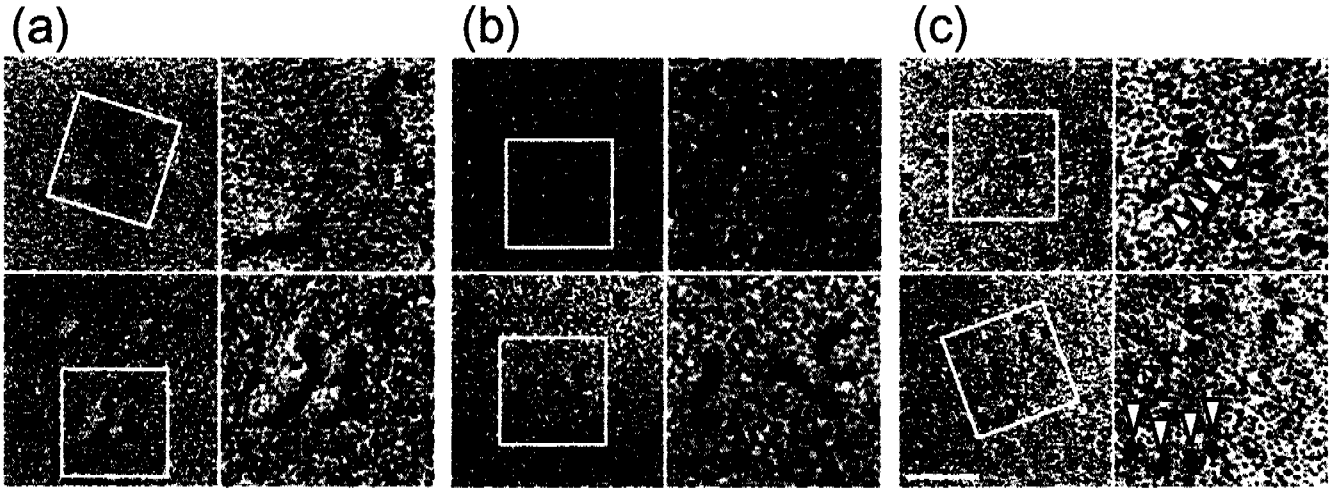

Figure 6.9: *TEM images of individual myomesin polyproteins.* $(My10)_9$ (a), $(My6)_8$ (b), and $(My6\text{-}EH)_4$ (c) molecules as seen after glycerol spraying/rotary metal shadowing. The right panels in (a), (b) and (c) represent 2-fold magnifications of the squares framed in the left panels. The $(My10)_9$ and $(My6)_8$ polyproteins are visible as randomly bent rod-like structures. The $(My10)_9$ molecules appear longer and slightly less compact than the $(My6)_8$ ones, which can be explained by the higher number of modules and by the longer linker length in the $(My10)_9$ polyprotein (35 aa) compared to $(My6)_8$ (15 aa). In contrast, rotary metal-shadowed images of the $(My6\text{-}EH)_4$ construct reveal the My6 modules as four small globules (arrowheads), evidently connected by an 'invisible thread' (i.e. the EH-segment). The scale bar represents 20 nm and applies to the left panels of (a), (b) and (c) (Schoenauer et al., 2005).

unfolded polypeptide chain and might act as an entropic spring similar to the PEVK domain of titin.

6.1.6 The EH-segment appears less compact as the Fn domains in molecules visualized in transmission electron microscopy (TEM)

The molecular anatomy of recombinant myomesin constructs was visualized by TEM to confirm the non-folded conformation of the EH-segment by glycerol spraying/rotary shadowing of myomesin polyproteins (Figure 6.9). Both, $(My10)_9$ (Figure 6.9 a) and $(My6)_8$ (Figure 6.9 b) polyproteins appear as randomly bent rod-like structures. In contrast, the micrographs of the $(My6\text{-}EH)_4$ polyproteins (Figure 6.9 c) show groups of 4 evenly spaced globular domains, evidently linked by an 'invisible thread'. Some molecules seem to be fragmented and contain fewer than 4 beads. We interpret these results as evidence of four tightly folded My6 domains giving rise to the bead-like structures separated by three EH-segments, which are not visible after rotary shadowing. Considering that the Fn domains are connected by 116 aa comprising the EH-segment and the linkers, this region has a contour length of 34.8 nm (0.3 nm/aa x 116 aa). However, the observed end-to-end length of the EH-domain is much smaller than its contour length, suggesting that this region is coiled in the relaxed state. The invisibility of the EH-segment in EM micrographs indicates that it forms a much less compact structure than the folded My6 domain and cannot be visualized by rotary shadowing. The difference between the appearance of My6 or My10 and the My6-EH polyproteins supports the view that the EH-region is largely a non-folded polypeptide also in the native state.

6.1.7 CD-spectrum of recombinant human EH-segment reveals the absence of a defined secondary structure

In order to further clarify the structural properties of the alternatively spliced EH-segment of human myomesin, we measured the CD-spectrum of this domain (Figure 6.10). The spectrum contains one strong minimum at 199 nm and a negative shoulder at ~215 nm, which corresponds to a mostly non-folded protein chain with residual secondary structure (Ma and Wang, 2003). This result strongly supports the hypothesis, based on computer predictions

(PONDR) and the experiments described above, that the EH-segment has no defined secondary structure and is present in a mostly non-folded state at physiological condition. In contrast, CD spectroscopy measurements of the full-length myomesin molecule lacking the EH-segment (Obermann *et al.*, 1995) show a beta-sheet spectrum typical for Ig domains (minimum at ~210 nm), which can be explained by the dominant presence of this type of secondary structure in the whole protein.

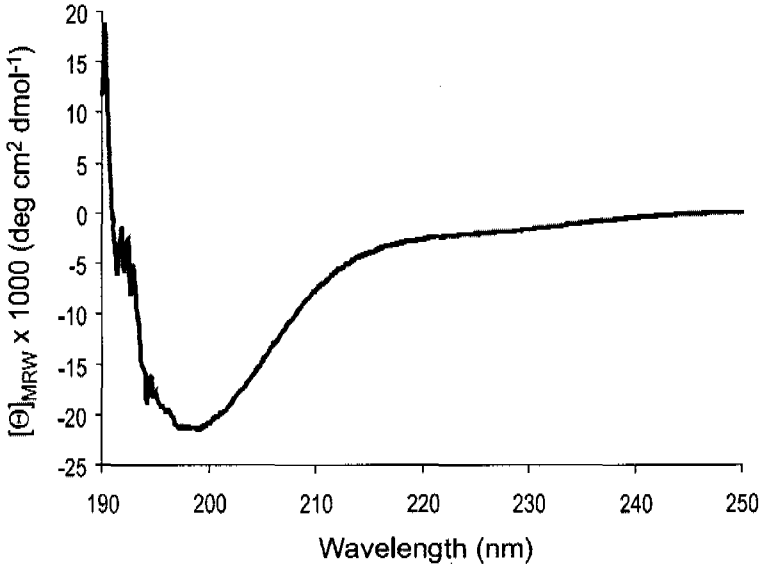

Figure 6.10: *Circular dichroism spectrum of the human EH-segment.* Note the strong minimum at 199 nm and a negative shoulder at ~215 nm, which corresponds to a mostly unstructured protein with no defined secondary structure. ($[\Theta]_{MRW}$) is the mean molar ellipticity (Schoenauer *et al.*, 2005).

6.2 The molecular composition of the sarcomeric M-band correlates with muscle fiber type

6.2.1 Introduction

Striated muscle consists of repeating structural units, the sarcomeres. Despite a lot of effort, the detailed ultrastructure of a sarcomere is still unclear, especially with respect to the molecular organization of the sarcomeric M-band. In electron microscopic images the M-band appears as a series of dark transversal lines in the center of the A-band, where no myosin crossbridges are present (Sjostrom and Squire, 1977). On cross sections of this zone, thin lines, called M-bridges, seem to connect adjacent thick filaments to form a regular hexagonal lattice. It has been suggested that the M-band appearance in electron microscopic preparations correlates with the physiological performance of a particular muscle type (Pask *et al.*, 1994) and can change during development (Carlsson and Thornell, 1987), but the molecular basis for this has not been elucidated yet. The proposed active role of the M-band during contraction (Agarkova *et al.*, 2003) implies that its mechanical properties, probably regulated by diverse molecular compositions, should depend on the myosin isoform content, which determines the contractile characteristics in a given muscle type (Hilber and Galler, 1997, Pette and Staron, 2000).

Only few structural components of the M-band have been identified so far. These are the C-terminal part of titin (Labeit and Kolmerer, 1995), myomesin (Eppenberger *et al.*, 1981, Grove *et al.*, 1984) and M-protein (Masaki and Takaiti, 1974). According to its general role as a sarcomeric template (Trinick, 1996) the M-band portion of titin might define the positions of the bridges that connect the myosin filaments transversally, with myomesin and M-protein playing the role of these bridges (Obermann *et al.*, 1996, Lange *et al.*, 2005b). Despite their strong similarity, these two proteins display different expression patterns. While myomesin was found in all striated muscle types, M-protein is absent from early embryonic heart and adult slow muscle (Carlsson *et al.*, 1990, Grove *et al.*, 1989). Moreover, myomesin localizes to the M-band already in the first nascent sarcomeres in embryonic heart (Ehler *et al.*, 1999) and can be detected in striated muscles of all vertebrates (Agarkova *et al.*, 2000). This suggests that myomesin is an essential sarcomeric component, controlling the assembly and maintenance of the A-band structure, whereas M-protein may increase the stability of the thick filament lattice in some kinds of muscles (Pask *et al.*, 1994).

According to the current M-band model the N-terminus of myomesin is involved in the interactions with titin and myosin (Obermann *et al.*, 1997), whereas the C-terminus (domain 13) can dimerize in an antiparallel manner (Lange *et al.*, 2005b). Interestingly, in the central part of the molecule an alternative splicing event can take place (Agarkova *et al.*, 2000, Steiner *et al.*, 1999). The insertion of an additional fragment between domains 6 and 7 of conventional myomesin leads to the EH-myomesin isoform (Fig. 1b), which was found in the embryonic heart of all higher vertebrates (Agarkova *et al.*, 2000). This myomesin isoform was previously characterized in mouse as a distinct M-band component, called "skelemin" (Price, 1987, Price and Gomer, 1993).

A study on the expression pattern of myomesin isoforms in chicken failed to detect EH-myomesin in breast muscle of any stage (Agarkova *et al.*, 2000). However, its mouse counterpart was initially cloned from adult mouse skeletal muscle (Price and Gomer, 1993). In addition, low amounts of the EH-myomesin transcript were detected by Northern blot analysis of murine skeletal muscle (Steiner *et al.*, 1999). This suggests that this isoform may be expressed in some special types of skeletal muscle. To address this question and to estimate the general significance of the EH-myomesin isoform for the M-band structure, we investigated its expression in different muscles of adult mouse.

6.2.2 Characterization of antibodies against EH-myomesin

In a previous study on myomesin isoform expression an antibody generated against the chicken EH-fragment of myomesin was employed. Unfortunately the sequence of this fragment is highly divergent between species, so this antibody reacts only weakly with mammalian muscle extracts (Agarkova *et al.*, 2000). In addition, an antibody against the human EH-fragment does not react with the mouse protein (Agarkova, I.; unpublished results). Consequently, to study the expression of EH-myomesin in mouse, it was necessary to generate an antibody against the mouse EH-fragment.

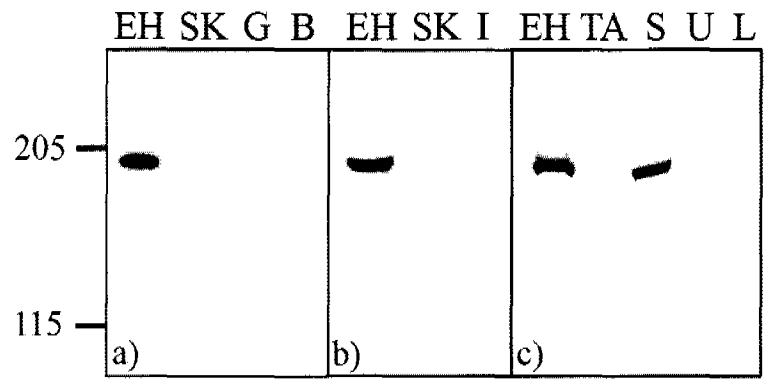

Figure 6.11: *Specificity of polyclonal rabbit antibodies directed against the EH-fragment of different species.* Antibodies specific for chicken (a, (Agarkova, 2000)), human (b, Agarkova, I., unpublished) and mouse (c, (Schoenauer, 2002)) EH-myomesin were tested on SDS-samples of different tissues of the corresponding species. Lane EH: embryonic heart (chicken: HH stage 45, human: 17 weeks, mouse: E16.5 pc, lane SK: skeletal muscle, lane G: gizzard, lane B: brain, lane I: intestine, lane TA: m. tibialis anterior, lane S: m. soleus, lane U: uterus, lane L: liver. Molecular weight markers are indicated in kDa. The anti-EH antibodies recognize a band of about 190 kDa in the embryonic heart extracts of all three species, which corresponds well with the expected size. In addition, a strong signal of EH-myomesin can be detected in mouse soleus (S), whereas skeletal muscle of chicken, human and tibialis anterior (fast muscle) of mouse do not express this isoform in significant amounts. No signal is detected in smooth muscle (gizzard, intestine and uterus) as well as in non-muscle tissue.

In Figure 6.11, polyclonal rabbit antisera generated by using the EH-fragment of chicken (a), human (b) and mouse (c) EH-myomesin were tested on different tissues of the corresponding species (a: chicken, b: human, c: mouse) by western blot analysis. All three antibodies recognize a band of about 190 kDa in the embryonic heart extracts (EH), which corresponds well to the expected size. Surprisingly, a strong signal of EH-myomesin can be detected in mouse soleus (S) as well, whereas skeletal muscle of chicken, human and tibialis anterior (fast skeletal muscle) of mouse do not express this isoform in measurable amounts. No signal is detected in smooth muscle (gizzard, intestine and uterus) as well as in non-muscle tissue. Consequently, EH-myomesin is expressed in the embryonic heart of all tested vertebrates and can be used as a marker for this tissue (Agarkova *et al.*, 2000). Because the sequence of the EH-fragment is not strongly conserved, the antibodies show no cross-reaction between the different species with the exception of the mouse antibody, which also reacts with rat EH-myomesin (data not shown, see (Schoenauer, 2002)).

6.2.3 The EH-myomesin isoform is expressed in slow muscle of adult mouse

After the specific reaction has been confirmed, the isoform-specific polyclonal antibody (anti-moEH) as well as an antibody directed against the first domain of myomesin (My-N), which recognizes both myomesin isoform, were applied in immunoblot analysis of different muscles of adult mouse (Figure 6.12). Previously it was shown that the EH-myomesin isoform appears in the embryonic heart of all higher vertebrates (Agarkova *et al.*, 2000). Therefore, mouse embryonic heart extract from day 16.5 p.c. was used as a positive control for the generated anti-moEH antibody (Figure 6.12, lane EH). Liver extract (lane L) was used as a negative control. The general myomesin antibody My-N detects myomesin in all tested muscle extracts (Figure 6.12, panel My-N), but not in the non-muscle extract (lane L). As expected, an additional band of higher molecular weight, corresponding to the EH-myomesin isoform, appears in the extract of embryonic heart (Figure 6.12, lane EH). The specificity of the generated anti-moEH antibody is confirmed by the strong reaction with the same band (Figure 6.12, lane EH) and by the absence of reactivity with the non-muscle extract (Figure 6.12, lane L). Surprisingly, the general myomesin antibody recognizes a band of higher molecular weight also in the extracts of soleus and extraocular muscle (EOM) of adult mouse (Figure 6.12, lanes S and EOM). This band corresponds to the EH-myomesin isoform, too, as indicated by the strong reactivity with the anti-moEH antibody. Interestingly, the proportion of EH-myomesin isoform in the extraocular muscle is extremely high and amounts to about 70% of total myomesin, which exceeds even its proportion in the embryonic heart (compare lanes EOM with EH). A small amount of the EH-myomesin isoform is detected also in adult heart and a subset of skeletal muscles, namely diaphragm, m. plantaris and m. gracilis (Figure 6.12, lanes AH, D, P and G). Interestingly, all these muscles are known to contain a significant number of slow-type fibers (Pette and Staron, 1990). This experiment confirmed that the anti-moEH antibody reacts specifically with the EH-myomesin isoform of mouse and indicated that EH-myomesin is expressed in the slow and extraocular muscles of adult mouse. Furthermore, it reacts specifically with rat muscle tissues (heart, soleus) as well, indicating that there might be species specific differences in the level of EH-myomesin expression (Agarkova *et al.*, 2004).

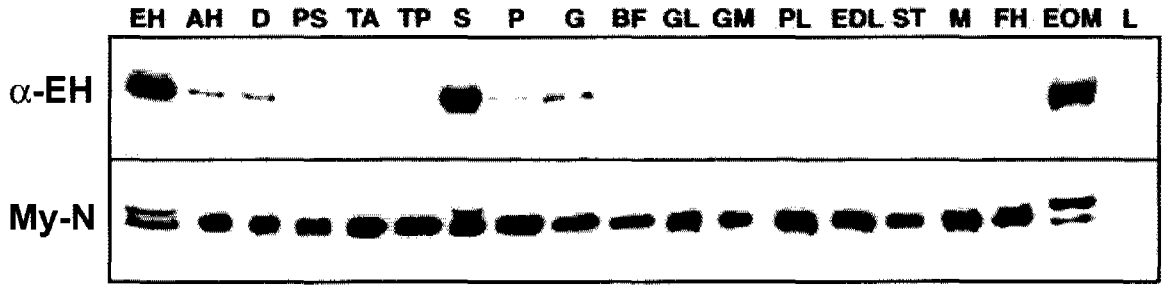

Figure 6.12: *The EH-myomesin isoform is expressed in slow muscle of adult mouse.* Extracts of embryonic heart, liver and different skeletal muscles of adult mouse were probed by immunoblot with the anti-moEH antibody (α-EH) and with an antibody My-N that recognizes all myomesin isoforms (My-N)). Lane EH: embryonic heart E16.5, lane AH: adult heart, lane D: diaphragm, lane PS: m. psoas, lane TA: m. tibialis anterior, lane TP: m. tibialis posterior, lane S: m. soleus, lane P: m. plantaris, lane G: m. gracilis, lane BF: m. bizeps femoris, lane GL: m. gastrocnemius lateralis, lane GM: m. gastrocnemius medialis, lane PL: m. peroneus longus, lane EDL: m. extensor digitorum longus, lane ST: m. semitendinosus, lane M: m. membranosus, lane FH: m. flexor hallucis, lane EOM: extraocular muscles and lane L: liver. The general myomesin antibody My-N detects myomesin in all tested muscle extracts (My-N), but not in the liver extract (lane L). An additional band of higher molecular weight appears in the extracts of embryonic heart, soleus and extraocular muscles of adult mouse (lanes EH, S and EOM). This band corresponds to the EH-myomesin isoform, as proved by the strong reactivity with the anti-moEH antibody (α-EH). A small amount of the EH-myomesin isoform is detected also in adult heart, and in some skeletal muscles, namely diaphragm, plantaris and gracilis, muscles known to contain a lot of slow fibers. The anti-moEH antibody does not react with extracts of muscles, containing only fast fibers or with non-muscle extract (lane L) (Agarkova *et al.*, 2004).

6.2.4 EH-myomesin is expressed in all type I and part of the type IIA fibers of the mouse hind limb

To compare the expression pattern of EH-myomesin with the myosin heavy chain isoform content in a given muscle fiber, we performed an immunofluorescence analysis of mouse hind limb muscles (Figure 6.13). For this and all following stainings tissue samples from 5-week-old mice were used. On one hand, the relatively small size of the hind limb at this age favors the analysis with confocal microscopy; on the other hand, the adult pattern of MHC isoform expression as well as of the M-band composition is already established in the hind limb muscles at this stage (Allen and Leinwand, 2001, Agarkova *et al.*, 2004). First, we stained hind limb cryosections with the anti-moEH antibody (Figure 6.13 d, blue in a) in combination with antibodies directed against the MHC-I/β (A4.840; Figure 6.13 b, green in a) and MHC-IIa (A4.74; Figure 6.13 c, red in a) isoforms. At this age, MHC-I/β is strongly expressed in the majority of the soleus fibers, but it is rare in most other muscles of the hind limb (Figure 6.13 b). MHC-IIa is expressed in the MHC-I/β-negative fibers of soleus and in some fibers of the neighboring gastrocnemius muscle (Figure 6.13 c). Coexpression of the MHC-I/β and MHC-IIa isoforms is not observed in any fiber (compare Figure 6.13 b with c). A high

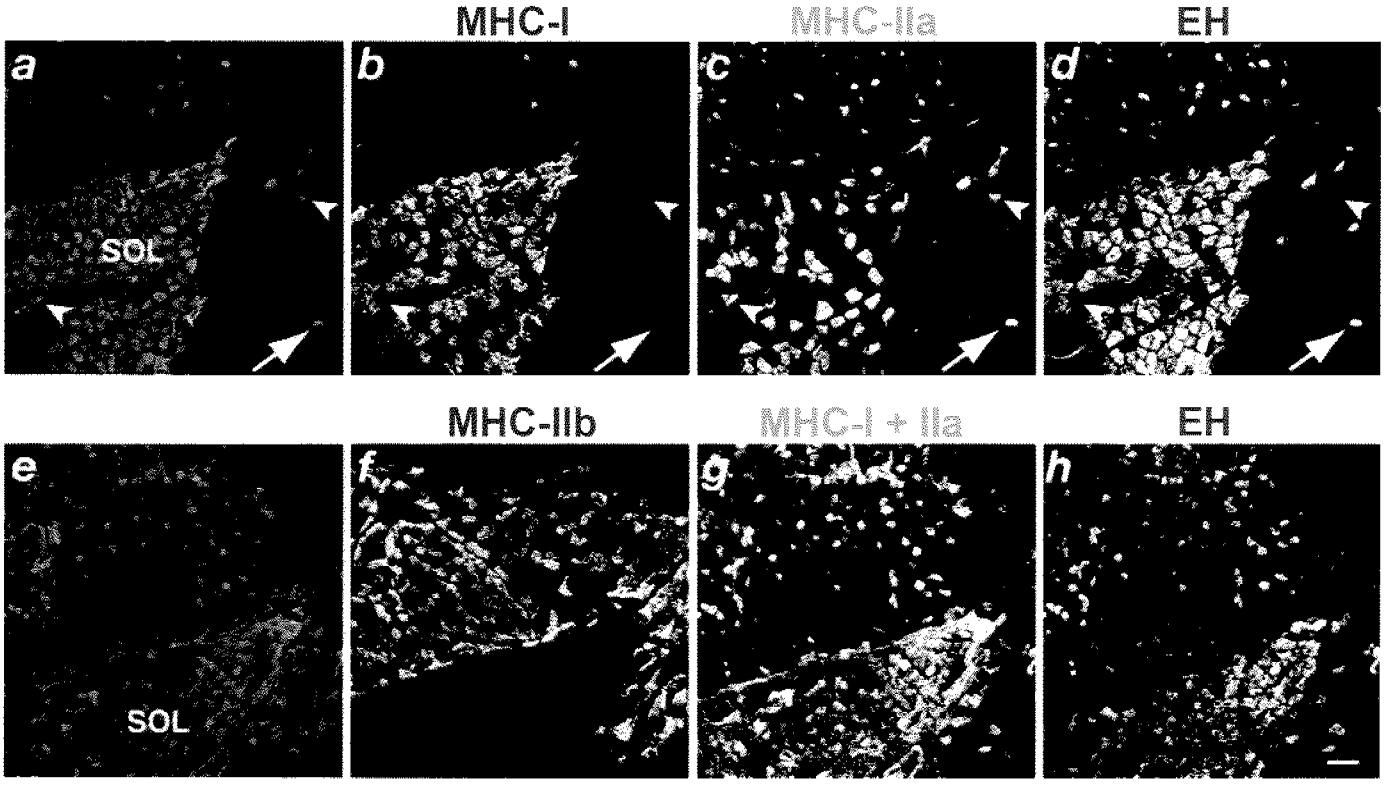

Figure 6.13: *EH-myomesin is expressed in all MHC-I/β and part of the MHC-IIa fibers of mouse hind limb.* Confocal images of hind limb cryosections of five-week-old mouse triple stained with the anti-moEH antibody and antibodies directed against different MHC isoforms. The position of the soleus is marked (SOL). Bar: 100 μm. The first section (upper panel) is stained with the anti-moEH antibody (d, blue in a) in combination with antibodies directed against MHC-I/β (b, green in a; A4.840) and MHC-IIa (c, red in a; A4.74). No co-expression of MHC-I and MHC-IIa isoforms can be detected in any fiber. The expression of EH-myomesin is detected in all fibers expressing the slow MHC-I/β isoform (compare b with d). EH-myomesin also appears in a subset of fibers expressing the fast MHC-IIa isoform (arrows), while a significant number of MHC-IIa-positive fibers both inside and outside the soleus are certainly negative for EH-myomesin (arrowheads). The second section (lower panel) is stained with the anti-moEH antibody (h, blue in e) in combination with antibodies directed against MHC-IIb (f, green in e; BF-F3) and both types I/β and IIa MHC (g, red in e; NCL-MHCs and A4.74). No EH-myomesin can be detected in any fiber expressing the fast MHC-IIb myosin isoform (compare f and h). Further, EH-myomesin is practically absent from fibers, which are not stained with any of the antibodies directed against type I, IIa and IIb MHC. Therefore the "pure" MHC IId fibers in the section are EH-myomesin negative as well (Agarkova et al., 2004).

expression of EH-myomesin can be detected in all MHC-I/β-positive fibers (compare Figure 6.13 d with b), but also in a big part of the fibers expressing MHC-IIa (upper panel, arrows). However, a significant number of type IIa fibers inside and outside the soleus lack EH-myomesin (upper panel, arrowheads). To further analyze a correlation between the EH-myomesin and myosin heavy chain isoform expression, hind limb cryosections were stained with the anti-moEH antibody (Figure 6.13 h, blue in e) in combination with antibodies directed against MHC-IIb (BF-F3; Figure 6.13 f, green in e) and a mixture of antibodies directed against MHC-I/β and MHC-IIa isoforms (mixture of NCL-MHCs and A4.74; Figure 6.13 g, red in e). There are currently no antibodies available that specifically recognize the MHC-IId isoform, but previous studies used this exclusion method for the detection of "pure" IId fibers in sections (Allen and Leinwand, 2001). The MHC-IIb isoform is hardly detectable in the soleus, but is strongly expressed in most fibers of fast muscles (Figure 6.13 f). MHC-IIb is not expressed in fibers with high levels of either MHC-I/β or MHC-IIa (compare Figure 6.13 f with g). This is consistent with the observation that hybrid fibers of types IIb/ IIa or IIb/I are not common in adult mammalian skeletal muscle (Pette and Staron, 2000). EH-myomesin is not detected in any fiber expressing the fast MHC-IIb myosin isoform (compare Figure 6.13 h with f) and is practically absent from fibers, which are not stained with any of the antibodies directed against MHC-I/β, -IIa and -IIb (Figure 6.13 e). Therefore the expression of EH-myomesin is restricted to MHC-I and part of MHC-IIa fibers of the adult mouse hind limb.

6.2.5 Comparision of EH-myomesin and M-protein expression pattern

To study the differences in M-band composition in respect to fiber type, hind limb cryosections were stained with antibodies directed against different M-band components. First, we compared the expression pattern of EH-myomesin and M-protein (Figure 6.14, upper panels). Mouse hind limb cryosections were stained with the anti-moEH antibody (Figure 6.14 b, green in a) in combination with the general myomesin antibody (mAb B4; Figure 6.14 c, red in a) and an antibody directed against M-protein (AA259; Figure 6.14 d, blue in a). The general myomesin antibody evenly stains all fibers in a section (Figure 6.14 c), whereas EH-myomesin and M-protein show a complementary expression pattern (compare Figre 6.14 b with d). EH-myomesin is expressed mainly in soleus, whereas M-protein appears predominantly in all neighboring muscles. However, the exclusive expression of either M-

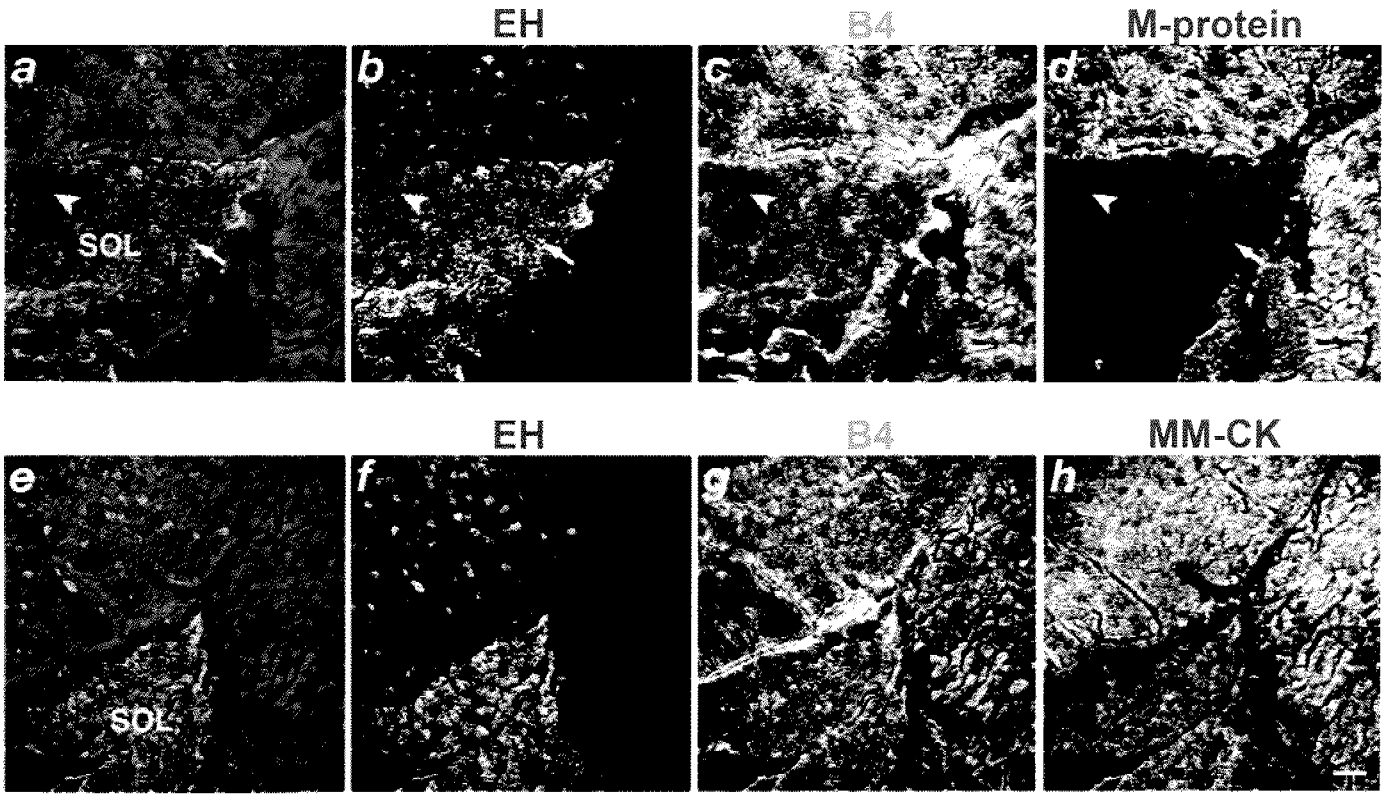

Figure 6.14: *EH-myomesin and M-protein show a complementary expression pattern.* Confocal images of hind limb cryosections of five-week old mouse triple stained with antibodies directed against different M-band components. The position of the soleus is marked (SOL). Bar, 100 μm. The first section (upper panel) is stained with the anti-moEH antibody (b, green in a) in combination with the general myomesin antibody (c, red in a; B4) and an antibody directed against M-protein (d, blue in a; AA259). The general myomesin antibody stains all fibers in a section (c), whereas the EH-myomesin and Mprotein are expressed in an exclusive manner, e.g. each fiber in a section being stained either with the anti-EH-antibody or with the anti-M-protein antibody (compare b with d). Exceptions are only observed in a few fibers, with some fibers showing a weak expression of both EH-myomesin and M-protein (arrowhead), whereas others seem to contain both components, although the level of the co-expressed counter player is rather low (arrow). The second section (lower panel) is stained with the anti-moEH antibody (f, green in e; Alexa488-anti-moEH) in combination with the general myomesin antibody (g, red in e; B4) and an antibody directed against the MM-creatine kinase (h, blue in e; anti-MM-CK). Both myomesin (g) and MM-creatine-kinase (h) are evenly expressed in all fiber types, whereas the EH-myomesin (d) is restricted to slow fibers in the mouse hind limb (Agarkova et al., 2004).

protein or EH-myomesin, although valid for the majority of fibers, is not true for every fiber in a section. Two kinds of exceptions occur. There are some fibers, which are negative for EH-myomesin, but express very little of M-protein (Figure 6.14, upper panel, arrowheads). On the other side, by careful analysis of the image one can find fibers, that strongly express EH-myomesin, but are weakly stained with the anti-M-protein antibody as well (Figure 6.14, upper panel, arrows). Thus, although counter players in general, the two M-band components can be both absent or coexpressed in small amounts at least at the level of the myofiber. Subsequently, we compared the expression pattern of the EH-myomesin isoform and the muscle isoform of creatine kinase (MM-CK), a metabolic enzyme, a small part of which localizes to the M-band in the sarcomere (Stolz *et al.*, 1998)(Figure 6.14, lower panels). For this purpose, hind limb cryosections were stained with the anti-moEH antibody (Alexa488-anti-moEH; Figure 6.14 f, green in e) in combination with the general myomesin antibody (B4; Figure 6.14 g, red in e) and an antibody directed against MM-creatine kinase (anti-MM-CK; Figure 6.14 h, blue in e). Whereas EH-myomesin (Figure 6.14 f) is restricted to the soleus muscle and to some fibers of the neighboring plantaris muscle, the MM-CK is expressed in all hind limb muscles of adult mouse (Figure 6.14 h). However, this immunofluorescence staining is not quantitative and cannot rule out the possibility that the level of MM-CK expression varies slightly between different fibers of the mouse hind limb.

6.2.6 Protein composition of the M-bands gradually changes during the first weeks of postnatal development

To investigate how the expression of EH-myomesin changes in the course of development we probed extracts of the entire hind limb and of the soleus muscle of different developmental stages with the anti-moEH antibody (Figure 6.15, panel EH) and with an antibody that recognizes all myomesin isoforms (Figure 6.15, panel My-N). To achieve the maximal sensitivity in the detection of myomesin isoforms all protein extracts were normalized to an equal amount of MHC, as judged by Coomassie Blue staining of a twin gel. Under these conditions nearly equal amounts of myomesin are expressed at all developmental stages as detected by the general myomesin antibody (Figure 6.15, panel My-N). In contrast, the EH-myomesin isoform is absent from the hind limb muscles of embryonic and neonatal mouse (Figure Ta, panel EH, lanes E14.5, P0 and P4). A weak signal of EH-myomesin appears in the hind limb extract only at day 10 after birth (Figure 6.15, panel EH, lane P10). The EH-

myomesin isoform seems to be upregulated very quickly after this time point and a nearly maximal expression level is detected in the soleus muscle at postnatal day 20 (Figure 6.15, panel EH, lane P20). In agreement with this, the incubation with the general myomesin antibody (Figure 6.15, panel My-N, line P20) shows a second band of higher molecular weight in the extract of this developmental stage. The maximal content of EH-myomesin in the soleus amounts to about 30% of total myomesin, as estimated by the comparison of the two bands, corresponding to the EH-positive and EH-negative isoform. Nearly the same expression level of EH-myomesin is detected at postnatal day 50 (Figure 6.15, line P50, panel EH). Thus, we conclude that EH-myomesin is absent from the embryonic and neonatal hind limb muscle and is up-regulated after birth, during the postnatal maturation of slow muscle fibers.

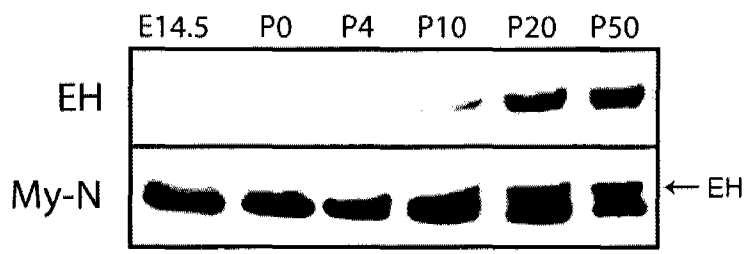

Figure 6.15: *The EH-myomesin isoform appears in the soleus muscle during the first weeks of postnatal development.* Immunoblots of entire hindlimb extracts and soleus muscle extracts of different developmental stages probed with anti-moEH antibody (panel EH) and with an antibody My-N that recognizes all myomesin isoforms (panel My-N). Lane E14.5: embryonic mouse E14.5 hindlimb, lane P0: newborn mouse hindlimb, lane P4: postnatal day 4 mouse hindlimb, lane P10: postnatal day 10 mouse hindlimb, P20: postnatal day 20 mouse soleus muscle, P50: postnatal day 50 mouse soleus muscle. To achieve the maximal sensitivity in the detection of myomesin isoforms, all protein extracts were normalized to an equal amount of MHC, as judged by Coomassie Blue staining of a twin gel. Under these conditions nearly equal amounts of myomesin are expressed at all developmental stages as detected by the general myomesin antibody (panel My-N). In contrast to this, the expression of EH-myomesin starts in the hind limb only at day 10 after birth (panel EH, lane P10). The proportion of this isoform rapidly increases and reaches nearly maximum expression levels in soleus muscle at postnatal day 20 (panel EH, lane P20). The same expression level of EH-myomesin is detected in soleus muscle at postnatal day 50, corresponding to the adult state (panel EH, line P50). In accordance to this, the second band of higher molecular weight appears in the same extracts incubated with the general myomesin antibody (panel My-N, lines P20 and P50). The comparison of the two bands, corresponding to the EH-positive and EH-negative isoform allowed an estimate that the maximal EH-myomesin content in the mouse soleus muscle amounts to about 30% of total myomesin (Agarkova *et al.*, 2004).

To study the expression pattern of EH-myomesin during postnatal development in more detail, hind limb cryosections of postnatal mouse (days 4, 10, 20 and 50) were triple stained with antibodies directed against M-protein, EH-myomesin and MHC-I/β (Figure 6.16). During the first days after birth all fibers, including the nascent slow fibers that express the type I MHC isoform, have an identical M-band composition: M-protein is strongly expressed in all muscles of the mouse hind limb, whereas EH-myomesin cannot yet be detected (row

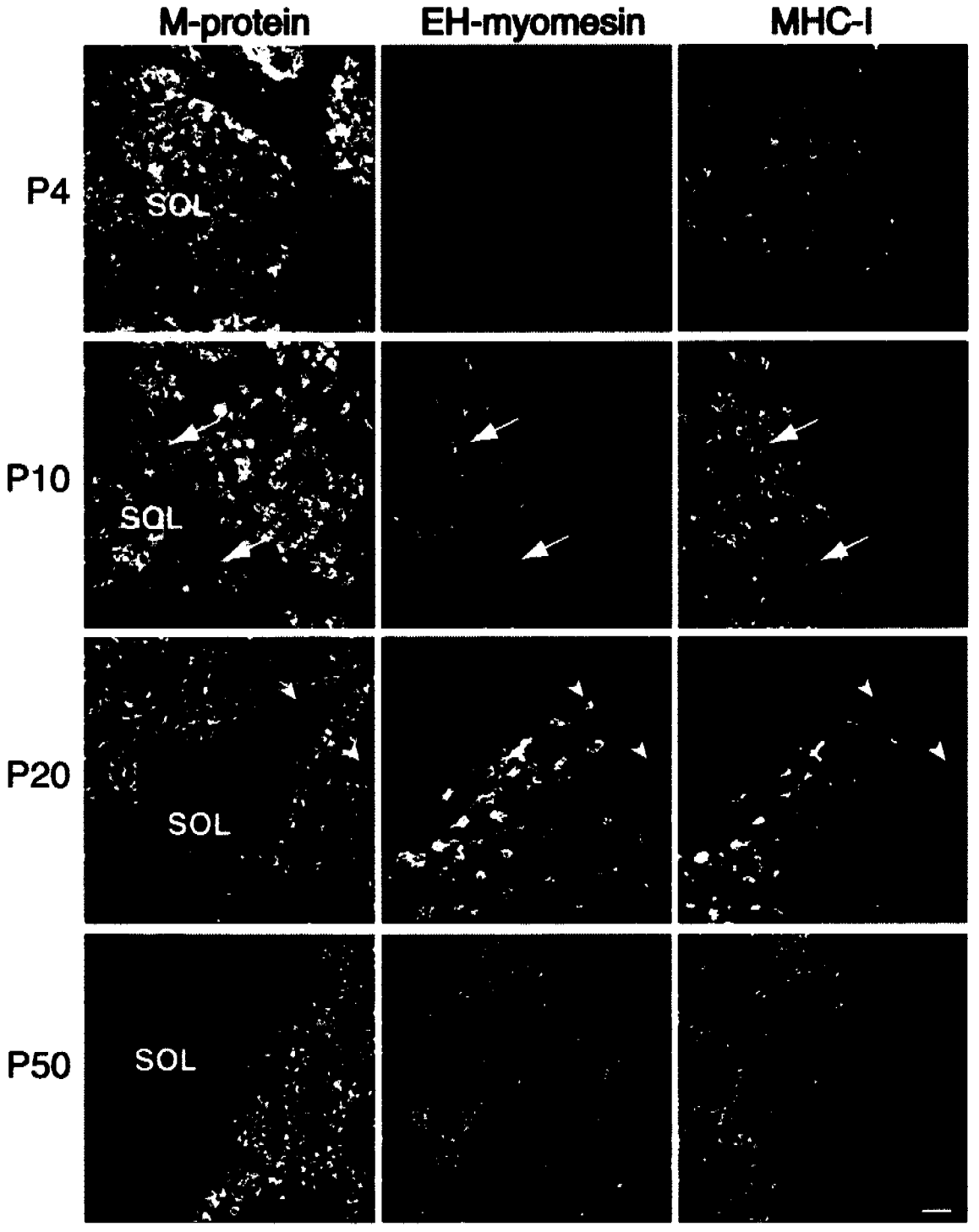

Figure 6.16: *M-protein is gradually replaced by EH-myomesin in slow fibers during postnatal development.* Confocal images of postnatal mouse hind limb cryosections (days 4, 10, 20 and 50), triple stained with antibodies directed against M-protein, EH-myomesin and MHC-I/b. The position of the soleus is marked (SOL). Bar, 50 μm. During the first days after birth all fibers in the hind limb, including the nascent slow fibers that express the type I MHC isoform, have an identical M-band composition. All of them express M-protein and are devoid of EH-myomesin (row P4). However, at postnatal day 10 (row P10) some of the type I fibers begin to down-regulate M-protein simultaneously with the upregulation of EH-myomesin (arrows). All other fibers, which at this stage begin the expression of the adult fast isoforms of MHC, just increase the expression of M-protein. This diversification continues during the next 10 days and leads to the appearance of a complementary expression pattern at postnatal day 20 (row P20). At this stage some fibers outside the soleus also express EH-myomesin and are devoid of M-protein, though they do not react with the anti MHC-I antibody (arrowhead). These fibers start the expression of the adult MHC-IIa isoform (data not shown). All other fibers express M-protein and are negative for EH-myomesin. This characteristic expression pattern remains also in the hind limb muscles of adult mouse (row P50) (Agarkova et al., 2004).

P4). At postnatal day 10 (row P10) most of the type I fibers start the expression of the EH-myomesin isoform (arrows). Although M-protein can still be detected in all muscles of the mouse hind limb and in most of the soleus fibers, its levels begin to drop in all EH-myomesin-positive fibers. Interestingly, at this developmental stage EH-myomesin-positive, MHC-I/β-expressing fibers are scattered through all hind limb muscles, before they concentrate mainly to the soleus muscle in the hind limb of the adult mouse. All other fibers, which at this stage upregulate the expression of the adult fast MHC isoforms, also increase the expression of M-protein. The diversification in the M-band composition in different fiber types continues during the next ten days and leads to the appearance of a complementary expression pattern at postnatal day 20 (row P20). At this point most of the soleus fibers already express EH-myomesin and are devoid of M-protein. Some fibers outside the soleus have a high level of EH-myomesin, but they do not react with the anti MHC-I antibody (arrowheads). Additional immunofluorescence stainings have shown that these are the developing type IIa fibers (data not shown), whereas all other fibers express M-protein and are negative for EH-myomesin. This exclusive expression pattern was detected in the hind limb muscles of adult mouse, too (row P50): M-protein can hardly be found in soleus but is present in all fast muscles at high levels, while EH-myomesin is highly accumulated in M-protein-negative fibers. It has to be noted, that the fiber size is continuously growing in the first weeks after birth and reaches its adult size at about P50.

Thus, we found that the expression of EH-myomesin gradually increases during postnatal maturation of slow fibers, in correlation with the progressive down-regulation of M-protein in the same fibers. This diversification process leads to the establishment of a fiber type-specific M-band composition in the hind limb muscles of three-week-old mice. In addition, these stainings demonstrate that EH-myomesin is absent from the MHC-I-positive fibers of the neonatal mouse, despite being expressed in all MHC-I-positive fibers in adult mouse (compare with Figure 6.13). Therefore, the distinct M-band composition is not firmly correlated to the program of MHC expression, but might be affected by other factors, like the level of activity of the respective fiber. Consequently, the progressively increasing nerve and locomotion activity of animals after birth may stimulate the development of specialized M-band structures in the maturing slow fibers leading to upregulation of EH-myomesin expression.

6.3 Myomesin 3, a novel component of the sarcomeric M-band

6.3.1 Introduction

The M-band is a prominent part of the sarcomeric cytoskeleteon, a complex network which ensures the proper interaction of contractile filaments in muscle. This transverse structure is believed to stabilize the thick filament lattice in the sarcomere during contraction (Agarkova *et al.*, 2003, Agarkova and Perriard, 2005, Lange *et al.*, 2005a). The main structural components of the sarcomeric M-band identified so far are the C-terminal part of titin (Labeit and Kolmerer, 1995) and two proteins from the myomesin family: myomesin (Eppenberger *et al.*, 1981, Grove *et al.*, 1984) and M-protein (Masaki and Takaiti, 1974), which are closely related proteins consisting of an intrinsically disordered N-terminal domain, followed by 12 identically arranged tandem repeats of Ig- and Fn-like domains. Myomesin can be found in all kinds of vertebrate cross-striated muscles (Agarkova *et al.*, 2000), whereas M-protein is expressed mainly in fast skeletal muscle and adult heart (Grove *et al.*, 1989, Carlsson *et al.*, 1990).

The molecular organization of the M-band has been recently further characterized by biochemical and biophysical methods. These studies have shown that myomesin not only can bind to myosin and titin (Obermann *et al.*, 1997), but has the ability to form antiparallel dimers via its C-terminal domain (Lange *et al.*, 2005b). These findings were integrated into the novel three-dimensional model of the sarcomeric M-band in which myomesin is considered to be the principal thick filament cross-linking protein analogous to α-actinin in the Z-disk (Lange *et al.*, 2005b). In addition, myomesin is a molecular spring with visco-elastic properties that are adaptable by alternative splicing of the EH-segment which has a disordered conformation and functions as entropic spring (Schoenauer *et al.*, 2005). Several muscle types express the EH-myomesin splice isoform, generated by the inclusion of the unique EH-segment of about 100 amino acids in the center of the molecule between the Fn domains My6 and My7 (Agarkova *et al.*, 2000, Agarkova *et al.*, 2004). The Ig and Fn domains might function as "shock absorbers" by reversible sequential unfolding in the case the sarcomeres are subjected to extremely high or long sustained stretching forces (Schoenauer *et al.*, 2005).

Using comparative sequence analysis we have now identified a novel gene in the vertebrate genome, which is closely related to both M-protein and myomesin and shares the same intron-exon and domain arrangement. To study the expression of all three myomesin family genes in

different types of adult and developing muscles we performed RT-PCR analysis of mouse tissues. We show that the new member of the myomesin family (myomesin 3) is differentially expressed in various kinds of striated muscle with the highest level in newborn skeletal and adult slow muscles, like soleus and diaphragm. To check the expression of myomesin-3 on the protein level, we generated the antibody recognizing an epitope in the disordered N-terminal domain. Using immuno-histochemistry and confocal microscopy we show that myomesin-3 is a novel protein component of sarcomeric M-band. Its expression in skeletal muscle is fiber-type specific with the highest expression level in IIa fibers of mouse hind limbs. Interestingly, myomesin-3 is absent from the mouse heart under normal conditions but can be expressed in a pathological situation. Furthermore, transfections of neonatal rat cardiomyocytes with constructs encoding N-terminal fragments of myomesin 3 show M-band localization.

We conclude that each muscle is characterized by its unique M-band protein composition, which can be adapted to divergent physiological needs in different muscle types. In several cases it correlates with the expression of titin isoforms (Opitz *et al.*, 2004, Lahmers *et al.*, 2004) and depends on the contractile parameters of a particular fiber (Agarkova *et al.*, 2004).

6.3.2 Exon–intron organization of the murine myomesin 3 gene

The subdivision of the complete murine myomesin 3 gene into exons and introns was analyzed and compared to myomesin and M-protein. The 5' region of the cDNA was fully sequenced (exon 2- 12) whereas the central and the 3' region was taken from the already published sequence (Ensembl gene ID: ENSMUSG00000037139). The exact sequence surrounding the intron–exon boundaries, intron and exon sizes, and intron phases are compiled in Table 6.1. The murine myomesin 3 gene is divided into 37 exons and 36 introns, resulting in a total length of about 55 kb. Exon sizes vary from 23 (exon 35) to 200 bp (exon 12) with the last exon as an exception. Intron sizes range between 149 bp (intron 34) and 5,37 kb (intron 20). The first intron is located in the 5' UTR, 18 bp 5' of the start codon. All other exons and introns are located within the protein coding region. Interestingly, the exon-intron organisation of the murine myomesin 3 gene is identical to M-protein and very similar to myomesin, which has an additional exon encoding the EH-segment. In addition, many exon sizes are identical to M-protein (grey in table 6.1) or even to M-protein and myomesin (dark grey in Table 6.1). Therefore, the gene structure of all three members of the myomesin family

Table 6.1: *Exon–intron organization of the murine myomesin 3 gene.* The first two columns give exon numbers and sizes, the third column shows the DNA sequence around the 5' exon–intron boundary (exon sequences in capital letters and intron sequences in lowercase letters). Column 4 indicates intron length in kilobases. The N-terminal part (exon 2 – exon 12) has been fully sequenced, the rest of the sequence was taken from already published data (Ensembl gene ID: ENSMUSG00000037139). Column 5 gives the DNA sequence around the 3' exon–intron boundary in the same manner as described. Codon phases are shown in the next column: phase 0 are introns that do not split codon triplets; phase I introns are inserted after the first nucleotide of the triplet, and phase II introns are inserted after the second nucleotide. The last column gives the amino acid residues encoded at the splice sites and their numbers in the translated cDNA sequence.

		5' Splice donor consensus		3'Splice acceptor consensus		
No.	Exon size (bp)	C a AG gtagt A g	Intron length (kb)	cc c G n ag G tt t T	Codon phase	Amino acid
1°	92	GTTTCT gtgagt	2.7	tcacag GTTATT		
2*	18/161	CAGCAG gtgggc	0.91	tggcag TGAGGA	II	54 Ser
3*	81	GTCCTG gtaagt	1.07	ctacag GGAAGC	II	81 Trp
4*	160	CAACGG gtgagg	0.60	ctccag ACAGAG	0	134/135 Arg/Thr
5*	158	CACCTG gtaagc	4.97	ccacag GTACAA	II	187Trp
6*	96	CATGAG gtaaag	0.77	ttttag GTGCAC	II	219 Arg
7*	89	TCCGCA gtaagt	2.15	tggcag ATTACC	I	249 Asn
8*	45	TTAAAC gtaagt	0.47	acccag GATCTA	I	264 Lys
9*	141	GAGATG gtgagc	1.12	ccacag GCAGGC	I	311 Gly
10*	162	TAAGAG gtaagg	0.63	gttcag ATGCTG	I	365 Asp
11*	142	TGAGAT gtgagt	1.56	ccacag GTGCCA	II	412 Met
12*	200	GTACAG gtgaga	1.12	tcctag AGATTC	I	479 Glu
13	54	TCGAAG gtatgt	0.39	ttccag ATGCTG	I	497 Asp
14	128	GAAAAG gtacag	3.09	ccttag TCCGTC	0	539/540 Lys/Ser
15	184	AGCCAG gtacca	2.62	ttccag CGACTC	I	601 Ala
16	175	CACCAA gtaagg	1.41	tcccag GTTCAC	II	659 Lys
17	122	CACTAG gtgagt	0.38	ctccag CCACTC	I	700 Ala
18	188	TGCAAG gtgagg	0.21	ctacag GTCACC	0	762/763 Lys/Val
19	127	AGCCAG gtaaga	1.12	caacag GTCCCC	I	805 Gly
20	179	CTCAGG gtgagt	5.37	ccccag GTGTCT	0	864/865 Arg/Val
21	115	AGCCAG gtagga	1.09	ccccag ACGCCC	I	903 Asp
22	157	TAGCAA gtgagc	0.53	tgccag GTCCAA	II	955 Lys
23	110	AGGAAG gtaatg	0.38	ccctag AGCTGA	I	992 Glu
24	45	ACCCAG gtaaac	0.80	tctcag TCATCA	I	1007 Val
25	137	TCCCCG gtaaat	2.57	cgccag AACCGC	0	1052/1053 Pro/Asn
26	145	ATGACG gtcagc	0.20	tcacag AATTTG	I	1101 Glu
27	60	AACAGG gtaagc	0.32	ttgcag GTCCCT	I	1121 Gly
28	68	TGCAAG gcaagt	1.39	cctcag GTAAGA	0	1143/1144 Lys/Val
29	111	GAGGGG gtgagt	2.72	ccttag TTTTCC	0	1180/1181 Gly/Phe
30	88	GTGAAG gtaggc	0.76	ctccag CCCTAG	I	1210 Ala
31	39	TTGGTG gtaagt	0.25	ccccag CTCTCT	I	1223 Ala
32	109	CCACAA gtaggt	1.52	ttccag AGATAA	II	1259 Lys
33	164	GACAAG gtgagg	1.79	ctacag CTTTTG	I	1314 Ala
34	37	ACTGAA gtaagt	0.15	tttcag GGCCTT	II	1326 Lys
35	23	AGAAGA gtgagt	1.49	ttccag ATCGGG	I	1334 Asn
36	56	GATAAG gtacta	1.66	aaacag ACCCTG	0	1352/1353 Lys/Thr
37	264/?					

Exon size is identical in M-protein gene	Exon size is identical in M-protein and Myomesin genes	° partially sequenced * fully sequenced

is highly conserved suggesting that they may have evolved by reduplication of one gene and that their function may be similar.

6.3.3 Sequence comparision of myomesin family members

The amino acid sequence of mouse myomesin 3 was aligned with the human sequence and with the murine sequences of M-protein and myomesin (without EH-segment). The identity level between mouse and human myomesin 3 is about 83% and decreases to 42% and 40% compared to murine M-protein and myomesin. These two proteins are more closely related (49% of identical amino acid residues). While identity values of the immunoglobulin-like (Ig) and fibronectin type III (Fn) repeats within the three proteins are between 38% and 52% demonstrating their close relationship, this value clearly decreases for the head domain (25% to 28%). The building principle of the repeating modular units is identical in all myomesin family members: a unique N-terminal domain, two Ig domains (Ig2-3), 5 Fn domains (Fn4-8) and 5 C-terminal Ig domains (Ig9-13). An exception is the EH-myomesin isoform which has the additional EH-segment in the center of the myomesin molecule. In Table 6.2 the results of this analysis showing the identity values of blocks of similar domains (head domain, repeats of Ig and Fn domains) are summarized.

TABLE 6.2

Conservation of myomesin family protein sequences

	head domain	Ig2-3	Fn4-8	Ig9-13	total
mouse myo3/myo	25	38	40	46	40
mouse myo3/M-prot	28	40	44	46	42
mouse myo/M-prot	27	48	52	51	49
myo3 mouse/human	80	84	82	85	83

Table 6.2. *Conservation of myomesin family protein sequences.* Identity levels were calculated for pairwise comparisons of translated mouse myomesin 3, M-protein and myomesin (without EH-segment) cDNA. In addition, the amino acid sequence of mouse myomesin 3 was aligned with the human one. To allow a more detailed analysis, sequences were divided in blocks of similar domains: head domain (the unique N-terminal domain), Ig2–3 (Ig-like domains), Fn4-8 (Fn type III modules), and Ig9-13 (C-terminal Ig-like domains). Values give the percentages of identical residues. Note the significantly lower identity in the N-terminal domain compared to the Ig-like and Fn type III repeats.

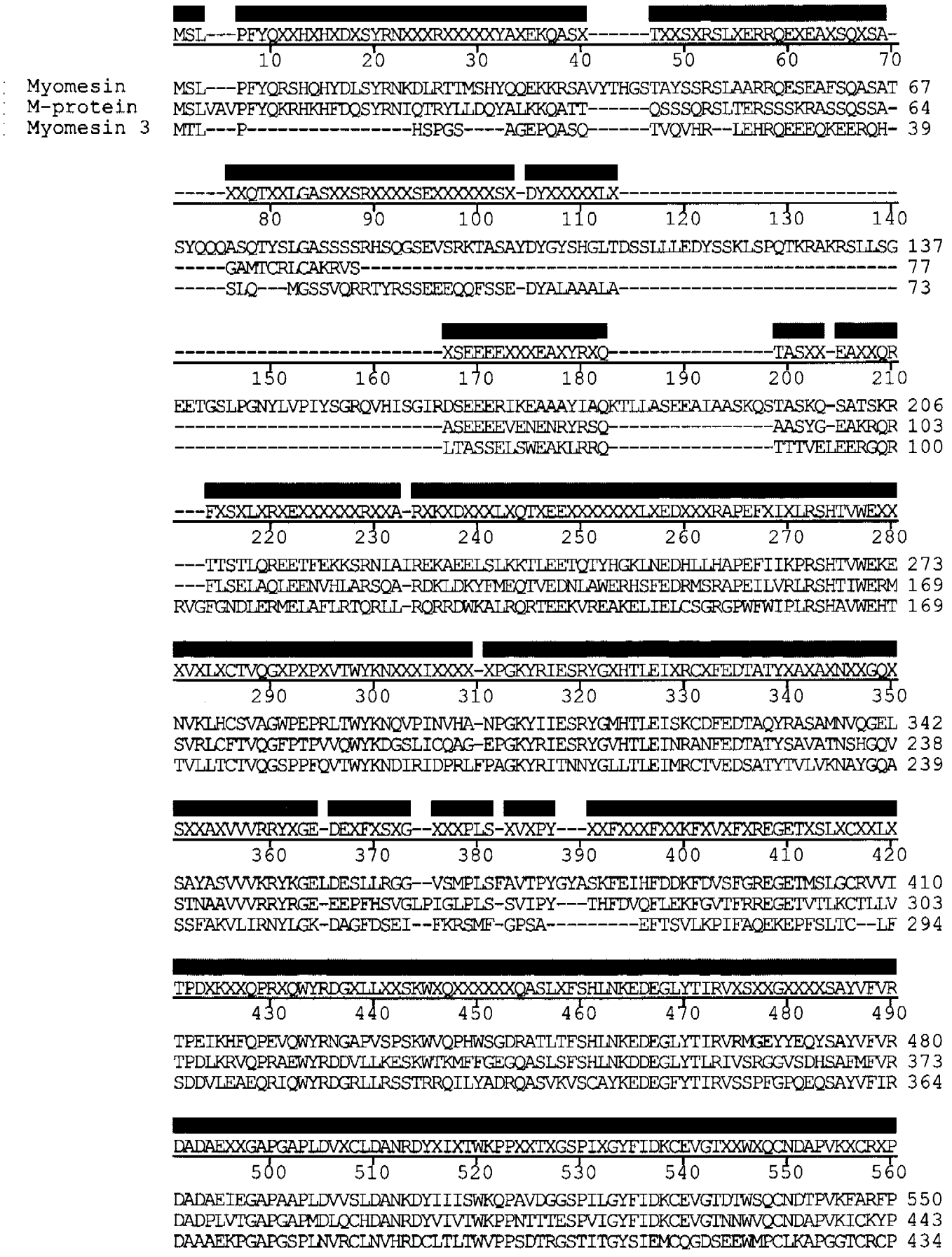
Myomesin
M-protein
Myomesin 3

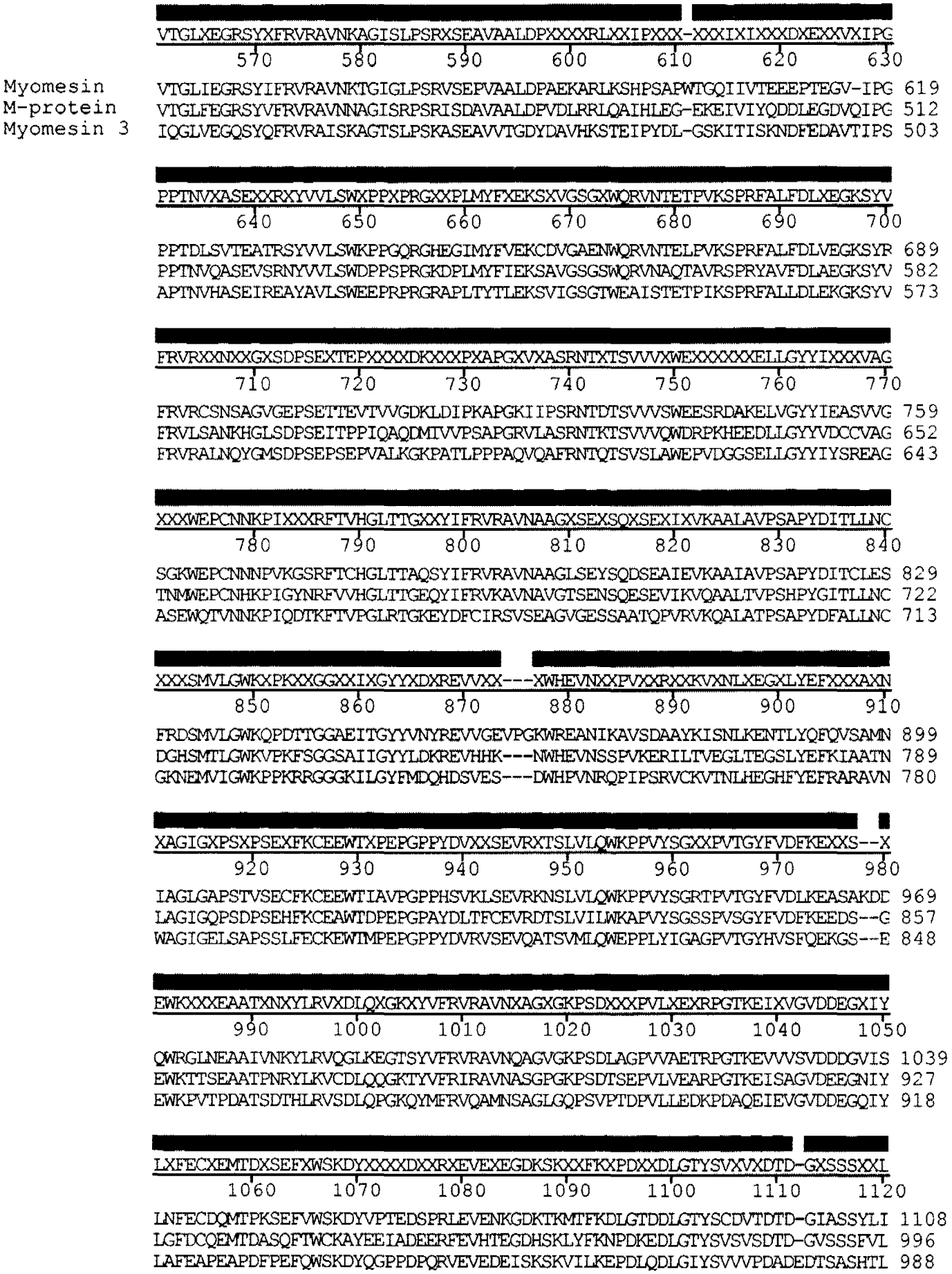
VTGLXEGRSYXFRVRAVNKAGISLPSRXSEAVAALDPXXXXRLXXIPXXX-XXXIXIXXXDXEXXVXIPG
570 580 590 600 610 620 630
Myomesin VTGLIEGRSYIFRVRAVNKTGIGLPSRVSEPVAALDPAEKARLKSHPSAPWTGQIIVTEEEPTEGV-IPG 619
M-protein VTGLFEGRSYVFRVRAVNNAGISRPSRISDAVAALDPVDLRRLQAIHLEG-EKEIVIYQDDLEGDVQIPG 512
Myomesin 3 IQGLVEGQSYQFRVRAISKAGTSLPSKASEAVVTGDYDAVHKSTEIPYDL-GSKITISKNDFEDAVTIPS 503
PPTNVXASEXXRXYVVLSWXPPXPRGXXPLMYFXEKSXVGSGXWQRVNTETPVKSPRFALFDLXEGKSYV
640 650 660 670 680 690 700
PPTDLSVTEATRSYVVLSWKPPGQRGHEGIMYFVEKCDVGAENWQRVNTELPVKSPRFALFDLVEGKSYR 689
PPTNVQASEVSRNYVVLSWDPPSPRGKDPLMYFIEKSAVGSGSWQRVNAQTAVRSPRYAVFDLAEGKSYV 582
APTNVHASEIREAYAVLSWEEPRPRGRAPLTYTLEKSVIGSGTWEAISTETPIKSPRFALLDLEKGKSYV 573
FRVRXXNXXGXSDPSEXTEPXXXXDKXXXPXAPGXVXASRNTXTSVVVXWEXXXXXXELLGYYIXXXVAG
710 720 730 740 750 760 770
FRVRCSNSAGVGEPSETTEVTVVGDKLDIPKAPGKIIPSRNTDTSVVVSWEESRDAKELVGYYIEASVVG 759
FRVLSANKHGLSDPSEITPPIQAQDMTVVPSAPGRVLASRNTKTSVVVQWDRPKHEEDLLGYYVDCCVAG 652
FRVRALNQYGMSDPSEPSEPVALKGKPATLPPPAQVQAFRNTQTSVSLAWEPVDGGSELLGYYIYSREAG 643
XXXWEPCNNKPIXXXRFTVHGLTTGXXYIFRVRAVNAAGXSEXSQXSEXIXVKAALAVPSAPYDITLLNC
780 790 800 810 820 830 840
SGKWEPCNNNPVKGSRFTCHGLTTAQSYIFRVRAVNAAGLSEYSQDSEAIEVKAAIAVPSAPYDITCLES 829
TNMWEPCNHKPIGYNRFVVHGLTTGEQYIFRVKAVNAVGTSENSQESEVIKVQAALTVPSHPYGITLLNC 722
ASEWQTVNNKPIQDTKFTVPGLRTGKEYDFCIRSVSEAGVGESSAATQPVRVKQALATPSAPYDFALLNC 713
XXXSMVLGWKXPKXXGGXXIXGYYXDXREVVXX---XWHEVNXXPVXXRXXKVXNLXEGXLYEFXXXAXN
850 860 870 880 890 900 910
FRDSMVLGWKQPDTTGGAEITGYYVNYREVVGEVPGKWREANIKAVSDAAYKISNLKENTLYQFQVSAMN 899
DGHSMTLGWKVPKFSGGSAIIGYYLDKREVHHK---NWHEVNSSPVKERILTVEGLTEGSLYEFKIAATN 789
GKNEMVIGWKPPKRRGGGKILGYFMDQHDSVES---DWHPVNRQPIPSRVCKVTNLHEGHFYEFRARAVN 780
XAGIGXPSXPSEXFKCEEWTXPEPGPPYDVXXSEVRXTSLVLQWKPPVYSGXXPVTGYFVDFKEXXS--X
920 930 940 950 960 970 980
IAGLGAPSTVSECFKCEEWTIAVPGPPHSVKLSEVRKNSLVLQWKPPVYSGRTPVTGYFVDLKEASAKDC 969
LAGIGQPSDPSEHFKCEAWTDPEPGPAYDLTFCEVRDTSLVILWKAPVYSGSSPVSGYFVDFKEEDS--G 857
WAGIGELSAPSSLFECKEWTMPEPGPPYDVRVSEVQATSVMLQWEPPLYIGAGPVTGYHVSFQEKGS--E 848
EWKXXXEAATXNXYLRVXDLQXGKXYVFRVRAVNXAGXGKPSDXXXPVLXEXRPGTKEIXVGVDDEGXIY
990 1000 1010 1020 1030 1040 1050
QWRGLNEAAIVNKYLRVQGLKEGTSYVFRVRAVNQAGVGKPSDLAGPVVAETRPGTKEVVVSVDDDGVIS 1039
EWKTTSEAATPNRYLKVCDLQQGKTYVFRIRAVNASGPGKPSDTSEPVLVEARPGTKEISAGVDEEGNIY 927
EWKPVTPDATSDTHLRVSDLQPGKQYMFRVQAMNSAGLGQPSVPTDPVLLEDKPDAQEIEVGVDDEGQIY 918
LXFECXEMTDXSEFXWSKDYXXXXDXXRXEVEXEGDKSKXXFKXPDXXDLGTYSVXVXDTD-GXSSSXXI
1060 1070 1080 1090 1100 1110 1120
LNFECDQMTPKSEFVWSKDYVPTEDSPRLEVENKGDKTKMTFKDLGTDDLGTYSCDVTDTD-GIASSYLI 1108
LGFDCQEMTDASQFTWCKAYEEIADEERFEVHTEGDHSKLYFKNPDKEDLGTYSVSVSDTD-GVSSSFVL 996
LAFEAPEAPDFPEFQWSKDYQGPPDPQRVEVEDEISKSKVILKEPDLQDLGIYSVVVPDADEDTSASHTL 988

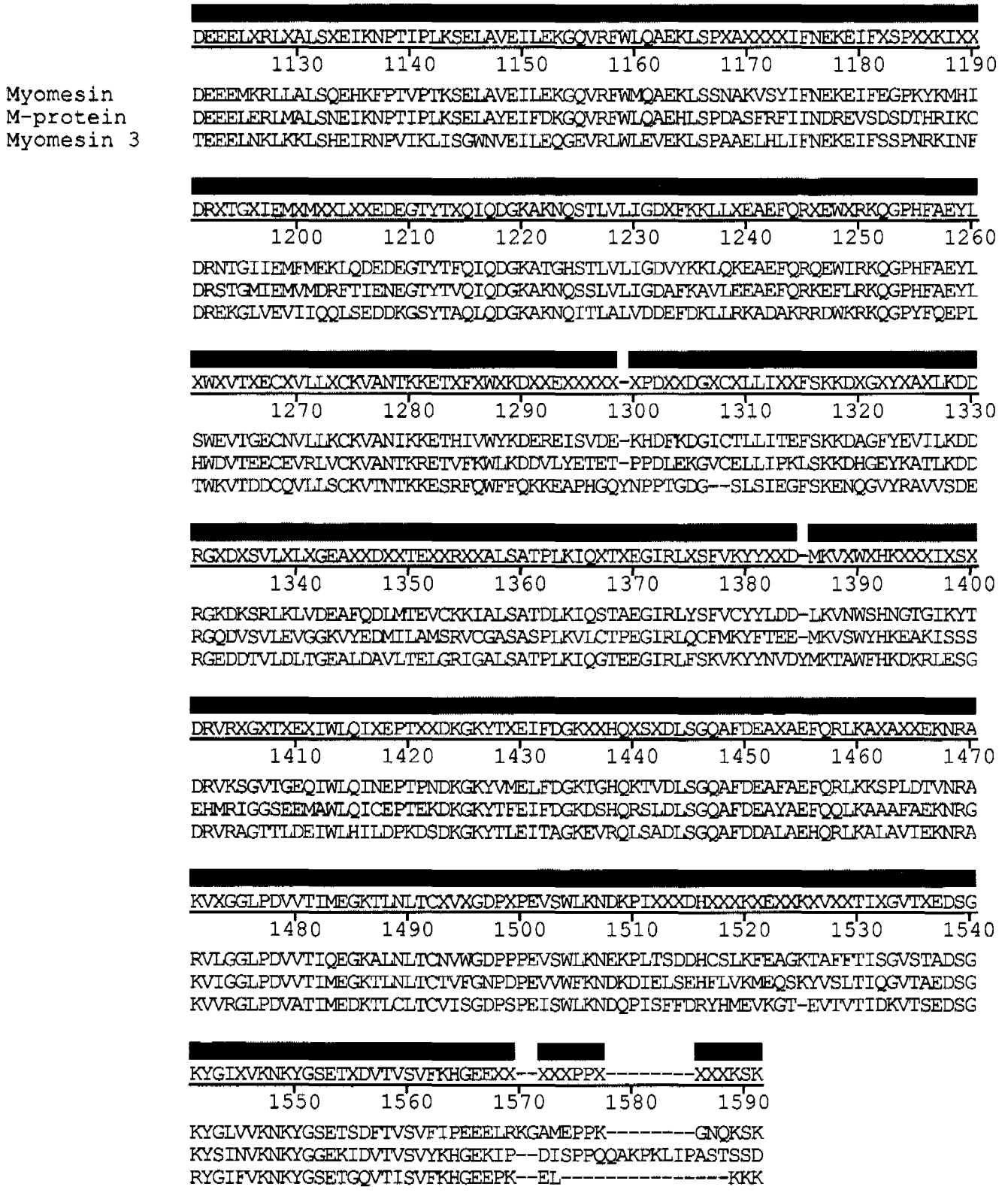

Figure 6.17: *Comparision of amino acid sequences of the myomesin family members.* The alignment of mouse myomesin, M-protein and myomesin 3 was performed using the MEGALIGN program (see materials and methods). Red boxes indicate identical residues in all three sequences, blue boxes indicate identical residues in two sequences, green boxes indicate no identical residues. Numbers correspond to the mouse myomesin sequence. Note the different degree of conservation in different regions of the sequence: E.g. the N-terminal domain is highly diverse between all three proteins whereas some C-terminal regions are highly conserved.

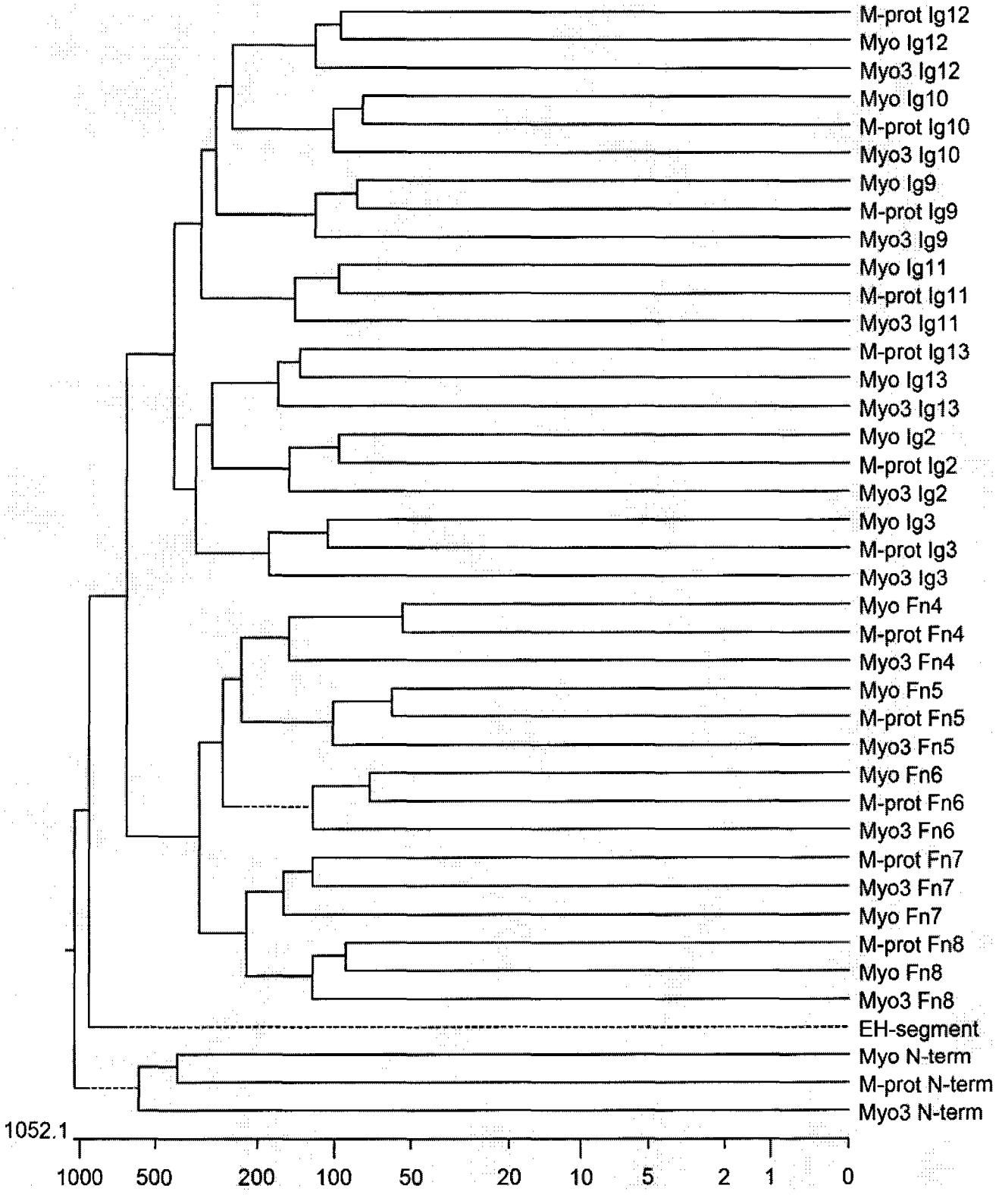

Figure 6.18: *Phylogenetic tree of all domains of the myomesin family proteins.* There are three big groups of domains which are closely related to each other: The fibronectin type III (Fn) domains (Fn4-8), a first group of immunoglobulin-like (Ig) domains (the N-terminal Ig2, Ig3 and the C-terminal Ig13) and a second group of Ig domains (Ig 9-12). Besides, there is the group of N-terminal domains and the EH-segment of myomesin which cannot be assigned to one of these groups and are much less conserved between species compared to the Ig or Fn domains. The corresponding domains (especially the Ig and Fn) are highly conserved between the three proteins indicating that they have a common ancestor. Myo=myomesin, M-prot=M-protein, Myo3=myomesin 3.

As a further illustration, Figure 6.17 shows an alignment of the amino acid sequences of mouse myomesin, M-protein and myomesin 3. The different degree of conservation in different regions of the sequence can clearly be recognized: The N-terminal domain is highly diverse between all three proteins whereas many regions of the Ig or Fn domains (e.g. the β-sheets) are highly conserved (especially parts of the C-terminal domain Ig13).
If we draw a phylogenetic tree of all domains of the myomesin family proteins (Figure 6.18), there are three big groups of domains which are closely related to each other: The fibronectin type III (Fn) domains (Fn4-8), a first group of immunoglobulin-like (Ig) domains (the N-terminal Ig2, Ig3 and the C-terminal Ig13) and a second group of Ig domains (Ig 9-12). The corresponding domains (Ig and Fn) are highly conserved between the three proteins leading to the assumption that they are derived from a common ancestor. The N-terminal domains and the EH-segment of myomesin cannot be assigned to one of these groups. They are much less conserved between species compared to the Ig or Fn domains and belong to the intrinsically unstructured proteins (IUP) according to their sequence.

6.3.4 The expression of myomesin, M-protein and myomesin 3 genes in mouse is tissue- and developmental stage-specific

To study whether mRNA transcripts of all myomesin family members are expressed in a tissue and stage-specific manner, we performed semi-quantitative RT-PCR analysis on total RNA isolated from mouse (C57/BL6) tissues at different developmental stages (Figure 6.19). Different embryonic stages of heart (embryonic heart (EH) 10.5 p.c. to 18.5 p.c.) and skeletal muscle (somites: 10.5 p.c., 12.5 p.c. and whole leg muscle: 12.5 p.c. to newborn) as well as adult tissues of heart, different skeletal muscle types and smooth muscle (stomach) have been tested with primers specific for myomesin, M-protein and myomesin 3. To monitor also the presence of the longer EH-myomesin isoform, the myomesin primers were derived from exon 15 (primer P1) and exon 18 (primer P2), flanking the alternatively spliced segment. This PCR reaction generates a product of 652 bp corresponding to the EH-myomesin isoform and a second product of 358 bp corresponding to myomesin lacking the EH-segment (first panel). In general, the myomesin transcript can be detected in all types of striated muscle but not in smooth muscle (e.g. stomach) which is in correlation to the analysis on the protein level (Agarkova *et al.*, 2004). In heart extracts the transcript of EH-myomesin shows the highest level in the earliest tested embryonic stage (10.5 p.c.) and is almost completely downregulated

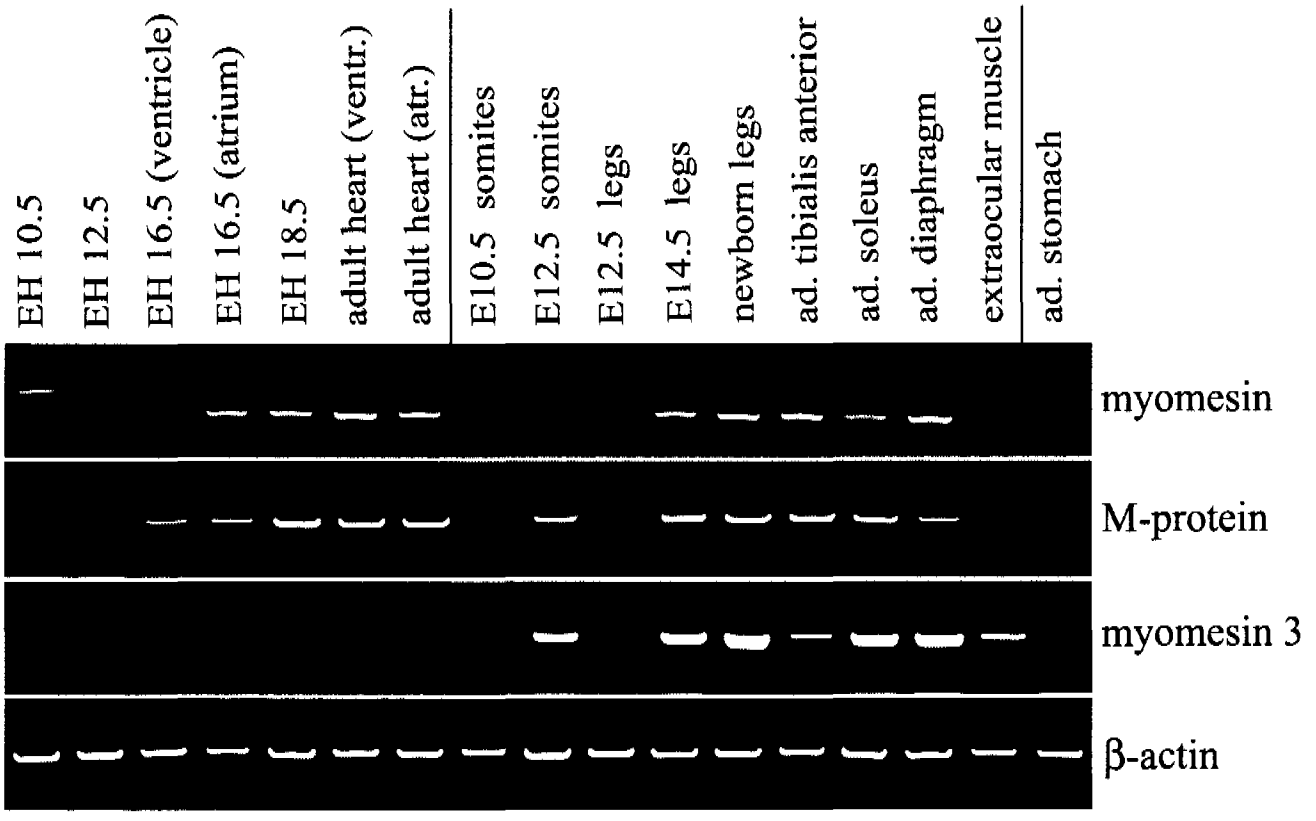

Figure 6.19: *Tissue- and developmental stage-specific expression of myomesin, M-protein and myomesin 3 genes in mice.* Total RNA extracted from mouse tissues of different developmental stages was used for RT-PCR analysis. Different sets of primers were used to detect myomesin (uppermost panel, primers P1 and P2), M-protein (second panel, primers P3 and P4), myomesin 3 (third panel, primers P5 and P6) and β-actin (lowest panel, primers P7 and P8). *Lanes 1–7:* heart extracts of embryonic day 10.5, 12.5, 16.5 (ventricle), 16.5 (atrium), 18.5 (ventricle) and of adult mouse (ventricle and atrium). *Lanes 8-9:* somite extracts of embryonic day 10.5 and 12.5; *lanes 10-12:* whole leg extracts of embryonic day 12.5, 14.5 and newborn stage. *Lanes 13–17:* m. tibialis anterior, m. soleus, diaphragm, extraocular muscle, stomach extracts of adult mouse. Myomesin can be detected in all types of striated muscle but not in smooth muscle (stomach, lane 17). EH-myomesin (longer product of 652 bp) shows the highest level in the early embryonic heart (EH10.5) and is downregulated in the adult heart ventricle. Its transcript can also be detected in the adult slow m. soleus and extraocular muscle. In the adult heart and skeletal muscle, the shorter myomesin isoform (without EH segment, product of 358 bp) is the major myomesin species with extraocular muscle as an exception. M-protein (second panel, product of 466 bp) can be found mainly in adult heart, newborn skeletal and adult skeletal muscle (highest level in m. tibialis anterior), whereas its expression is weak in the early embryonic heart (EH10.5, EH12.5). High levels of myomesin 3 mRNA can be detected in skeletal muscle of newborn mice (newborn legs) and in slow muscle (m. soleus, diaphragm) of adult animals (third panel, product of ...bp). In addition, the myomesin 3 gene is highly expressed already in the somites (E12.5) and legs (E14.5) of the embryo, whereas it is not expressed in any of the heart stages. None of the three myomesin family members can be detected in smooth muscle (stomach). Specific primer for β-actin (P7 and P8, product of 416 bp) have been used to confirm equal loading.

until the late embryonic stage (18.5 p.c.), while the shorter myomesin (without EH-segment) is upregulated at the same time reaching the highest level in the adult heart ventricle. In the adult heart ventricle, EH-myomesin is almost not detectable by RT-PCR, whereas the atrium shows a slightly higher level of this isoform. Furthermore, its transcript can be detected in the adult slow m. soleus, in the extraocular muscle and to minor amounts in the somites (10.5 p.c., 12.5 p.c.) and embryonic leg muscle (12.5 p.c., 14.5 p.c.). The second PCR product of 358 bp (corresponding to the myomesin transcript without EH-segment) can be found mainly in the adult heart and skeletal muscle (strongest signal in newborn leg, adult m. tibialis anterior and adult diaphragm). Similar observation of a relatively fast change in the expression profile from the longer to the shorter myomesin isoform has already been analyzed in chicken (Agarkova *et al.*, 2000).

To detect the transcript of M-protein (myomesin 2), the second member of the myomesin protein family, primers located in the N-terminal part (P3 in exon 4, P4 in exon 7) have been used generating a product of 466 bp. The second panel of Figure 6.19 clearly shows that M-protein can be found mainly in the tissue samples which show a high level of the short myomesin isoform and a low amount of EH-myomesin, such as adult heart, newborn skeletal and adult fast muscle (m. tibialis anterior). It is gradually upregulated in the heart during embryonic development while EH-myomesin is downregulated. This inverse correlation between M-protein and EH-myomesin has already been shown by immunofluorescence analysis (Agarkova *et al.*, 2004).

The tissue specific expression pattern of the myomesin 3 transcript has been checked by primers (P5 in exon 10, P6 in exon 12) located in the N-terminal region generating a product of 446 bp. Interestingly, myomesin 3 shows a different tissue specific expression pattern on the mRNA level compared to M-protein or myomesin (third panel). It can be detected at high levels in the skeletal muscle of newborn mice (whole leg) and in slow muscle (m. soleus, diaphragm) of adult animals, whereas the fast muscle (extraocular muscle, m. tibialis anterior) accumulate smaller amounts of the transcript. In addition, a strong signal of myomesin 3 can be found already in the somites (12.5 p.c.) and legs (14.5 p.c.) of the embryo. Surprisingly, in all the heart stages, myomesin 3 is not detectable at significant levels by RT-PCR suggesting that it is not needed for normal heart function. None of the three myomesin family members can be found in smooth muscle (stomach), demonstrating that their expression is restricted to striated muscle.

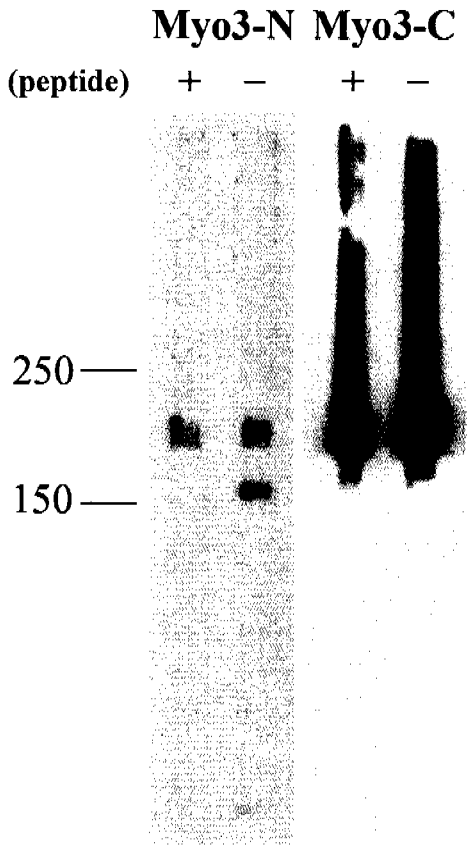

Figure 6.20: Specificity of polyclonal rabbit-anti-mouse myomesin 3 antibodies. Antibodies generated against a N-terminal peptide (Myo3-N, R295) and a C-terminal peptide (Myo3-C, R3036) of mouse myomesin 3 were tested on SDS-samples of mouse soleus extract. The anti-Myo3-N antibody recognizes a band of about 160 kDa (lane -) which corresponds well to the calculated size (162 kDa) and can be totally blocked by the peptide used for immunization (lane +). In addition, an unspecific cross-reaction against myosin heavy chain (MHC) can be detected which is not blocked by the N- terminal peptide. The antibody against the C-terminal peptide (Myo3-C) shows a very strong reaction with MHC (lane -), which is unspecific and cannot be blocked the peptide (lane +). In this case, two weaker bands could be detected, which might be unspecific cross-reactions against myomesin and M-protein according to the sizes of about 170 and 190 kDa. Unfortunately, this antibody does not recognize a band of the expected size and consequently does not react with myomesin 3. Molecular weight markers are indicated in kDa.

6.3.5 Characterization of myomesin 3 antibodies

To study the expression of myomesin 3 at the protein level, we generated two polyclonal rabbit antibodies against a N-terminal peptide (Myo3-N) and a C-terminal peptide (Myo3-C) of mouse myomesin 3. The specificity of these polyclonal antibodies was checked by immunoblot analysis of mouse soleus extracts. A band of about 160 kDa (lane -, Figure 6.20) is detected by the Myo3-N antibody, which corresponds well to the expected size of of myomesin 3 (162 kDa). This reaction can be totally blocked by the N-terminal peptide used for immunization (lane +), confirming the specificity of the reaction. In addition, an unspecific cross-reaction against myosin heavy chain (MHC) can be detected which is not blocked by the N- terminal peptide but can be slightly reduced by optimizing the dilution and blocking with normal goat serum and myosin.
The antibody against the C-terminal peptide (Myo3-C) shows a very strong but unspecific reaction with MHC, which cannot be blocked by the peptide. In addition, two additional weak bands could be detected, which might be unspecific cross-reactions against myomesin and M-protein. Unfortunately, this antibody does not react with myomesin 3.

6.3.6 Myomesin 3 accumulation in mouse skeletal muscle

After having confirmed the specificity of the N-terminal myomesin 3 antibody (Myo3-N), we further analyzed the expression in different mouse tissues on the protein level (Figure 6.21). In addition to the strong signal in mouse soleus, high levels of myomesin 3 can be detected in extraocular muscle and diaphragm, but also in embryonic and neonatal skeletal muscle (18.5 p.c. back muscle, neonatal leg), which confirms the results of the RT-PCR analysis. The specific reaction of this antibody is underlined by the absence of reactivity with heart, smooth muscle (uterus) and non-muscle extracts (brain). Minor amounts of the protein can be detected in the somites (14.5 p.c.) and adult fast muscle (m. tibialis anterior). To summarize, myomesin 3 is mainly expressed in slow muscle, extraocular muscle and embryonic/neonatal skeletal muscle.

Figure 6.21: *Myomesin 3 is accumulated in different types of skeletal muscle.* Immunoblot analysis of mouse tissue extracts representing different embryonic stages and of several adult muscle types (age: 2 months). The polyclonal myomesin 3 antibody (Myo3-N) reacts specifically with m. soleus, diaphragm and extraocular muscle extracts of adult mouse, revealing a band of the expected size (162 kDa) which disappears by specific blocking of the antibody with the peptide used for immunization. Besides, several embryonic/neonatal skeletal muscle extracts show a positive reaction with this antibody (E18.5 back muscle, E18.5 legs, neonatal legs). The specific reaction is further shown by the absence of reactivity with all tested heart extracts and smooth muscle (stomach). Minor amounts of the protein can be detected in E14.5 somites and in the adult m. tibialis anterior. As loading control, an antibody against all actin isoforms has been used (lower panel).

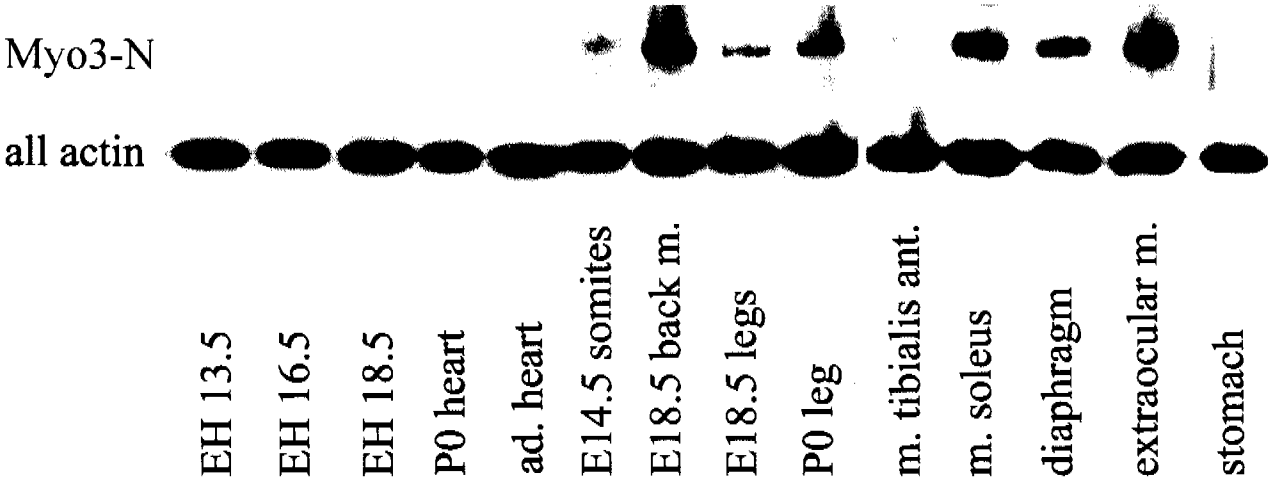

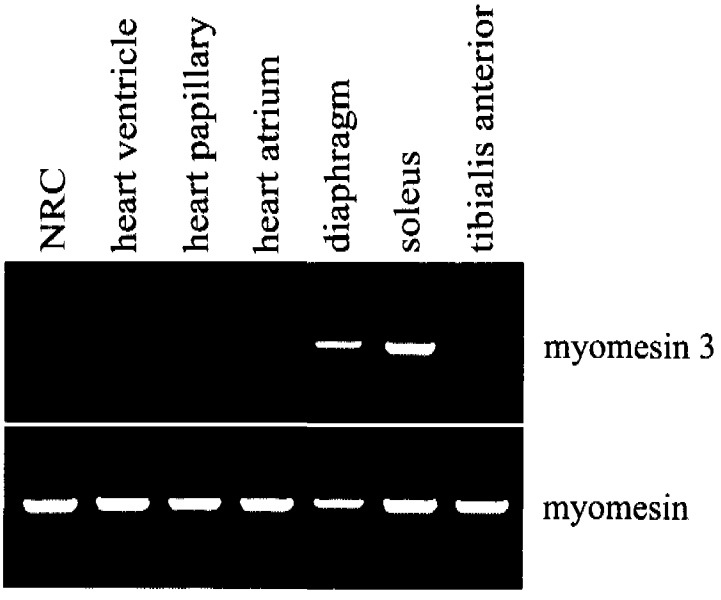

Figure 6.22: *Slow muscle of rat accumulate high levels of myomesin 3 mRNA.* RT-PCR analysis was performed on total RNA isolated from different rat tissues (heart ventricle, atrium and papillary muscle, m. soleus, m. tibialis anterior and diaphragm). All tested rat samples of striated muscle express the myomesin transcript at high levels (lower panel), low amounts of the EH-myomesin isoform (upper band) can be detected in neonatal rat cardiomyocytes (NRC) and diaphragm. The myomesin 3 transcript (upper panel) is expressed at high levels in slow muscle (m. soleus, diaphragm) but not in the adult heart (ventricle, atrium, papillary muscle), only minor amounts can be detected in NRC and fast muscle (m. tibialis anterior).

6.3.7 Myomesin 3 gene is expressed in slow muscle of rat

The finding that the myomesin 3 gene is expressed in mouse skeletal muscle but not in the heart raises the question whether this may also be true for other mammalian species. To address this question, we performed semi-quantitative RT-PCR analysis on total RNA isolated from different rat tissues, such as heart ventricle, atrium and papillary muscle, m. soleus, m. tibialis anterior and diaphragm (Figure 6.22). All these tissues have been tested with primers specific for myomesin and myomesin 3 (the same as used for the analysis of mice tissues). The myomesin transcript is present at high levels in all tested rat samples of striated muscle (lower panel). In addition, low amounts of the EH-myomesin isoform (upper band) can be detected in neonatal rat cardiomyocytes (NRC) and diaphragm. Concerning the expression pattern of myomesin 3, the picture looks similar compared to mice: myomesin 3 (upper panel) is expressed at high levels in slow muscle (m. soleus, diaphragm) but not in the adult heart (ventricle, atrium, papillary muscle). In NRC and fast muscle (m. tibialis anterior), the transcript is almost not detectable.

6.3.8 The myomesin 3 transcript can be detected in human skeletal muscle and adult heart

The next step was to perform RT-PCR analysis on total RNA isolated from different human tissues to analyze whether mRNA transcripts of the myomesin family members are expressed in a tissue-specific manner (Figure 6.23). Different muscle tissue samples have been tested with primers specific for all myomesin family members. To analyze the presence of both myomesin isoforms, again primers flanking the alternatively spliced EH-segment have been used for RT-PCR analysis (P9 in exon 15, P10 in exon 18). These primers generate a product of 670 bp corresponding to the EH-myomesin isoform and a second product of 382 bp corresponding to myomesin lacking the EH-segment. Figure a (first panel) shows that the myomesin transcript can be detected in all types of human striated muscle but not in smooth muscle (small intestine, uterus), which is in agreement to the RT-PCR analysis of mice tissues (Figure 6.19). In addition, a primer (P11, exon 17) specific for the EH-segment of human was used (together with primer P9, generating a product of 382 bp) to confirm the presence of the EH-myomesin isoform in the human embryonic heart (Figure 6.23, second panel).
The transcript of M-protein has been detected using primers located in the N-terminal part of the sequence (P12 in exon 3, P13 in exon 5) generating a product of 287 bp. This analysis

Figure 6.23: *Expression of myomesin, M-protein and myomesin 3 genes in human tissues.* Total RNA extracted from different human muscle tissues was used for RT-PCR analysis using primers specific for all myomesin family members. To check the presence of myomesin, primers located in the central part of myomesin flanking the alternatively spliced EH-segment have been used generating a product of 670 bp (EH-myomesin) and a second product of 382 bp (myomesin lacking the EH-segment). Myomesin can be detected in all types of human striated muscle but not in smooth muscle. In addition, a primer specific for the EH-segment was used (generating a product of 382 bp) to confirm the presence of the EH-myomesin isoform in embryonic heart (second panel). High levels of M-protein (N-terminal primers generating a product of 287 bp) mRNA are detectable in embryonic skeletal muscle (psoas) and adult heart, in addition it can be found in adult m. tibialis anterior, tongue and in the embryonic heart (third panel). The expression pattern of myomesin 3 has been analyzed by N-terminal primers generating a product of 149 bp (fourth panel). Its transcript can be detected not only in skeletal muscle with the highest level in the embryo (embryonic psoas), but also in the adult heart. In addition, m. tibialis anterior and tongue of the adult human show higher expression of myomesin 3 mRNA whereas in smooth muscle, it is not detectable. As loading control, primers specific for β-actin have been used (fifth panel).

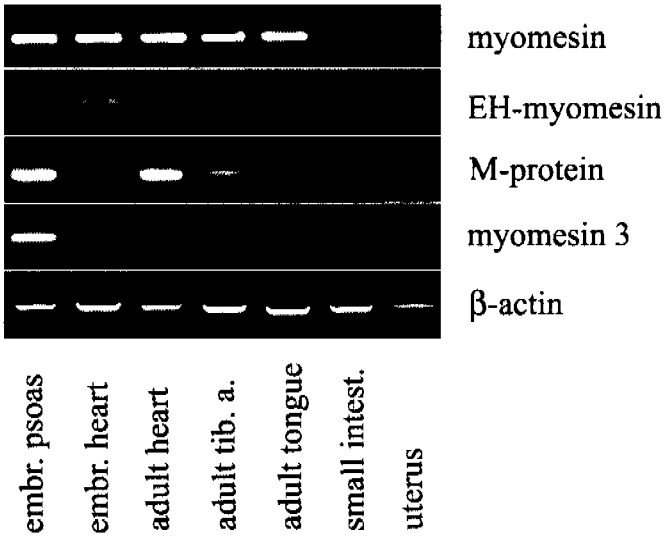

demonstrates a high level of M-protein mRNA in embryonic skeletal muscle (psoas) and adult heart of human, besides the transcript can be found in m. tibialis anterior and tongue of the adult and in the embryonic heart (Figure 6.23, third panel).
Concerning the abundance of the myomesin 3 transcript in different muscle types of human, the picture looks slightly different compared to mouse. Here, the expression pattern has been analyzed by primers P14 (located in exon 5) and P15 (located in exon 6) generating a product of 149 bp. Interestingly, it can be detected not only in skeletal muscle with the highest level in the embryo (embryonic psoas), but also in the adult heart (Figure 6.23, fourth panel). Moreover, m. tibialis anterior and tongue of the adult human show measurable levels of myomesin 3 mRNA whereas in smooth muscle, the transcript is not detectable in significant amounts.

6.3.9 Skeletal muscle and adult heart of human accumulate high levels of myomesin 3

The same antibody which was used for the Western Blot analysis of mouse tissues (Myo3-N) has been used to check the expression level of myomesin 3 in several human muscle tissues (Figure 6.24, upper panel). This antibody reacts specifically with the human protein, which is shown by a strong reaction with a band of the expected size (162 kDa) in all skeletal muscle tissues (embryonic psoas, adult limb muscle, diaphragm and tongue) and by the absence of a signal in embryonic heart (day 175) and smooth muscle. Besides, high levels of myomesin 3 are detectable in the adult heart, in this way confirming the results of the RT-PCR analysis, where the myomesin 3 transcript could be found not only in skeletal muscle, but also in the adult human heart. Interestingly, a weaker second band of slightly smaller size is detectable in adult heart, indicating partial degradation or modification of myomesin 3 in the human heart.

6.3.10 Myomesin 3 is a novel component of the sarcomeric M-band

To check whether myomesin 3 shows a sarcomeric localization in skeletal myofibers, confocal images of longitudinal sections of mouse soleus fibers were triple-stained with antibodies against myomesin 3 (Myo3-N: Figure 6.25 b, green in a, e and g), myomesin (My-N: Figure 6.25 c, red in a, e and f) and α-actinin (EA-53: Figure 6.25 d, blue in a, f and g). This experiment clearly shows that myomesin 3 localizes to the sarcomeric M-band as

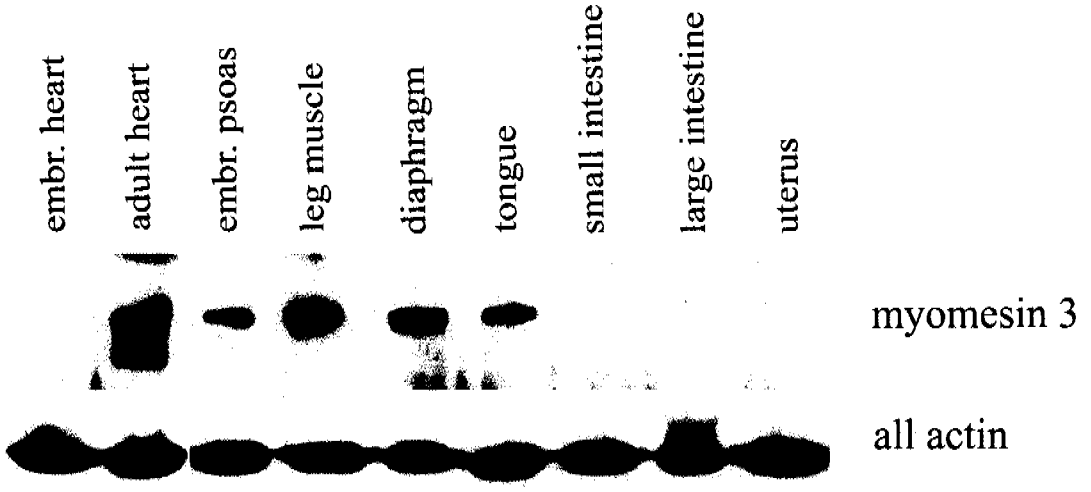

Figure 6.24: *Myomesin 3 is accumulated at high levels in skeletal muscle and adult heart of human.* The expression level of myomesin 3 in several human muscle tissues has been checked by western blot analysis (upper panel). The polyclonal antibody against mouse myomesin 3 (Myo3-N) reacts specifically with the human protein and recognizes a band of the expected size (162 kDa) in all skeletal muscle tissues while the signal is absent in embryonic heart (day 175) and smooth muscle. In addition, high levels of myomesin 3 are detectable in the adult human heart. The antibody against all actin isoforms confirms the equal loading of all tissue extracts (lower panel).

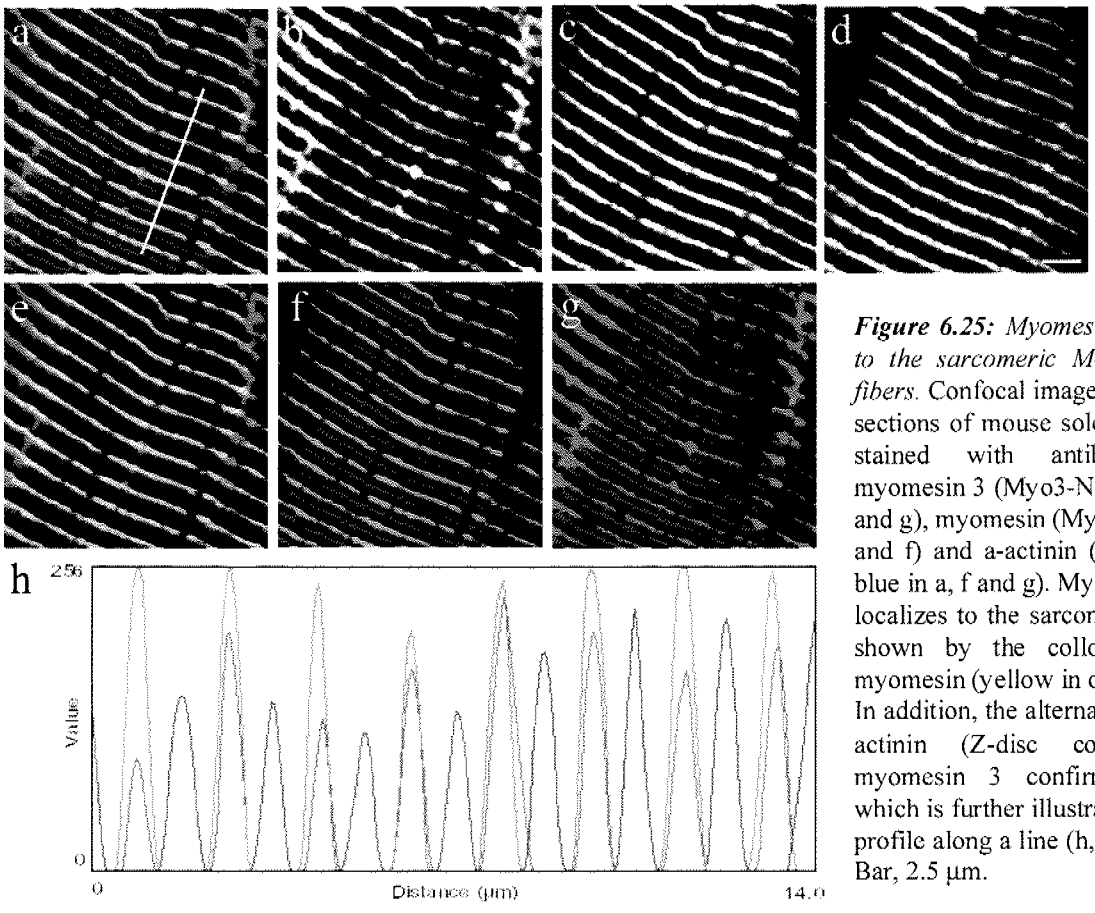

Figure 6.25: *Myomesin 3 is localized to the sarcomeric M-band in soleus fibers.* Confocal images of longitudinal sections of mouse soleus fibers triple-stained with antibodies against myomesin 3 (Myo3-N: b, green in a, e and g), myomesin (My-N: c, red in a, e and f) and a-actinin (mAb EA-53: d, blue in a, f and g). Myomesin 3 clearly localizes to the sarcomeric M-band as shown by the collocalization with myomesin (yellow in overlays a and e). In addition, the alternating signal of α-actinin (Z-disc component) and myomesin 3 confirms this result, which is further illustrated by the RGB profile along a line (h, white line in a). Bar, 2.5 µm.

confirmed by the collocalization with myomesin (yellow in overlays a and e). In addition, the alternating signal of α-actinin (Z-disk component) and myomesin 3 confirms this result (Figure 6.25 g). A further illustration is given by the RGB profile along a line (Figure 6.25 h, white line in a) verifying the collocalization of myomesin (red in h) and myomesin 3 (green in h) and clearly demonstrating that these two proteins are localized in the center between two Z-disks stained by α-actinin (blue in h).

Interestingly, a specific reaction of the antibody against myomesin 3 in immunofluorescence was achieved only by a special procedure using SDS treatment before and during fixation with paraformaldehyde. As an alternative (for cross-sections), acetone fixation was used after the SDS treatment (for details see materials and methods). The need of SDS treatment in immunofluorescence suggests that the epitope, which is localized in the N-terminal domain, is not accessible in the native state maybe because it is hidden through its presumed binding to the huge myosin filament. Fortunately, the peptide can be opened by denaturating agents such as SDS resulting in a specific reaction of the antibody in immunofluorescence.

6.3.11 All type IIA and part of the type I fibers of the mouse hind limb express high levels of myomesin 3

Immunofluorescence analysis of mouse hind limb muscles (Figure 6.26) was performed to compare the expression pattern of myomesin 3 with the myosin heavy chain isoform content in a given muscle fiber. For this and the following stainings tissue samples from 1-month-old mice were used. According to earlier studies, the adult pattern of MHC isoform expression is already established in the hind limb muscles at this stage (Allen and Leinwand, 2001). We stained hind limb cryosections with the anti-myomesin 3 antibody (Myo3-N; Figure 6.26 b and e, green in a and d) in combination with antibodies directed against the MHC-I/β (A4.840; Figure 6.26 c, red in a) or MHC-IIa (A4.74; Figure 6.26 f, red in d) isoforms. At the age of 1 month, most fibers of the m. soleus express either MHC-I/ β or MHC-IIa. In most other muscles of the hind limb, only few fibers express MHC-I/ β whereas some fibers (e.g. in the gastrocnemius) are positive for MHC-IIa (Agarkova *et al.*, 2004). A high expression of myomesin 3 can be detected in all MHC-IIa-positive fibers (compare Figure 6.26 e and f, yellow in d), but also in a small part of the fibers expressing MHC-I/ β (arrow in Figure 6.26 a, b and c). However, most of the MHC-I/β expressing fibers have less myomesin 3 compared to the MHC-IIa-positive fibers. According to these results we can conclude that high levels of

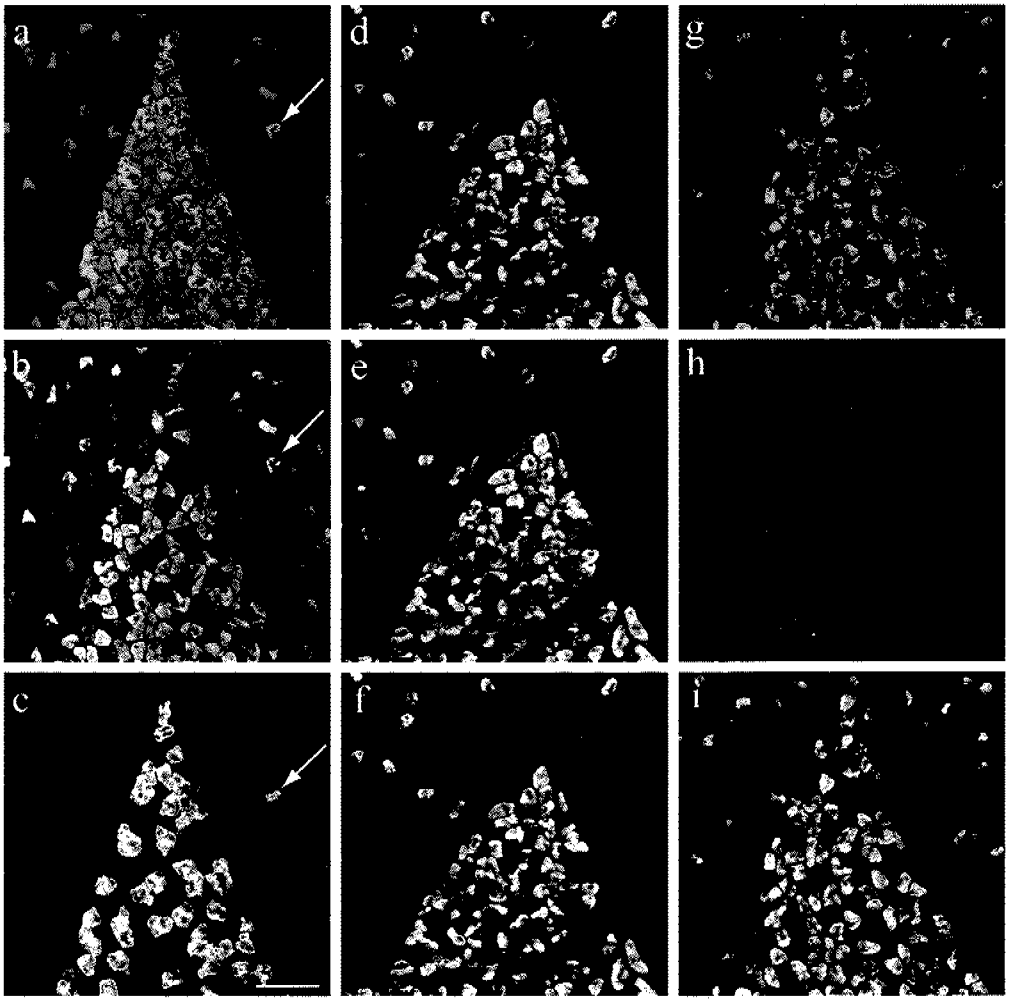

Figure 6.26: *All type IIA and part of the type I fibers of the mouse hind limb accumulate high levels of myomesin 3.* Mouse hind limb cryosections were stained with the anti-myomesin 3 antibody (Myo3-N; b and e, green in a and d) in combination with antibodies directed against the MHC-I/b (A4.840; c, red in a) or MHC-IIa (A4.74; f, red in d) isoforms. Myomesin 3 is highly accumulated in all MHC-IIa-positive fibers (compare e with f) and in a small part of the fibers expressing MHC-I/ b (arrow in a, b and c). Most of the type I fibers have lower levels of myomesin 3 compared to the type IIA fibers. Other fiber types (IID/IIB) do not express this protein. The specificity of the myomesin 3 antibodies is confirmed by blocking with the peptide used for immunization (h, green in g) counterstained with the anti-MHC-IIa antibodies (i, red in g). Bar: 100 μm.

myomesin 3 can be found mainly in type IIA fibers and partially in type I fibers, but not in other fiber types (IID, IIB) of the mouse hind limb. Yet we can not exclude lower levels of myomesin 3 expression in these fast fiber types. Blocking of the antibody with the peptide used for immunization (Figure 6.26 i, red in g) clearly exstinguishes its signal (Figure 6.26 h, green in g) and further confirms its specificity.

6.3.12 Comparision of expression pattern of all myomesin family members

To analyze the differences in M-band composition in respect to fiber type, hind limb cross-sections of mouse were stained with antibodies directed against all proteins of the myomesin family. The cryosections were triple-stained with the polyclonal myomesin 3 antibody (Myo3-N; Figure 6.27 b, green in a) in combination with the general myomesin antibody (B4; Figure 6.27 c, red in a) and an antibody directed against M-protein (AA259; Fig. 6.27 d, blue in a). The general myomesin antibody stains all fibers in a section, demonstrating that this protein is evenly expressed in all fiber types. Besides, myomesin 3 and M-protein show a very specific expression pattern (Figure 6.27 b and d, respectively). Fibers expressing high levels of M-protein (mainly type IIB fibers) do not accumulate a lot of myomesin 3, whereas fibers with high levels of myomesin 3 (mainly IIA fibers) only show low amounts of M-protein. In addition, many of M-protin negative fibers in the m. soleus have only intermediate levels myomesin 3. An additional staining of myomesin 3 combined with M-protein and the EH-myomesin isoform (not shown) reveals that fibers strongly positive for myomesin 3 accumulate in most cases intermediate amounts of M-protein and EH-myomesin. A high level of EH-myomesin (mainly in type I fibers, (Agarkova *et al.*, 2004)) correlates well with intermediate levels of myomesin 3.

To check wether all myomesin family proteins can be expressed in the M-bands of the same fiber, longitudinal sections of mouse soleus were triple stained with the same antibodies against myomesin (Figure 6.27 g), M-protein (Figure 6.27 h) and myomesin 3 (Figure 6.27 f). This staining clearly demonstrates that all three proteins can be collocalized (Figure 6.27 e) in the M-bands of the same fiber (e.g. in type IIA fibers).

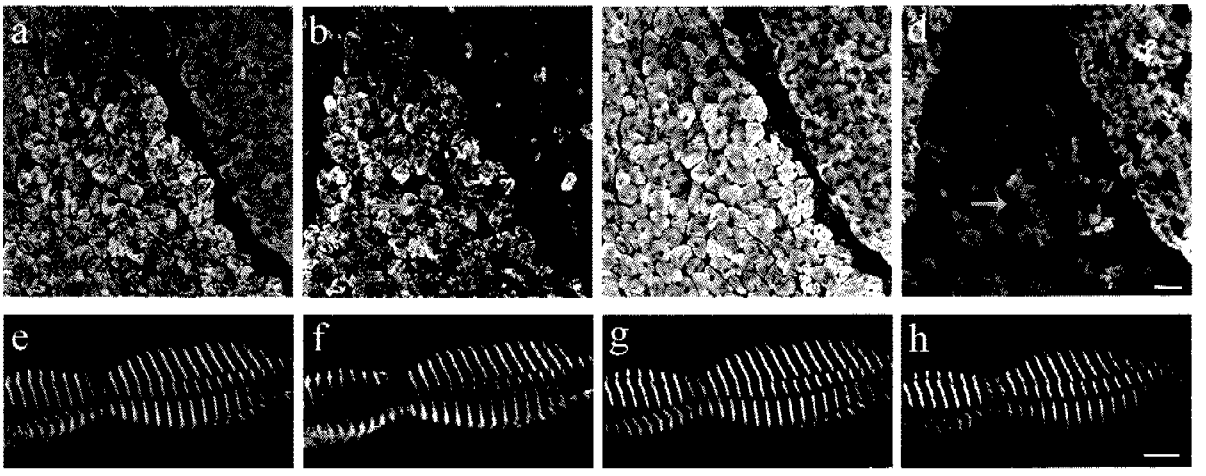

Figure 6.27: *Comparative analysis of expression pattern of all myomesin family proteins in skeletal muscle.* Mouse hind limb cross-sections and longitudinal sections of m. soleus were stained with the polyclonal myomesin 3 antibody (Myo3-N; b and f, green in a and e) in combination with the general myomesin antibody (B4; c and g, red in a and e) and an antibody directed against M-protein (AA259; d and h, blue in a and e). The general myomesin antibody stains all fibers evenly in a section (c), whereas myomesin 3 and M-protein show a more specific expression pattern (compare b and d). Most fibers with high levels of M-protein do not accumulate myomesin 3, whereas many fibers strongly positive for myomesin 3 (mainly IIA fibers) show only intermediate amounts of M-protein (arrows in b and d). In addition, the soleus fibers which are negative for M-protein (mainly type I fibers) have in most cases intermediate levels of myomesin 3. The longitudinal sections of soleus fibers further demonstrate that all 3 myomesin family proteins can be colocalized in the M-bands of the same fiber (e.g. in type IIA fibers). Bars: 50 (d) or 5 μm (h).

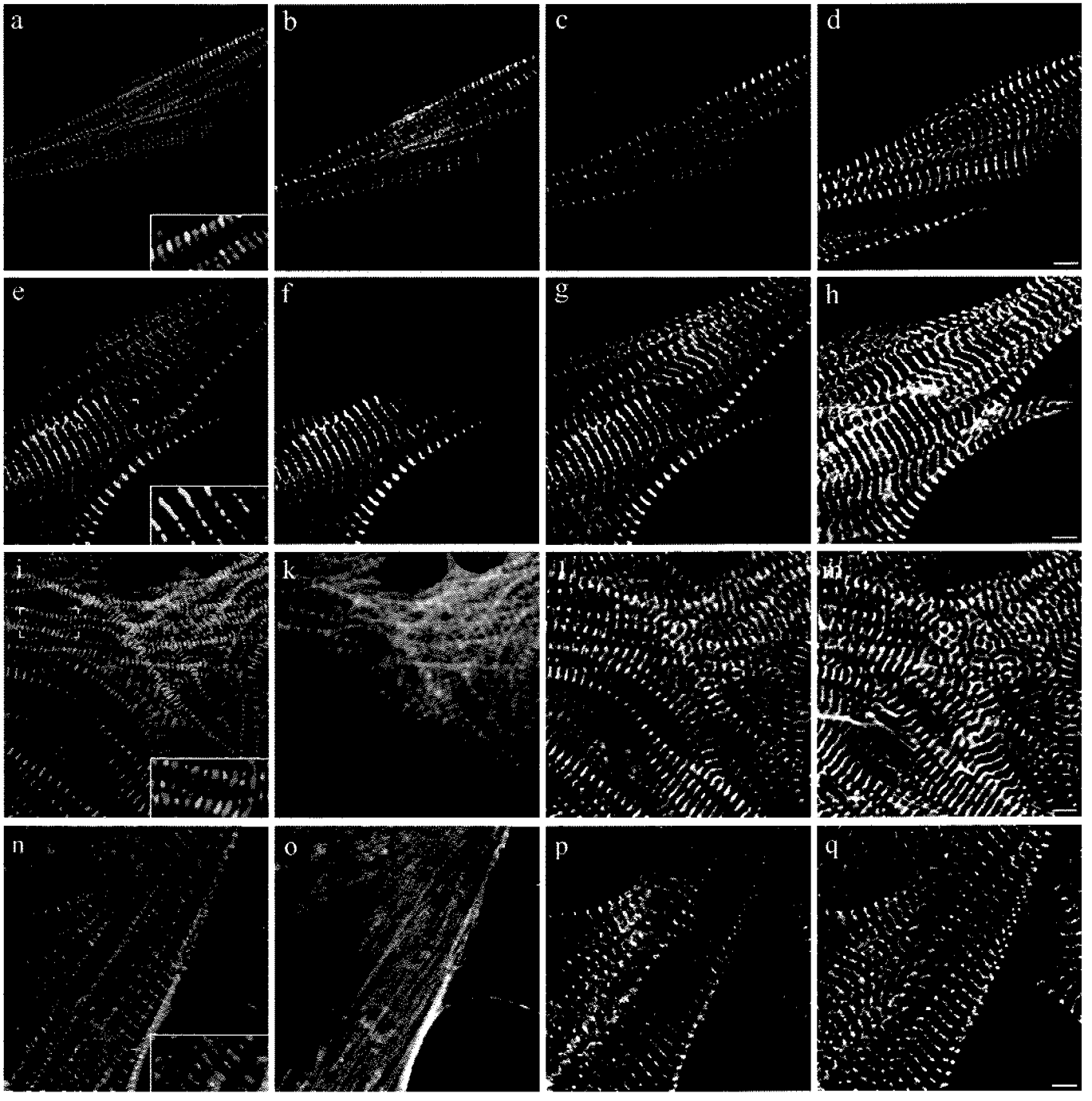

Figure 6.28: *Myomesin 3 N-terminal and C-terminal truncation mutants expressed in NRC.* Confocal images of neonatal rat cardiomyocytes expressing the following GFP-tagged myomesin 3 truncation mutants (b,f,k,o; green in overlays): Myo3-d1 (domain 1; b, green in a), Myo3-d1-3 (domains 1-3; f, green in e), Myo3-ig11-13 (domains 11-13; k, green in i) and Myo-ig13 (domain 13; o, green in n). Cells were stained with an antibody against myomesin (anti-EHmyomesin, c, g and p; anti-S-myomesin, l) and with an antibody against sarcomeric α-actinin (EA-53, d , h, m and q). Myo3-d1-3 and partially Myo3-d1 are incorporated into the M-band region of the myofibrils, as demonstrated by the collocalization with myomesin (yellow in a and e, see inset). The constructs Myo3-ig11-13 and Myo3-ig13 are diffusely distributed in the cytoplasm and show some unspecific interaction with the myofibrils. Bars: 5μm.

6.3.13 N-terminal part of myomesin 3 is responsible for M-band targeting

To investigate if the N- or C-terminal parts of myomesin 3 are able to direct the incorporation of the protein into the M-band, four fusion constructs were generated with the green fluorescent protein (GFP) fused N-terminally to the following myomesin 3 truncations: Myo3-d1 encoded only the head domain of myomesin 3, Myo3-d1-3 encoded the head domain and the following two immunoglobulin-like domains, Myo3-ig11-13 encoded the three C-terminal immunoglobulin-like domains and Myo3-ig13 encoded only the C-terminal domain. In Figure 6.28, neonatal rat cardiomyocytes (NRC) transfected with all 4 truncation constructs of mouse myomesin 3 are shown. In cells expressing Myo3-d1-3, the recombinant protein is incorporated into the M-bands of the myofibrils (Figure 6.28 f, yellow in e, inset) as confirmed by a counterstaining with antibodies against α-actinin (EA-53; Figure 6.28 h, blue in e) and myomesin (α-EH; Figure 6.28 g, red/yellow in e). Myo3-d1 (Figure 6.28 b, green/yellow in a, inset) is only partially incorporated into the M-band and shows also Z-disk localization. From these results we conclude that the N-terminal part of the protein is sufficient for M-band targeting in NRC. The truncations Myo3-ig11-13 (Figure 6.28 k, green in i) and Myo3-ig13 (Figure 6.28 o, green in n) are distributed in a diffuse manner in the cytoplasm and show some unspecific interaction with the myofibrils (Z-disk). Because the α-actinin and myomesin stainings show that myofibrils are still present in transfected cells, the constructs have no major antimorphic effects on the myofibrils.

6.3.14 Myomesin 3 is reexpressed in mouse models of dilated cardiomyopathy

To investigate whether genes of the myomesin family members change their expression level in the adult heart in pathological situations, several mouse models for hypertrophic or dilated cardiomyopathy were examined by RT-PCR analysis (Figure 6.29). The following mouse models have been checked: AngiotensinII (AngII) overexpressing mice (Mazzolai *et al.*, 2000), one-kidney-one-clip (1k1c) mouse model (Wiesel *et al.*, 1997) and isoproterenol (Iso) treated mice (Kudej *et al.*, 1997) as models for hypertrophic cardiomyopathy; retinoic acid receptor (RAR) overexpressing mice, (Colbert *et al.*, 1997), MyBPC transgenic mice (MyBPC, McConnel et al., 1999), tropomodulin-overexpressing transgenic (TOT) mice (Sussman *et al.*, 1998), muscle LIM protein (MLP) knockout mice, (Arber *et al.*, 1997) and dystrophin knockout (mdx) mice (Quinlan *et al.*, 2004) as models for dilated cardiomyopathy.

Figure 6.29: *Reexpression of myomesin 3 in mouse models of dilated cardiomyopathy.* Several mouse models for hypertrophic (HCM: AngII, 1k1c, Iso) or dilated cardiomyopathy (DCM: RAR, MyBPC, TOT, MLP, mdx) were examined by RT-PCR analysis using primers specific for all myomesin family members. The expression levels of myomesin (third panel) or M-protein (second panel) transcripts show no significant differences between hypertrophic, dilated and control hearts. In several mouse models of DCM, myomesin 3 is reexpressed (first panel) with the highest level in MLP knockout mice, but also TOT mice show a strong reexpression of this gene. RAR and mdx mice show only a slight increase in myomesin 3 expression, whereas MyBPC transgenic and all models of HCM show no significant differences compared to control hearts.

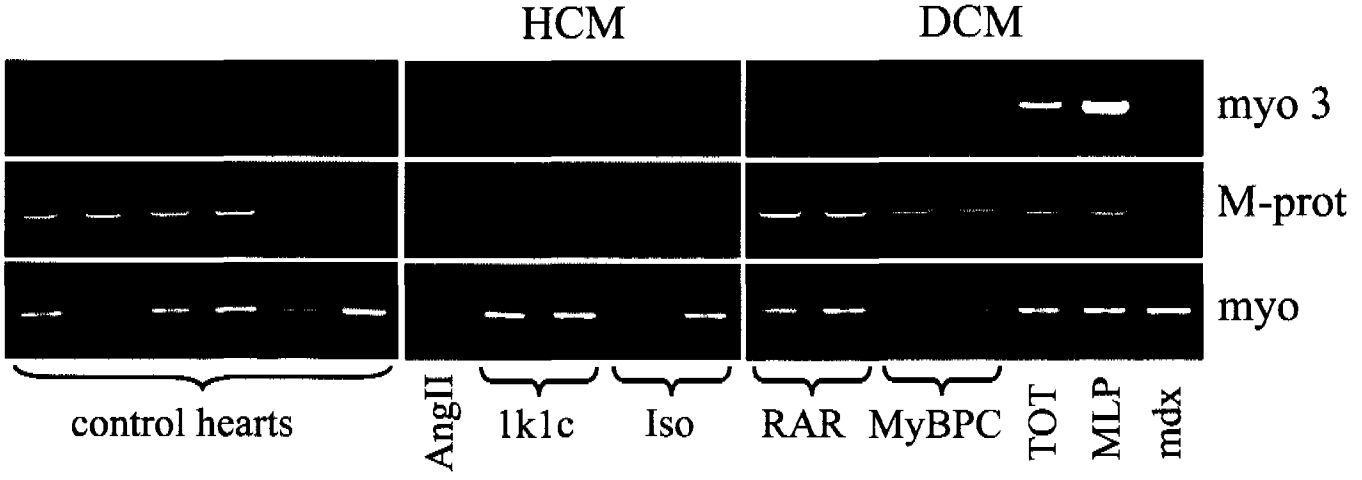

Total RNA extracted of all these models has been tested by RT-PCR with primers specific for myomesin, M-protein and myomesin 3 as described in chapter 6.3.4. No significant differences can be detected in the expression level of myomesin (third panel) or M-protein (second panel) transcripts between hypertrophic, dilated and control hearts. Interestingly, in several mouse models of dilated cardiomyopathy, the expression of the myomesin 3 gene is upregulated (first panel). The highest level of myomesin 3 reexpression can be found in MLP knockout mice, but also TOT mice show a high level of the myomesin 3 transcript. In addition, RAR and mdx mice show a slight increase in myomesin 3 expression. MyBPC transgenic mice and all models of hypertrophic cardiomyopathy show no significant differences in the expression of myomesin genes compared to control hearts.

6.3.15 Reexpression of EH-myomesin in human patients with dilated cardiomyopathy

To check the expression of the myomesin, M-protein and myomesin 3 genes in humans suffering from cardiomyopathies, RT-PCR analysis was carried out using total RNA isolated of different human patients suffering from hypertrophic or dilated cardiomyopathy and compared to control hearts (Figure 6.30). The samples have been tested with the same primers used for the analysis of different human tissues: The myomesin transcript is evenly expressed in all heart samples (first panel) whereas the EH-myomesin isoform is clearly upregulated in all patients suffering from dilated cardiomyopathy (DCM, second panel) compared to hypertrophic cardiomyopathy (HCM) and controls, with a rather big variability in the level of expression. This is in agreement to mouse models of DCM such as the tropomodulin-overexpressing transgenic (TOT) mouse (Sussman *et al.*, 1998) and the muscle LIM protein (MLP) knockout mouse (Arber *et al.*, 1997) showing also an upregulation of this EH-myomesin (Agarkova *et al.*, 2000). This re-expression of the longer myomesin isoform in DCM correlates well with the already described re-expression of fetal isoforms of several sarcomeric proteins in diseased hearts (Chien, 1999). No significant differences could be found in the total expression level of all myomesin isoforms and of the M-protein and myomesin 3 genes, even though the alternative splicing machinery produces a bigger amount of the longer EH-myomesin isoform in the hearts of DCM patients.

Figure 6.30: *EH-myomesin is reexpressed in human patients suffering from dilated cardiomyopathy.* RT-PCR analysis of human patients suffering from hypertrophic or dilated cardiomyopathy and of control hearts using again primers specific for myomesin, M-protein and myomesin 3. Myomesin is evenly expressed in all heart samples (first panel) whereas the EH-myomesin isoform is upregulated in all patients suffering from dilated cardiomyopathy (second panel). No significant differences can be detected in the expression of the M-protein (third panel) and myomesin 3 (fourth panel) genes suggesting that the transcript level of all myomesin family members is unchanged.

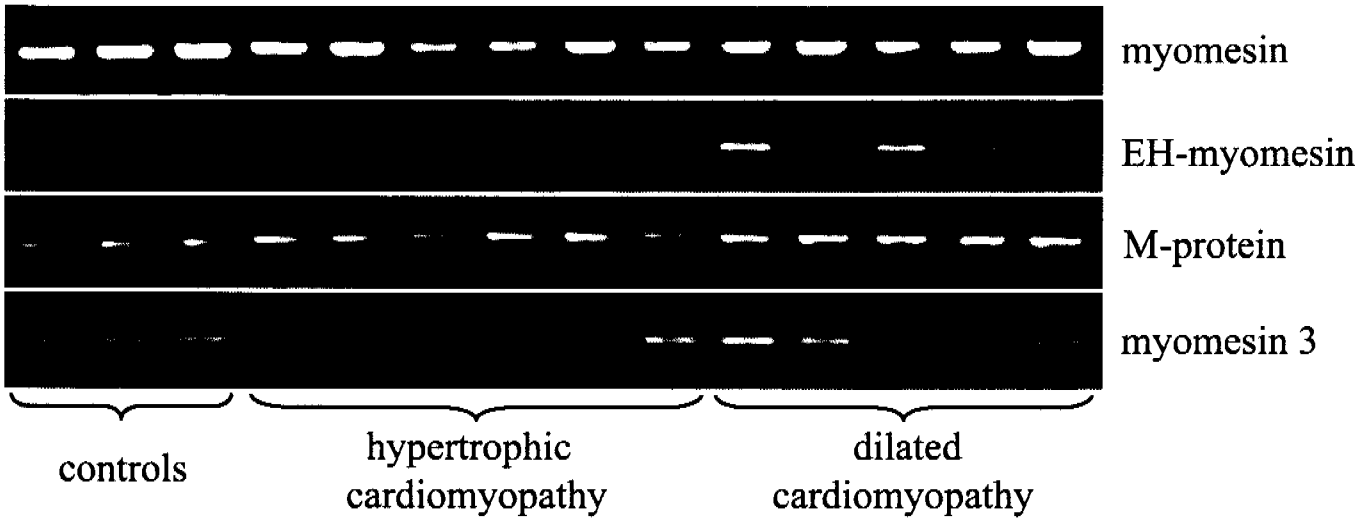

7 DISCUSSION

7.1 Myomesin is a molecular spring with adaptable elasticity

The sarcomeric cytoskeleton is responsible for ensuring the optimal interaction of the contractile filaments and proper transmission of the generated force. These functions are based largely on its remarkable elasticity, which is believed to originate from the titin filaments. We show for the first time that not only titin, but also myomesin, which was suggested to link the thick filaments in the center of the sarcomere, functions like a molecular spring. We analyzed the mechanical properties of the M-band component myomesin by AFM, TEM and CD spectroscopy. The AFM measurements of concatemers of individual myomesin domains My6 (Fn) and My10 (Ig) show a typical saw-tooth pattern in the force-extension curves, with the unfolding forces comparable with those of the Ig domains of I-band titin. The domains readily refold after relaxation. AFM measurements characterize the alternatively spliced EH-segment of myomesin as an entropic spring comparable to the PEVK domain of titin (Linke *et al.*, 2002). This characterization is complemented by TEM and CD spectroscopy indicating that the EH-segment is a random coil with a mostly non-folded conformation.

7.1.1 Structural role of myomesin in the sarcomere

Myomesin is a constitutive component of the sarcomeric M-band. It is expressed in all types of vertebrate striated muscle (Agarkova *et al.*, 2000) and can be detected in the M-bands of the first sarcomeres during myofibrillogenesis (Ehler *et al.*, 1999). The tight association with titin and myosin (Obermann *et al.*, 1997) suggests that myomesin is an integral component of the sarcomeric cytoskeleton. The myomesin molecule consists of a unique head domain, followed by twelve Fn and Ig domains. The EH-myomesin isoform contains an additional unique segment of about 100 aa between the domains My6 and My7. This isoform, which was previously known as skelemin (Price, 1987, Price and Gomer, 1993) was originally found in embryonic heart (Agarkova *et al.*, 2000) and later in the slow and extraocular muscle fibers of adult mice (Agarkova *et al.*, 2004).

According to the current M-band model the neighboring myosin filaments are connected by myomesin molecules that bind with their N-terminal domains to the myosin rod (Obermann *et*

al., 1995, Obermann *et al.*, 1997, Auerbach *et al.*, 1999). Via their C termini they dimerize in an antiparallel fashion (Lange *et al.*, 2005b) and in this way crosslink the thick filaments in the M-band, playing a role analogous to that of *a*-actinin in the Z-disk. Interestingly, both myomesin and α-actinin are modular proteins consisting of Ig/Fn domains or spectrin repeats, respectively, and may regularly be subjected to mechanical stress during contraction.
Considering the interaction of titin domain m4 with myomesin fragment My4-6 (Obermann *et al.*, 1997), myomesin in a complex with titin forms the M-band filament system, which is responsible for the lateral alignment of myosin filaments. It was suggested that this system might be under tension in the activated sarcomere because the myosin filaments will try to escape from the central position due to random deviations of the cross-bridge forces on both halves (Agarkova *et al.*, 2003), the so-called intrinsic instability. This active mechanical role implies some structural basis for the generation of a restoring force, which counterbalances these shearing stresses. Recent single-molecule manipulations helped to explain a potential mechanism of the restoring force generated by elastic titin filaments (Granzier and Labeit, 2004). However, nothing was known until now about the mechanical properties of M-band components.

7.1.2 Myomesin Fn/Ig domains have mechanical properties similar to titin Ig domains

Here, we performed for the first time single-molecule measurements on myomesin. The stretching of polypeptides, constructed from the domains My6 (Fn) and My10 (Ig) resulted in a typical saw-tooth pattern demonstrating the sequential unfolding of the individual modules. The mechanical stability of the My10 (Ig) domain of myomesin is comparable with the Ig domains (I65-70) of the differentially spliced region of titin (Watanabe *et al.*, 2002a), which is in agreement to the evolutional relationship between these domains (Kenny *et al.*, 1999). The similarity is supported by the finding that most of the Ig domains of myomesin have near their C-terminal end a glutamic (or aspartic) acid which is conserved in most of the Ig domains of this alternatively spliced part of titin (Witt *et al.*, 1998). In contrast to previous measurements which showed that Fn domains in titin have a mechanical stability that is in average 20% lower than the one of Ig domains (Rief *et al.*, 1998), we could not find a significant difference between the forces necessary to unfold My6 (Fn) and My10 (Ig). In addition, insect flight muscle proteins projectin and kettin were recently reported to have similar mechanical properties compared to titin with weaker Fn domains compared to Ig domains (Bullard et al.,

2006). Since domain My6 interacts with titin (Obermann *et al.*, 1997) in the M-band it might participate in the formation of the M-filaments (Luther and Squire, 1978). This is reflected by the close relation to the Fn domains of A-band titin (Kenny *et al.*, 1999), which tightly associate with the thick filament. Interestingly, My6 and My10 can refold again after a relaxation phase and the folding is correct even after multiple repetitions of the stretch-release cycles, suggesting a physiological role under extreme conditions.

7.1.3 The EH-segment is a mini-analogon of the PEVK domain of titin

Some muscle types express the EH-myomesin isoform, generated by the inclusion of the EH-segment of unknown secondary structure in the centre of the molecule. The analysis of the primary structure suggests that this segment has characteristic properties, despite the rather low sequence homology between different vertebrates (Agarkova *et al.*, 2000). Computer simulations (PONDR) predict the EH-segment to be a disordered region with a significantly lower probability of β-sheet conformation. In agreement with this prediction we found that the CD spectra of the recombinant human EH-segment show the characteristics of a largely non-folded protein with residual secondary structure. Furthermore, the EH-segment is not visible in rotary shadowed specimen viewed by TEM, indicating that it is not as well folded as the Ig and Fn domains and does not form a compact structure. Interestingly, these properties of the EH-segment of myomesin are shared by the PEVK domain of titin (Ma and Wang, 2003, Li *et al.*, 2002). Moreover, the AFM stretching of the $(My6\text{-}EH)_4$ polypeptide clearly shows that the EH-segment has elastic properties represented by the presence of the initial spacer equivalent to the sum of EH-segment contour lengths of 35 nm in the force-extension curves before the unfolding peaks of My6. The measured persistence length shows a clear peak at ~0.3 nm, which is close to the theoretical value of a random coil (0.18 nm) and to the measured value of an unfolded polypeptide strand (0.4 to 0.8 nm (Rief *et al.*, 1997, Rief *et al.*, 1998)). The persistence length of this segment seems to be smaller compared to the PEVK domain of titin, which shows a relatively wide range of values from 0.15 to 2.3 nm (Tskhovrebova *et al.*, 1997, Watanabe *et al.*, 2002b, Li *et al.*, 2002, Leake *et al.*, 2004). However, it has been suggested that the PEVK region may not be a pure random coil but contains structured elements by sequence-specific hydrophobic (Leake *et al.*, 2004) or charge interactions (Forbes et al., 2006). In addition, multiple elastic conformations resulting from varying degrees of proline isomerisation have been postulated (Li *et al.*, 2001), which has

been questioned by a recent study (Sarkar et al., 2005). In addition, these proline-rich sequences seem to be candidates as major hubs of SH3-dependent signaling pathways, which could play an important role in mechanical sensing (Ma et al., 2006). In this context, the EH-segment of myomesin could play a similar function in the M-band, even though the presence of polyproline helices is rather unlikely for this domain because of the smaller amount of proline residues compared to the PEVK domain. Interestingly, measurement of the apparent persistence lengths of different parts of the PEVK region of titin revealed a hierarchical arrangement according to local flexibility: the N-terminal segment is the most rigid and the C-terminal part is the most flexible segment within the domain (Nagy et al., 2005).

By using several methods, based on different physical principles, we demonstrated that the EH-segment lacks an obvious secondary structure and functions like an entropic spring. Therefore, we propose that the EH-domain of myomesin belongs to the rapidly growing family of intrinsically unstructured proteins (IUPs) (Tompa, 2002). The functional state of these proteins or protein fragments depends on the flexible, random-coil conformation under physiological conditions, which is provided by the special composition with a predominance of the so called disorder-promoting amino acids (like E, P, K) and a scarcity of order-promoting amino acids (like W, C, F) (Tompa, 2002).

7.1.4 EH-myomesin is the small brother of titin

In summary, EH-myomesin is a kind of miniature titin, which is also composed of stretches of Ig and Fn modules separated by largely unstructured segments, the PEVK domain and the N2A or N2B sequence insertions, which are differentially expressed in heart and skeletal muscles (Labeit and Kolmerer, 1995, Trombitas *et al.*, 1999). Titin generates a restoring force based on the mechanism of entropic elasticity. In the absence of external force its entropic springs take a random conformation trying to maximize the entropy of its segments, while extension or compression of the chain generates a restoring force due to reduction of entropy. The elasticity of entropic components allows titin to be extended fully reversibly at physiological forces, without the need to unfold the Ig domains (Tskhovrebova *et al.*, 1997). Recently, it was shown that the elasticity of such entropic components (e.g. the unique N2B sequence) could also be modulated by reversible formation of disulfide bridges (Leake et al., 2006). Similar to titin, the probability for myomesin domains to unfold decreases with rising pulling speed. Thus, the domains can resist rather strong forces acting for a short time,

whereas even a weak force can unfold it, being applied for a long time. Once unfolded, the domains need seconds of complete relaxation to refold. Therefore, the stability of myomesin domains is mostly endangered in the M-bands of slow twitch skeletal fibers, which are characterized by prolonged twitch duration and are active over long periods of time. Two EH-modules present in the myomesin dimers could considerably increase the elastic working range in the M-bands of slow twitch fibers and prevent the unfolding of the Fn / Ig domains of myomesin. Considering the persistence length of 0.3 nm, the end-to-end length of the EH-segment in zero-force (slack) conformation is about 6 nm, while in the fully extended state it amounts to 35 nm. The elastic force might rapidly align the thick filaments during relaxation, while the refolding of Fn and Ig modules might be not completed before the next contraction in constantly active muscles. Although the significance of this is not completely clear at the moment, the expression of myomesin isoforms seems to correlate with the expression of titin isoforms at least in some muscle types. Indeed, the developmental control of titin isoform expression leads to a shift from longer isoforms in the fetal heart to shorter isoforms in the adult heart (Lahmers *et al.*, 2004, Opitz *et al.*, 2004), similar to the predominant expression of the EH-isoform in the embryonic heart compared to a predominance of myomesin lacking the EH-segment in adult heart. The expression of longer titin isoforms in soleus muscle (Freiburg *et al.*, 2000) also correlates with the presence of EH-myomesin there (Agarkova *et al.*, 2004). This coordinated regulation of the M-band protein composition, as well as the titin isoform content probably reflects adaptations of the sarcomeric cytoskeleton to the special functional regime in different muscles.

7.1.5 Mechanical portrait of myomesin

We suggest that myomesin is a molecular spring characterized by complex visco-elastic properties and propose a mechanical portrait for this protein, which describes the behaviour of myomesin under stretch (Figure 7.1). The elastic component arises from the straightening of the serially linked Fn / Ig domains chain and the alternatively spliced EH-segment. These behave as two entropic springs with different stiffness in a similar way as the tandem Ig segments and the PEVK domain of titin (Trombitas *et al.*, 1998). In the relaxed muscle, the myomesin dimers are in a compact state. During sarcomere activation the myomesin molecules may be straightened due to small misalignments of the neighboring myosin filaments. The compliable Fn / Ig domains chain will be stretched first, followed be the

extension of the stiffer EH-segment. The additional elasticity brought in by the EH-segment seems to be correlated to the working length range of sarcomeres (Agarkova *et al.*, 2003) and may help to prevent the opening of Fn / Ig modules, which need a rather long period of relaxation for refolding. However, in the case of extremely high or extremely long lasting stretching forces the tightly folded Ig and Fn domains might function as reversible "shock absorbers" to avoid rupture of the M-bands (Figure 7.1). These mechanical properties of the myomesin molecule are probably crucial for the stability of the sarcomeric cytoskeleton during contraction.

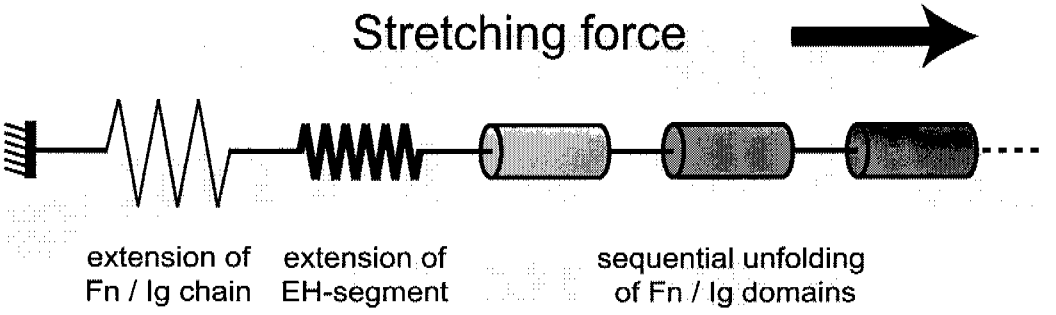

Figure 7.1: Myomesin is a molecular spring: In the relaxed state it is in a coiled conformation. Its behaviour during extension might be modelled as series of elastic springs with different stiffness together with the viscous elements, corresponding to the unfolding of individual domains. Stretch would result first in the straightening of the Fn / Ig domains chain, followed by the extension of the stiffer EH-segment. The tightly folded Fn and Ig domains might function as "shock absorbers" by reversible unfolding only in the case of extremely high or extremely long stretching forces. This mechanism might prevent the permanent rupture of the M-band filaments due to overstretching in the process of sarcomere contraction (Schoenauer *et al.*, 2005).

7.2 The molecular composition of the sarcomeric M-band correlates with muscle fiber-type

The basic principles of sarcomeric organization are the same in all kinds of vertebrate striated muscle. However, sarcomeres in different muscle types modulate their functional characteristics by using distinct isoforms of contractile proteins. In this respect it is remarkable that slow fibers of skeletal muscle express a number of protein isoforms specific for cardiac muscle (Schiaffino and Reggiani, 1996). This might be due to a similar working regime since both types of muscle have to be active continuously over long periods of time. The data discussed in this section show that slow fibers of adult mouse skeletal muscle express the EH-myomesin isoform, which was characterized previously as an M-band component specific for embryonic heart (Agarkova *et al.*, 2000). This isoform is generated by the insertion of the additional EH-segment in the central part of the myomesin molecule. As discussed above, this domain works as an entropic spring similar to the PEVK domain of titin, which protects the immunoglobulin-like domains from unfolding during extreme stretching (Linke et al., 1998).

EH-myomesin is strongly expressed in all type I/β and in a part of the IIa fibers, but is absent from the type IId and IIb fibers of the adult mouse hind limb. Interestingly, IIa fibers accumulate high levels of myomesin 3 (discussed chapter 7.3.2) and in IIb fibers, M-protein is highly expressed (discussed chapter 7.2.1). The contractile parameters, measured in single muscle fibers, depend mainly on the myosin isoform content and have been shown to increase in the order: type I<IIa<IId<IIb (Bottinelli, 2001). Thus, EH-myomesin expression is restricted to fibers that are characterized by more slow motor properties, though formally IIa fibers belong to the "fast-twitch" class of fibers. The EH-myomesin expression pattern does not overlap precisely with the MHC isotypes, because it appears only in part of the type IIa fibers. The reason for such heterogeneity between the type IIa fibers is not clear at the moment, but probably reflects some differences in the contractile characteristics. The IIa fibers negative for EH-myomesin might represent the hybrid IIa/IId fibers, which are rather common in rat skeletal muscle (Bottinelli *et al.*, 1994a). Alternatively, the difference in the functional properties between IIa fibers characterized by a differential M-band composition could result from various myosin light chain combinations (Bottinelli *et al.*, 1994b).

7.2.1 EH-myomesin and M-protein have a complementary expression pattern

Expression of EH-myomesin starts in slow fibers of mouse leg muscles only several days after birth, i.e. when its accumulation ceases in cardiac muscle. All fibers in the hind limb muscles of the neonatal mouse have the same M-band composition, expressing about equal amounts of M-protein and being negative for EH-myomesin. This is also the case for the numerous fibers that express MHC-I at this time (Maggs *et al.*, 2000). However, all type I fibers in the adult mouse are EH-myomesin positive. Therefore, we assume that the special molecular composition of M-bands in slow fibers, in particular the EH-myomesin expression, is not completely controlled by the genetic mechanisms leading to co-expression with certain slow MHC isoforms. The progressively increasing locomotion activity of animals after birth may stimulate the development of specialized M-band structures in the maturing slow fibers. The postnatal increase of EH-myomesin expression is accompanied by the down-regulation of M-protein in the same fibers, which was reported in previous studies on rat muscle (Carlsson and Thornell, 1987, Grove *et al.*, 1985, Grove *et al.*, 1989). As a result, EH-myomesin and M-protein show a complementary expression pattern in adult mouse skeletal muscle.

Thus, it seems that M-protein and EH-myomesin are counter players that provide some mutually exclusive properties to the M-bands. Assuming that the neighboring myosin filaments are connected in the M-band by a set of distinct molecules characterized by different lengths and elasticity, it is their relative amount that will control the mechanical properties of the thick filament lattice. The M-bands of fast fibers are characterized by the expression of high levels of M-protein and the shorter myomesin isoform, lacking the EH-fragment. This molecular composition probably improves the alignment and stiffness of the thick filament lattice in the fast fibers, characterized by the quick development of force (Pask *et al.*, 1994). In the M-bands of mouse slow fibers M-protein is practically absent and a significant part of the myomesin molecules are longer due to the addition of the EH-segment, which probably renders the A-band lattice more loose and elastic.

7.2.2 M-bands containing a high proportion of EH-myomesin look "fuzzy" in electron microscopic preparations

A strong argument, favoring the assumption that the level of EH-myomesin can influence the elastic properties of the M-band, is provided by studies on embryonic hearts that express much more of the EH-myomesin isoform than slow fibers. Electron-microscopic pictures reveal that the electron-dense M-band becomes visible in cardiac sarcomeres only around birth (Smolich, 1995). This phenomenon was previously attributed to the appearance of the muscle isoform of creatine kinase (MM-CK) (Forsgren *et al.*, 1982, Wallimann *et al.*, 1983). In contrast to the clear absence of MM-CK in embryonic heart, the slow fibers of the hind limb express this enzyme, as was shown in previous studies of rat muscles (Carlsson *et al.*, 1990) and confirmed here.

However, the diaphragm type I fibers of rat hardly express MM-CK and show indistinct M-bands on electron-microscopic preparations (Thornell *et al.*, 1990). Our data cannot rule out the possibility that slow fibers of mouse hindlimb expresses less MM-CK than fast fibers and that this is the reason, why the M-band looks diffuse in some of the soleus fibers. Future experiments using immunoelectron microscopy might resolve this question. However, the finding that extraocular muscles (EOM) express high levels of EH-myomesin and low levels of MM-CK (Andrade *et al.*, 2003) suggests that muscles, which need an "elastic" sarcomere skeleton might also have different metabolic requirements.

According to recent studies the molecules of MM-CK bind in the M-band either directly to myomesin and M-protein (Hornemann *et al.*, 2003) or via DRAL/FHL-2 to titin (Lange *et al.*, 2002). However, only a minor fraction of the MM-CK molecules (5 ± 10%) localizes to the M-band of the myocytes, while the majority is found diffuse in the cytoplasm (Schäfer and Perriard, 1988, Wallimann *et al.*, 1992). Therefore, the less dense M-band appearance seen in the EM might potentially be caused by the weaker MM-CK incorporation into M-bands that contain the EH-myomesin isoform. However, such an assumption is not supported by the observation that ectopically expressed creatine-kinase was effectively targeted to the M-bands of embryonic chicken cardiomyocytes, which express 100% of the EH-myomesin isoform (Schäfer and Perriard, 1988).

In addition to their lack of clearly visible M-bands the embryonic heart sarcomeres are characterized by significant misalignments of the thick filaments (Smolich, 1995). This was originally explained by the absence of M-bridges in such sarcomeres (Anversa *et al.*, 1981, Carlsson *et al.*, 1982). However, since then, it was established that myomesin appears in the

M-bands even in the first sarcomeres formed in the developing heart (Agarkova *et al.*, 2000, Ehler *et al.*, 1999). Recent studies explained the poorly registered A-band and the absence of distinct M-bands in the extraocular muscles by the low levels of myomesin and M-protein (Andrade *et al.*, 2003, Porter *et al.*, 2003).

In contrast, our data show that the total myomesin content in EOM sarcomeres is comparable to all other striated muscles, whereas myomesin is present mainly in the EH-isoform. Thus, the muscles that express a significant proportion of EH-myomesin (embryonic heart, EOM and slow fibers of mouse soleus muscle) show less defined (fuzzy) M-bands on electron micrographs at least in some of the fibers. We suggest that in addition to the altered incorporation of creatine kinase, this effect might be explained by small misalignments of the M-bands containing a high proportion of EH-myomesin. The about 100 amino acids of the unfolded EH-segment might add 30 additional nm to the myomesin molecule, which is a significant gain of length, considering the overall myomesin length of 50 nm (Obermann *et al.*, 1995). This effect might be augmented by the addition of the Mex-5 exon to the titin M-band region in soleus and diaphragm muscle (Kolmerer *et al.*, 1996). Interestingly, not all type I fibers of mouse soleus show the diffuse M-bands on EM pictures, despite the finding that all of them are EH-myomesin positive (Agarkova *et al.*, 2004). This indicates that even the elastic M-bands might be aligned after sufficient relaxation time. Thus the proportion between diffuse and distinct M-band appearance in type I fibers of mouse soleus might depend not only on the level of EH-myomesin in a particular fiber but also on the relaxation procedure.

7.2.3 M-band and eccentric contraction

Therefore, the M-band protein composition, as well as the titin isoform content probably reflects the adaptations of the sarcomeric cytoskeleton to the special functional regime in different muscles rather than the MHC isoform profile per se. This is supported by the observation that EOM, which contains predominantly fast-twitch fibers express a high proportion of EH-myomesin and low level of M-protein (Andrade *et al.*, 2003, Porter *et al.*, 2003). The M-band composition seems to depend more on the level of activity or the working length range of the sarcomeres in a given fiber. Interestingly, a specific feature of all murine muscles with decreased levels of M-protein accompanied by increased levels of EH-myomesin (e.g. diaphragm, soleus and EOM muscles) is their special functional regime. All

these muscles are committed to continuous contractile activity often accompanied by stretching (Collins et al., 1975; (Gillis, 1996, Walmsley *et al.*, 1978). It is known that such stress like activation of the extending sarcomere (eccentric contraction) can lead to the damage of the contractile structures (for review see (Allen, 2001)).

The hypothesis of the importance of the EH-myomesin isoform for the mechanical properties of the M-band has to be tested by resolving the molecular organization of this structure in more detail. However, the relevance of the structural integrity of the M-band for the overall stability of the sarcomere is underlined by numerous studies that are published on eccentric contraction. They reveal that the disruption of M-band bridges is one of the most prominent signs of damage after eccentric contraction (Macpherson *et al.*, 1996, Ogilvie *et al.*, 1988). Future experiments will show whether the increased vulnerability of the M-bands in the unloaded or diseased muscle is accompanied by alterations in M-band composition.

7.3 Myomesin 3 – a novel component of the sarcomeric M-band

7.3.1 Myomesin, M-protein and myomesin 3 have evolved from a common ancestor

We have shown, that myomesin 3 is the third member of the myomesin protein family and a novel component of the sarcomeric M-band in skeletal muscle generated from a distinct gene. According to the alignment of the amino acid sequences, the identity level between myomesin 3 and myomesin or M-protein is about 40 %, and all three proteins share the same domain arrangement (Figure 7.2). The structure of the myomesin and M-protein genes have already been analyzed in earlier studies (Steiner *et al.*, 1998, Steiner *et al.*, 1999), revealing that intron positions and phases are essentially identical. Putting these results together with the analysis of the myomesin 3 gene and with sequence alignments on the level of single domains, we can conclude that all three genes have evolved from a common ancestor. Interestingly, the unique N-terminal domains of the three proteins are much less conserved compared to the rest of the molecule and belong to the intrinsically unstructured protein sequences (IUPred), whose exact 3-dimensional structure does not seem to be essential for its function (the binding to the myosin filament (Obermann *et al.*, 1997)). It was exciting to find myomesin 3 as the third member of this protein family after almost 25 years of research in this field (Eppenberger *et al.*, 1981, Grove *et al.*, 1984). But the interesting question arises: Why do some muscle types need a third component in the M-band, which is very similar to myomesin and M-protein and shares exactly the same domain arrangement?

Myomesin seems to be the universal M-band component because its total amount in the sarcomere remains approximately the same in all kinds of striated muscle (Agarkova *et al.*, 2004). According to the 3-dimensional model of the M-band (Lange *et al.*, 2005b), dimers of myomesin are the fundamental bridge between the myosin filaments. The mechanical properties of these bridges can be adjusted by the alternatively spliced EH-segment (Schoenauer et al., 2005), an intrinsically unstructured polypeptide which functions as an entropic spring comparable to the PEVK domain of titin. The addition of the EH-domain may render the myosin crosslinks more elastic, which could also be part of an adaptation process of the sarcomeric cytoskeleton to an altered contractile behaviour of the sarcomere. Interestingly, the expression level of the longer EH-myomesin seems to be linked to the presence of longer titin isoforms, e.g. in the embryonic heart (Agarkova *et al.*, 2000, Lahmers *et al.*, 2004, Opitz *et al.*, 2004) suggesting that the isoform expression pattern of different components of the sarcomeric cytoskeleton is correlated. Because of the high degree of

sequence conservation between all myomesin family members (same domain arrangement), it can be assumed, that M-protein and myomesin 3 play a similar structural role in the M-band as myomesin. Although the essential function of myomesin has not been proven, evidence for its importance is provided by mice with a truncated titin (lacking the myomesin binding site) that show a gradual destruction of their muscles (Gotthardt *et al.*, 2003).

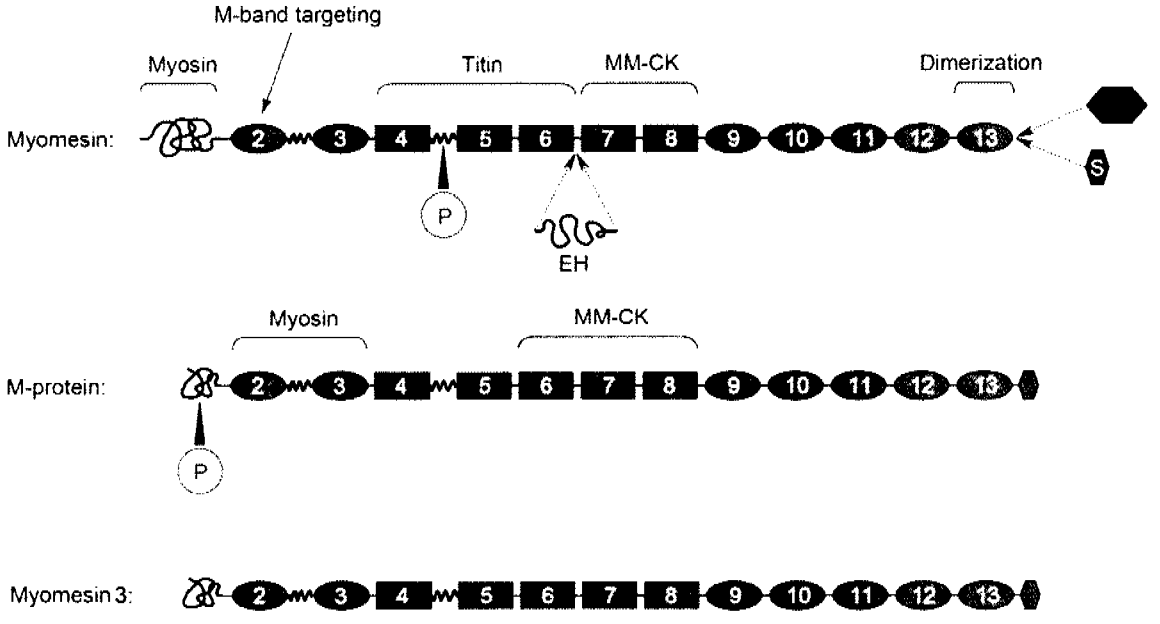

Figure 7.2: *Schematic representation of all myomesin family members.* The main part of myomesin, M-protein and myomesin 3 consists of identically arranged tandem repeats of Ig (ellipses) and Fn (rectangles) domains. The N-terminal parts as well as the alternatively spliced EH-segment are predicted to be in an intrinsically disordered state. Myomesin has two sites of alternative splicing. The one at the C-terminus is specific for birds and leads to the expression of H (heart) and S (skeletal) myomesin isoforms. Mammalian muscles express the shorter S-myomesin in all muscle types. The EH-myomesin isoform is generated by the inclusion of the EH-segment in the central part of the molecule. Phosphorylation sites (P, blue circles) (Obermann *et al.*, 1997, Obermann *et al.*, 1998) and interacting partners (identified above brackets) (Obermann *et al.*, 1997, Obermann *et al.*, 1998, Hornemann *et al.*, 2003, Lange *et al.*, 2005b) are indicated (adapted from (Agarkova and Perriard, 2005)).

7.3.2 Myomesin 3 shows a fiber-type specific expression pattern

In combination with the other members of the myomesin family, myomesin 3 shows a muscle-type specific expression pattern in mouse. It is strongly accumulated in different types of skeletal muscle such as embryonic (neonatal) muscle, adult slow muscle and extraocular muscle. In addition myomesin 3 shows a fiber-type specific expression pattern in adult skeletal muscle with the highest level in IIA fibers (intermediate speed). We also could confirm that myomesin is an ubiquitous component of the myofibrillar M-band and that M-

protein and the EH-myomesin isoform are differentially expressed in striated muscle. The expression of M-protein in chicken heart (Grove *et al.*, 1985), chicken fast skeletal muscle (Grove *et al.*, 1985, Grove *et al.*, 1987);Grove et al., 1988;(Grove *et al.*, 1989) and rat fast fibers (Thornell *et al.*, 1987) has already been shown in many studies. Its correlation with the expression pattern of the EH-myomesin isoform, which is accumulated not only in the embryonic heart (Agarkova *et al.*, 2000), but also in slow muscle of mouse, has been revealed only recently (Agarkova *et al.*, 2003, Agarkova *et al.*, 2004).

It is remarkable that the levels of EH-myomesin, M-protein and myomesin 3 are regulated in a fiber-type dependent manner. In mouse, EH-myomesin is expressed mainly in type I fibers and part of the type IIA fibers (Agarkova *et al.*, 2004) whereas myomesin 3 can be detected at high levels in type IIA fibers and at low levels in type I fibers. M-protein, the counter-player of EH-myomesin, is highly accumulated in fast IIB fibers, while IIA fibers express only low amounts of this protein. In the mouse heart, EH-myomesin is the major myomesin species in the embryo, whereas myomesin (without EH-segment) and M-protein can be detected at high levels in the adult heart. Interestingly, myomesin 3 is not expressed in the mouse heart at any stage, suggesting that this protein is not essential for sarcomere function. This differentially regulated expression pattern of the myomesin family proteins suggests, that the relative amounts of EH-myomesin, M-protein and myomesin 3 in the M-band of the sarcomere is linked to the contractile characteristics of a certain fiber. Consequently, each muscle is characterized by its unique M-band protein composition, which can be adapted to divergent physiological needs in different muscle types.

7.3.3 Is myomesin 3 an integral component of the M6 line?

In this context, it has to be emphasized, that different vertebrate muscle fiber-types have different M-band appearances in electron microscopic preparations. Generally, the slowest fibers have four-line M-bands (M6, M4, M4', M6' visible), the fastest have three-line M-bands (M4, M1, M4' visible) and fibers of intermediate speed have variations of a five-line M-band (M6, M4, M1, M4', M6' visible; (Sjostrom and Squire, 1977, Thornell *et al.*, 1987, Edman *et al.*, 1988, Carlsson *et al.*, 1990). Consequently, the M-band appearance in EM could be used as an indicator of the physiological properties of a given muscle fiber. Data from immunoelectron microscopy suggest myomesin as an integral component of the M4 line (Obermann *et al.*, 1996), which is supported by the fact that myomesin is expressed in all

types of vertebrate striated muscle (Agarkova *et al.*, 2000, Agarkova *et al.*, 2004). In addition, the expression of the longer EH-myomesin isoform seems to correlate with a fuzzy appearance of the M-band in the EM, underlining that myomesin is involved in the longitudinal alignment of the myosin filaments (Agarkova *et al.*, 2003). The presence of M-protein was proposed to be responsible for the appearance of the M1 line (Obermann *et al.*, 1996), which is confirmed by the simultaneous absence of M-protein and the M1 line in slow fibers (Carlsson *et al.*, 1990).

The expression of myomesin 3 in type IIA and type I fibers and its localization to the M-band of the sarcomere fits well in this picture and seems to correlate nicely with the appearance of the M6 line in these fiber types. Consequently, we suggest that myomesin 3 may be an integral component of the M6 line in the M-band of the sarcomere. Myomesin 3 (in intermediate fibers) and M-protein (in fast muscle and heart) might improve the stability of the thick filament lattice during contraction. Since M-protein and myomesin 3 are absent in special muscle types such as slow muscle (no M-protein) and heart or fast fibers (no myomesin 3), it seems likely that they have not only a simple structural, but also a functional role by offering binding places for enzymes or signaling molecules at specific sites in the M-band according to the particular physiological needs of the fiber type. It is important to mention, that the muscle-type isoform of creatine kinase binds to the central parts of myomesin and M-protein, but with different binding affinity (Hornemann *et al.*, 2003).

7.3.4 The N-terminal part of myomesin 3 is sufficient for M-band localization

In addition, our experiments showed that the N-terminal part of myomesin 3 (domains 1-3) is sufficient for the targeting to the M-band of the sarcomere in neonatal rat cardiomyocytes. Even the N-terminal domain alone localizes mainly to the M-band, but less specific compared to the longer construct. Similar studies have been already performed with myomesin revealing that the two N-terminal domains are targeted to specific sites in the sarcomere (Auerbach *et al.*, 1999): The unique head domain of myomesin, possessing the binding site for myosin (Obermann *et al.*, 1997), localized to a central area within the A-band, and the adjacent immunoglobulin-like domain localized to the M-band. It has to be underlined, that the N-terminal domain(s) of myomesin 3 are targeted to the M-band even in a cell type (cardiomyocyte), which does not express this protein under normal conditions. Surprisingly, the N-terminal domain of myomesin 3 seems to localize even more specifically to the M-band

in cardiomyocytes than the N-terminal domain of myomesin (Auerbach *et al.*, 1999). This could be explained by the fact that the binding places for myomesin are occupied by the endogenous protein, whereas the binding places for myomesin 3 are free because of the lack of endogenous protein.

7.3.5 Species specific differences in M-band protein composition

Interestingly, the expression levels of EH-myomesin and myomesin 3 show not only tissue-specificity, but also species-specific differences. Myomesin 3 can easily be detected in the hearts of human, while in the heart of mouse or rat, it is totally absent. In addition EH-myomesin is highly expressed in slow muscle of mice (Agarkova *et al.*, 2004), but not of chicken (Agarkova *et al.*, 2000) and shows some variability in different species. What could be the reason for this discrepancy?

First, it is known that in the hearts of different species the predominating myosin heavy chain isoform varies. Furthermore, the beating frequency is increasing from big to small mammals and seems to be somehow correlated with the appearance of the electron-dense M-band in electron microscopic preparation (Pask *et al.*, 1994), suggesting that the appearance of the M6 line may vary according to the expression level of myomesin 3. The expression of myomesin 3 in the heart of humans may be one of the adaptations of the M-band as a part of the sarcomeric cytoskeleton to the altered contractile behaviour of the human cardiomyocytes compared to mouse. In addition, changes in the proportion of different M-band proteins may also reflect the different shortening velocity or contractile force of the same fiber types (myosin isoforms) in different animals (Widrick *et al.*, 1997).

7.3.6 Myomesin family proteins and cardiomyopathies

Consequently, the expression level and proportion of the different myomesin family members in the M-band seems to be in an equilibrium, which may be able to adapt to changed physiological or mechanical properties of a given myofiber. This seems to be the case not only in respect to different fiber types in skeletal muscle, but also in disease states such as cardiomyopathies. Our experiments show that such adaptations of the M-band may vary with the type of disease model, but may also be species-specific. In the case of dilated

cardiomyopathy (DCM), we see a clear upregulation of myomesin 3 in most of the mouse models tested, and some of these models also re-express the EH-myomesin isoform (MLP and TOT, (Agarkova, 2000)).

In human, the picture looks different: In hearts of patients suffering from DCM, the expression level of EH-myomesin is clearly elevated, whereas the myomesin 3 gene is expressed at similar levels in control, DCM and HCM (hypertrophic cardiomyopathy) hearts. The re-expression of EH-myomesin (the "embryonic heart" myomesin isoform) in the case of DCM in mice and humans correlates well with the already described re-expression of fetal isoforms of several sarcomeric proteins in diseased hearts (Chien, 1999). Interestingly, the upregulation of EH-myomesin in DCM also correlates with the increased expression level of longer titin isoforms (Makarenko *et al.*, 2004), which depresses the proportion of titin-based stiffness in the end-stage failing heart. Interestingly, in hypertrophic hearts of mice or humans, no changes in the expression level of the myomesin family members could be detected. In addition, most of the mutations associated with HCM are linked to contractile proteins or proteins binding directly to such molecules, whereas many mutations associated with DCM could be found in components of the (sarcomeric) cytoskeleton (Chien, 1999).

7.4 Outlook

This study reports a significant progress in the understanding of myomesin function in the sarcomeric M-band of vertebrates. The mechanical properties of myomesin were thoroughly measured by biophysical techniques and the expression of all myomesin family members (mainly in mouse) was analyzed by different methods. In addition, several cardiomyopathic hearts (DCM and HCM) of human patients as well as of mouse models were tested for the expression of M-band components. Interestingly, most of the hearts in the state of DCM show higher levels of EH-myomesin or myomesin 3, suggesting that the M-band tries to adapt to the changed mechanical stress in the diseased state.

We propose additional experiments to continue the investigation of M-band protein expression in cardiomyopathies started in chapter 7.3.6. It would be interesting to test the hearts of mouse models showing a clear progression from HCM to DCM (e.g. trans-aortic constriction, TAC). In such models, it may be possible to correlate the changes in M-band protein levels to specific states in the progression of the disease which would help to clarify the role the myomesin proteins in the whole process. In addition, the analysis of transgenic mouse models with a cardiomyopathy phenotype (e.g. MLP KO) could help to clarify the role of the M-band in cardiac disease. It would also be interesting to test the effect of training on the expression of M-band components in heart or skeletal muscle.

Another important project is the myomesin KO model, which will help to further analyze myomesin and M-band function. This mouse has been recently generated (Perriard, J.-C. and Chen, J., University of California, San Diego) and no major disease phenotype was described until now. It will be very interesting to characterize these mice which possibly may have changes in the M-band stability or protein composition. Maybe it will be necessary to stress the myomesin KO mouse by a disease model such as TAC to see a clear phenotype. Single-fiber stretching or contraction experiments may be useful to analyze the stability of the sarcomeric M-band in this KO model. In addition, transgenic mice expressing only the EH-myomesin isoform (or myomesin without EH-segment) by using the myomesin KO background could be used to analyze the functions of both myomesin isoforms separately in an *in vivo* model.

Finally, the biophysical analysis of myomesin could be extended by using the AFM method to measure the binding strength between two myomesin molecules. The dimerization of myomesin via its C-terminal domain was recently reported (Lange *et al.*, 2005b) and its characterization by X-ray analysis is underway (Lange, S., pers. comm..). Measurements of

the stability of this dimer may be important to further characterize the function of myomesin in the sarcomeric M-band.

The detailed analysis of the structure and function of the M-band proteins (myomesin, M-protein and myomesin 3), which seem to be important building blocks of the sarcomere, will hopefully bring us closer to the full understanding of mechanisms underlying muscle assembly and contraction.

8 MATERIALS AND METHODS

8.1 Molecular biology

8.1.1 PCR

PCR reactions were carried out in a total volume of 25 µl with the following components: 100 pg - 1 ng template DNA, 1x Taq polymerase buffer, 1 µM of each primer, 0.2 mM dNTP mixture, 2 units of Taq polymerase (BioTherm DNA Polymerase; GeneCraft GmbH, Lüdinghausen, Germany) or proof-reading DNA polymerase (EasyA cloning enzyme, Stratagene, Amsterdam, Netherlands). Reactions were covered with mineral oil and runüp on an Eppendorf mastercycler gradient (Eppendorf scientific inc., New York, USA).

8.1.2 RT-PCR

Total RNA was isolated from embryonic heart (EH10.5, EH12.5, EH16.5 (ventricle and atrium), EH18.5), adult heart (ventricle and atrium), somites (E10.5, E12.5) , whole leg (E12.5, E14.5, newborn), musculus (m.) tibialis anterior, m. soleus, diaphragm, extraocular muscle and stomach of adult mouse using the TRIZOL Reagent (Invitrogen AG, Basel, Switzerland). RT-PCR was carried out on approximately 1 µg of total RNA, cDNA was produced with the Thermoscript RT-PCR System (Invitrogen, Basel, Switzerland) and amplified with the TAQ-polymerase (BioTherm DNA Polymerase; GeneCraft GmbH, Lüdinghausen, Germany). Primers used for the amplification of the fragments of myomesin, M-protein and myomesin 3 were derived from the corresponding mouse sequence (myomesin: Ensembl gene Myom1, ID ENSMUSG00000024049; M-protein: Ensembl gene Myom2, ID ENSMUSG00000031461; myomesin 3: Ensembl gene XP_144099.6, ID ENSMUSG00000037139). Forward primer used for myomesin: P1-TGACCGTCGTAGGGGACAAACT (exon 15); reverse primer used: P2-TCAAGACAAGTGATGTCATAGG (exon 18), generating products of 652 bp (EH-myomesin) or 358 bp (myomesin without EH-segment). Primers used for M-protein: P3-CGGTCTCAAGCGGCTTCTTACG (forward primer, exon 4), P4-CCACCGCAGCATTGGTAGACAC (reverse primer, exon 7), generating a product of 466

bp. Forward primers used for myomesin 3: P5- GCAGATACTCTACGCAGACCGC (exon 10), P6- CCGTGACAACTGCTTCTGAGGC (exon 12), generating a product of 446 bp. Primers used for the amplification of β-actin were derived from the human sequence: Ensembl gene ACTB, ID ENST00000331789. Primers used for β-actin: P7- GAAGAGCTACGAGCTGCCTGACG (forward primer, exon 4), P8- AGAAGCATTTGCGGTGGACGAT (reverse primer, exon 6), generating a product of 416 bp.

8.1.3 Isolation of DNA-fragments

Digests were run on a preparative 1-2% gel in 0.5x Tris-borate EDTA (TBE) buffer (Aushubel et al., 1987). Bands were visualized by ethidium bromide (using a long-range ultraviolet light source, excised with a clean scalpel and purified using the Nucleospin extract kit (Macherey-Nagel GmbH & Co., Düren, Germany). Yield and purity of the isolated fragments were judged by running fragments on a 1-2% agarose gel and comparing with a standard DNA ladder (Smart ladder).

8.1.4 Plasmid digests

For preparative digests, 3-5 μg plasmid DNA were digested with 10-20 units of enzyme for about 3 hours. Alternatively, DNA was digested with 1-10 units over night. When required, digestion mixes were supplemented with BSA. Restriction enzymes used were from New England Biolabs (NEB, Bioconcept, Allschwil, Switzerland).

8.1.5 Dephosphorylation of 5' ends

When cloning into a single site of a vector, 5' ends were dephosphorylated to inhibit selfligation of the vector.,). Dephoshorylation was done by incubating maximally 2 pg of linearized vector with 1x SAP buffer and 1U of SAP (shrimp alkaline phosphatase; Amersham Pharmacia Biotech) for 30 minutes at 37°C, followed by an inactivation step at 75°C for 10 minutes. After inactivation, an additional unit of SAP was added, incubation was

continued at 37°C for 30 minutes and the reaction was terminated by incubation at 75°C for 10 minutes.

8.1.6 Ligation of DNA fragments

Ligations were carried out in a total volume of 10 µl using 20-50 ng of vector and insert:vector ratios of 3:1, 1:1 and 1:3. As control, vector without insert was ligated. Vector DNA, insert DNA, T4 ligation buffer and 1 µl T4 DNA ligase were mixed and incubated either at at a temperature of 25°C for 2 hours or at 16°C over night. In general, 5 µl of reaction mixture were used for transformation of chemically competent bacteria.

8.1.7 Preparation of chemically competent bacteria

4 ml LB medium containing tetracycline was inoculated with XL-1 blue, BL-21 (DL3) Star or BLR (DE3) (Invitrogen, Basel, Switzerland) bacteria and incubated over night at 37°C. The over night culture was tranfered to 500 ml SOB medium and grown at 37°C to a density of OD_{600} = 0.5-0.8. The suspension was incubated for 15 min on ice before the cells were centrifuged for 5 min at 3000 g. The supernatant was discarded and cells were resuspended in 200 ml of TfbI buffer and incubated for another 15 min on ice. Cells were centrifuged again and the pellet was resuspended in 20 ml of TfbII buffer, incubated on ice for another 15 min and aliquoted into 200 – 500 µl aliquots, snap frozen in liquid nitrogen and stored at -80°C.

8.1.8 Transformation of chemically competent cells (Inoue method)

Bacteria were thawed on ice and divided into 100 µl aliquots. Subsequently, 5 µl of ligation mix or 1-10 ng of supercoiled plasmid DNA were added and cells were incubated for 30 minutes on ice. Afterwards, the cells were heat-shocked at 42°C for 90 seconds and incubated on ice for 3 additional minutes. 300 µl SOC medium were added and the cells were incubated on a shaker for 15 to 45 min. 100-300 µl were spread on bacterial plates with the appropriate antibiotic and incubated over night at 37°C.

8.1.9 Plasmid DNA isolation

The NucleoSpin Plasmid kit (Macherey-Nagel GmbH & Co., Düren, Germany) was used to isolate Plasmid DNA. Isolated clones from bacterial plates were grown in 4 ml LB medium supplemented with the appropriate antibiotic over night at 37°C. After centrifugation at 3500 rpm, bacterial pellets were suspended in 250 µl buffer S1 by vortexing. Lysis of cells was induced after adding 250 µl buffer S2 (alkaline lysis) and incubation for 5 minutes at room temperature. Lysed cells were incubated with buffer S3 (acidic precipitation buffer) and centrifuged for 10 minutes at 13000 rpm to precipitate cell debris and genomic DNA. The supernatant was loaded on the gel-affinity column and centrifuged for 1 minute at 13000 rpm. Bound DNA was washed once with 600 µl buffer N3 and after a final step of 2 minutes at 13000 rpm (to remove residual ethanolic washing buffer) eluted with 50 µl N5 buffer by centrifugation for 1 minute.

8.1.10 DNA sequencing

Sequencing reactions were done using the ABI PRISM^{TM} BigDye Terminator Cycle Sequencing Reaction Kit (PE Applied Biosystems). Approximately 200 ng template was used per sequencing reaction. Sequencing buffer, primer (10 pmol/µl) and termination ready reaction (TRR) mix were added to the DNA and the mixture was diluted with dd-water to a total volume of 20 µl. The thermocycler was run according to the following program: denaturation for 10 sec at 96°C, annealing for 10 sec at 50°C and elongation for 4 min at 60°C, with a cycle number of 25. The amplified DNA was purified on a Sephadex G-50 column, transferred to a small spin column and centrifuged for 2 min at 13000 g. 4 µl of the purified DNA was mixed with 20 µl of Template Suppression Reagent. The mixture was incubated for 2 min at 95°C , mixed, centrifuged shortly and loaded into an ABI PRISM capillary sequencer. Sequences were analyzed using the SeqMan program (DNASTAR Inc., Madison, USA).

8.1.11 Constructing polyproteins

Polyproteins made of either identical repeats of a single myomesin domain (My6, My10) or repeats of two neighboring domains (My6-EH) were constructed using directional DNA concatemerization by self-ligation of the sticky ends of the Ava I restriction site (Carrion-Vazquez *et al.*, 1999b, Hartley and Gregori, 1981). Myomesin fragments with flanking Ava I sites were produced by PCR from the human sequence using a cDNAclone (Vinkemeier *et al.*, 1993) as a template. This restriction site was used since it is asymmetrical, allowing directional assembly of the monomers. The repeats were connected by a Leu-Gly linker, corresponding to the translation of codons of the Ava I site. The ligation products were transformed into the recombination-defective *Escherichia coli* strain SURE 2 (Stratagene, Milano, Italy) and the colonies were analyzed directly by restriction digestion. A modified pET vector (pETAvaI) (Carrion-Vazquez et al. 2000) was used for expression in the *Escherichia coli* strain BLR(DE3) (Novagene, Heidelberg, Germany), consisting of a His-tag at the N-terminus, a unique CTCGGG Ava I cloning site (verified by sequencing), and two cysteine residues on the C-terminus (for covalent attachment to gold coated coverslips). The bacteria were lysed using lysozyme (1mg/ml) and the proteins were purified by Ni^{2+} affinity chromatography (Protino Ni 2000; Macherey-Nagel AG, Oensingen, Switzerland). The purified polyproteins were dialyzed to PBS buffer (137 mM sodium chloride, 6.5 mM sodium phosphate, 2.7 mM potassium chloride and 1.5 mM potassium phosphate, pH 7.4) and the purity and integrity was monitored by SDS-polyacrylamide gel electrophoresis(SDS-PAGE) (Agarkova *et al.*, 2000). Then the proteins were kept in PBS containing 5 mM DTT at 4°C or -20°C.

8.1.12 Expression of recombinant EH-segment of myomesin

The human EH-segment was amplified by PCR from EST clone (AA248352) and subcloned into the BglII and EcoRI sites of pGEX-2T (Amersham Biosciences Europe GmbH, Freiburg, Germany). It was expressed in the *Escherichia coli* strain BL-21(DE3)star (Novagene, Heidelberg, Germany) as a glutathione *S*-transferase fusion protein and was purified from crude bacterial lysates by affinity chromatography on glutathione-agarose (Amersham Biosciences Europe GmbH, Freiburg, Germany) and by thrombin (isolated from human plasma, T-6884; Sigma, Buchs, Switzerland) digestion. The recombinant EH-segment was

dialyzed to PBS buffer and the purity and integrity was monitored by SDS-PAGE. Then the protein was kept at -20°C.

8.2 Immunohistochemistry

8.2.1 Frozen sections of mouse hind limbs

Mouse hind limbs or m.soleus were dissected, snap-frozen in isopentane cooled by liquid nitrogen and stored at -80°C until sectioning. 10-15 µm thick cross-sections through the whole limb were cut on a Microm HM560 cryostat with a cutting temperature of about -20°C. The sections were collected on gelatin-coated glass slides, dried for 1 h at room temperature and stored at -20°C.

8.2.2 Immunostaining

Muscle fibers and cross-sections of mouse hind limbs were fixed with 4% PFA/PBS for 10 minutes at room temperature, blocked with 0.1 M glycine in PBS for 5 minutes and permeabilized in 0.2% Triton X100/PBS for 10 minutes. Alternatively, for immuofluorescence staining with antibodies against myomesin 3, sections were first treated with 0.3 % SDS in PBS for 1 min before fixation with 4% paraformaldehyde/0.1% SDS in PBS for 10 min at room temperature. For stainings with antibodies against different isoforms of MHC, frozen sections of mouse hind limb were fixed with acetone for 5 minutes at –20°C. After blocking with 5% goat serum in 1% BSA/PBS for 30 minutes, primary antibodies (diluted in 1% BSA/PBS) were added and incubated for 1 hour at room temperature or overnight at 4°C. After washing 3 times with PBS for 5 minutes, secondary antibodies were added for 45 minutes. After washing again 3 times in PBS for 5 minutes, the specimens were embedded in glycerol embedding medium [0.1 M Tris-HCl (pH 9.5) /glycerol (3:7) containing 50 mg/ml n-propyl gallate as anti-fading reagent (Agarkova *et al.*, 2000)].

8.2.3 SDS-PAGE and Immunoblotting

Tissue samples were carefully dissected from the animal, homogenized by freeze-slamming and resuspended in SDS-sample buffer (3.7M urea; 134.6 mM Tris pH 6.8; 5.4% SDS; 2.3% NP-40; 4.45% β-mercaptoethanol; 4% glycerol and 6 mg/100 ml bromophenol blue) and boiled for 1 minute. SDS-samples were run on 6% polyacrylamide/30% glycerol minigels together with broad range molecular weight marker (Biorad). Equal amounts of protein were loaded for the different tissue extracts as judged by Coomassie blue staining of a test gel. Blotting was carried out over night onto nitrocellulose Hybond-C extra (Amersham). Unspecific binding sites were blocked with 5% non-fat dry milk in washing buffer (PBS, pH 7.4, 0.3% Tween-20) for 1 hour at room temperature or overnight at 4°C. Primary and secondary antibodies were diluted in washing buffer supplemented with 2% non-fat milk powder and incubated for 1 hour. After the incubation, the blot was washed 3 times with washing buffer for 10 minutes. Chemiluminescence reaction was performed using a mixture of water, luminol, iodophenol, 1 M Tris-HCl (pH 7.5) and H_2O_2 or Supersignal and visualized on X-Ray films.

8.2.4 Antibodies

The antibodies against mouse myomesin 3 (anti-Myo3-N or anti-Myo3-C) were generated by immunizing adult rabbits with the N-terminal peptide LLRQRRDWKALRQRT (Eurogentec, Seraing, BE) or the C-terminal peptide GEEPKELKKK (Sigma-Aldrich, Epalinges, Switzerland), respectively. Antibodies against mouse EH-myomesin were generated by immunizing adult rabbits with the recombinant EH-segment fused to glutathione S-transferase. As soon as strong and specific responses were detected, the animals were sacrificed and sera were collected. For the conjugation with Alexa488, the IgG fraction was prepared by ammonium-sulfate precipitation. The conjugate was produced using an Alexa Fluor 488 Protein Labeling Kit (Molecular Probes).

The following primary antibodies against other proteins have been used for indirect immunofluorescence and immunoblotting:

Antigen	Antibody	Dilution	Source
actin	A2066 (pAb, R)	1:2000 (WB)	Sigma
sarcomeric α-actinin	mAb EA-53	1:500 (IF)	Sigma
MM-creatine kinase	pAb (R)	1:50 (IF)	raised in our lab
M-protein	mAb AA259 (IgA)	1:2 (IF)	gift from D. Fürst
myomesin	pAb My-N (Rt)	1:1000 (IB)	gift from M. Gautel
myomesin	mAb B4	1:50 (IF)	raised in our lab
EH-myomesin	pAb mo EH (R)	1:1000 (IF), 1:30000 (IB)	raised in our lab
S-myomesin	pAb ch My-S (R)	1:200 (IF)	raised in our lab
myomesin 3	pAb Myo3-N (R)	1:200 (IF), 1:2000 (IB)	raised in our lab
MHC-IIa	mAb A4.74 (IgG)	1:2 (IF)	DHSB
MHC-IIb	mAb BF-F3 (IgM)	1:2 (IF)	DHSB
MHC-Iβ	mAb A4.840 (IgM)	1:2 (IF)	DHSB
MHC-Iβ	mAb MHCs (IgG)	1:50 (IF)	Novocastra

Table 2: Primary antibodies, which were used in this study. DHSB denote Developmental Studies Hybridoma Bank, Jowa.

For immunofluorescence and immunoblot, the following secondary antibodies or reagents had been used:

Reactivity / Reagent	Conjugation	Dilution	Source
donkey-anti-rat	Cy3	1:200	Jackson
donkey-anti-rat (no X reaction mouse)	Cy3	1:100	Jackson
goat-anti-mouse	Cy3	1:500	Jackson
goat-anti-mouse (IgA)	FITC	1:20	Sigma
goat-anti-mouse (IgG)	Cy3	1:200	Jackson
goat-anti-mouse (IgG,Fab)	Cy3	1:300	Jackson
goat-anti-mouse (IgM)	Cy5	1:50	Jackson
goat-anti-mouse (IgM)	FITC	1:100	Sigma
goat-anti-rabbit	biotin	1:100	AMRAD
goat-anti-rabbit	Cy5	1:100	Jackson
goat-anti-rabbit (IgG)	FITC	1:100	Cappel
goat-anti-rabbit (IgG)	HRP	1:3000	Calbiochem
goat-anti-rabbit (Igs)	Cy3	1:500	Jackson
horse-anti-mouse (no X reaction rat)	FITC	1:50	Vector
rabbit-anti-mouse EH-myomesin	Alexa488	1:10	raised in our lab
rabbit-anti-rat (Igs)	HRP	1:1000	DAKO
phalloidin	Alexa633	1:100	Molecular Probes
streptavidin	FITC	1:100	DAKO

Table 3: Secondary antibodies and labelled reagents.

8.2.5 Culture and transfection of NRC

Newborn rat hearts were dissected, digested with collagenase (Worthington Biochemical Corp., Freehold, NY, USA) and pancreatin (Gibco Lab., Grand Island, NY, USA) and cultured as described (Komiyama et al., 1996; Sen et al., 1988). Cells were plated onto fibronectin- or collagen-coated dishes (10µg/ml fibronectin) with a density of 400'000 cells per 35 mm dish in plating medium. After 1 day, transfections were carried out using the Trojene™ transfection reagent (Avanti Polar Lipids, Alabaster (AL), USA). 1 µg supercoiled plasmid DNA (pEGFP-C1 vector from: Clontech, Mountain View, CA , USA) as well as 4 µl Trojene™ were diluted into 100 µl OptiMEM in separate siliconised tubes and mixed by pipetting. The DNA and Trojene™ transfection reagent were mixed and incubated at room temperature for 15 minutes allowing the DNA-lipid complex to be formed. Cells were washed with antibiotica-free and serum-free OptiMEM. The DNA-lipid complex was added to 0.8 ml transfection medium (maintenance medium without antibiotics + 4% horse serum) and pipetted onto washed cells. Cell cultures were incubated for max. 4 h at 37°C (5% CO_2) and subsequently the medium was replaced by normal maintenance medium.

8.3 Microscopy and spectroscopy

8.3.1 Confocal microscopy

Analysis of the stained fibers and sections was carried out using a Leica confocal unit equipped with an inverse microscope, argon & helium-neon lasers and a Leica PL APO 10x/0.3 NA or 63x/1.32 NA lens. Image processing was done on a PC workstation using the image processing software Imaris (Bitplane AG, Zurich, Switzerland) and Photoshop (Adobe Systems, San Jose, CA, USA).

8.3.2 Electron Microscopy

After dialysis against PBS, the purified polyproteins were either kept on ice or snap-frozen in liquid nitrogen and kept at −20°C. Immediately before spraying the samples onto a piece of freshly cleaved mica, glycerol was added to a final concentration of 30%. Sprayed samples were dried in an evaporator and then rotary shadowed at a low elevation angle (3-5°) with

platinum/carbon. Micrographs were recorded on a Hitachi H-7000 transmission electron microscope (Hitachi Ltd., Tokyo, Japan) operated at 100 kV. For preparing figures, micrographs were digitized with a scanner (HP Scan Jet IIcx) at a step size of 600 dpi. The digitized micrographs were processed using Adobe Photoshop CS 8.0 software (Adobe Systems Inc., Mountain View, CA).

8.3.3 Atomic force microscopy

Atomic force spectroscopy measurements were performed using a commercial atomic force microscope (AFM) instrument (Nanoscope III, Digital Instruments, Santa Barbara, CA). Acquisition of the cantilever deflection data and control of the piezoelectric positioner were done by means of a PCI-MIO-16XE-10 data-acquisition board driven by LabVIEW software (National Instruments, Austin, TX) in connection with an additional personal computer and a home-built high voltage amplifier. The program allowed us to repeatedly unfold and refold one molecule. The cantilevers used in this study were silicon nitride (Si_3Ni_4) cantilevers from Olympus (with typical spring constants of ~30 and ~6 pN/nm) and from Park Scientific (with typical spring constants of ~10 pN/nm). Calibration of the spring constants of all cantilevers is done in the experimental buffer and using the equipartition theorem (Hutter and Bechhoefer, 1993) with an absolute uncertainty of 20%.

$(My6)_8$ and $(My10)_9$ proteins (50 µl of a 10-30 µg/ml solution in PBS) were allowed to adsorb to freshly evaporated gold surfaces or to pre-cleaned glass microscope slides. After the incubation process (~two hours for gold surfaces and 20 minutes for pre-cleaned glass microscope slides) the sample was rinsed with PBS. Similar results were obtained on both substrates. $(My6\text{-}EH)_4$ proteins (50 µl of a 1 µg/ml solution in PBS) were allowed to bind to a pre-cleaned glass microscope slide for one minute before unbound molecules were washed away. We optimized the likelihood of stretching single molecules using low protein concentrations. During continuous probing of the surface with the AFM, only few contacts were made (5 to 10% when stretching $(My6)_8$ and $(My10)_9$, less than 0.5% when studying $(My6\text{-}EH)_4$. All force–extension measurements were carried out in PBS with 5 mM dithiothreitol at pulling speeds from 125 to 4000 nm/s. The room temperature was regulated and always in the range 23-25°C.

8.3.3.1 Treatment and analysis of experimental AFM data

Representation and curve fitting of the data were done using Origin 7.0 (OriginLab Corporation, Northampton, MA). We employed a series of steps in our analysis of single-molecule force data. We corrected the raw force-extension curves for several factors: (1) determination of the zero length / zero-force data point from the force response that corresponded to the cantilever tip reaching (or departuring from) the substrate surface; (2) correction for baseline slope using the force response of the displaced but unloaded cantilever; (3) calculation of the end-to-end length (x) of the tethered molecule by correcting the cantilever base displacement (s) with cantilever bending (ratio of force (F) and cantilever stiffness (k)) as:

$$x = s - \frac{F}{k}$$

and (4) using the worm-like chain (WLC) equation (Rief et al. 1999) to model the force versus extension characteristics of the unfolded polypeptide, in which p is the persistence length that describes the polymer stiffness, L is the contour length, or total length of the polymer backbone, kB is the Boltzmann's constant, T is the temperature in Kelvin, and x is the distance between the ends of the polymer:

$$F(x) = \frac{k_B T}{p}\left(\frac{1}{4(1 - x/L)^2} - \frac{1}{4} + \frac{x}{L}\right)$$

8.3.4 Circular dichroism spectroscopy

Circular dichroic experiments were performed at room temperature using a Jasco J-810 spectropolarimeter. The far-CD spectrum was recorded from 190 to 250 nm with quartz cells of 1 mm path length. After dialyzing to PBS, the protein concentration was determined by the absorbance coefficient at 280 nm. The purified EH-segment was diluted to 20 µM in PBS for obtaining the CD spectrum, which was corrected by subtracting the buffer baseline.

8.4 Sequence analysis

The boundaries of domains My6 and My10 of human myomesin were determined on the basis of crystal structures of the nearest neighbors, predicted by ncbi (conserved domain database). These were a Fn domain of the cytokine-binding region of human Gp130 (for My6) and an Ig domain of the mouse immunoglobulin Fab fragment (heavy chain, for My10). According to this structural analysis, the My6 domain has 88 aa residues and a linker length of 15 residues. The My10 domain spans 95 aa with 35 aa long linkers between the domains. The EH-segment has a length of 96 aa (116 aa including natural linkers in the polyprotein). Protein disorder analysis of myomesin was performed using PONDR® (Predictors of Natural Disordered Regions, developed by Dunker and colleagues). Access to PONDR® was provided by Molecular Kinetics (6201 La Pas Trail - Ste 160, Indianapolis, IN 46268; 317-280-8737; E-mail: main@molecularkinetics.com). VL-XT is copyright©1999 by the WSU Research Foundation, all rights reserved. PONDR® is copyright©2004 by Molecular Kinetics, all rights reserved.

Multiple alignments of myomesin, M-protein and myomesin 3 sequences were produced by the Megalign program (DNASTAR, Madison, WI, USA). Sequences were taken from the Ensembl sequence database (www.ensembl.org). Immunogenicity of peptides used for immunization of rabbits was analyzed by the Protean program (DNASTAR, Madison, WI, USA).

8.5 Vectors

8.5.1 Eukaryotic expression vectors

All used GFP vectors were derived from the pEGFP-C1 vector (Clontech, BD Bioscience, www.clontech.com). The HA-tagged vector pHA-C1 was constructed using the pEGFP-C1 vector backbone and linker-ligation.

8.5.2 Bacterial expression vectors

The pGEX-2TK vector was constructed and sold by Pharmacia, the pET-AvaI vector was derived from the pET-3a vector by inserting the AvaI cloning site.

8.6 Primers

8.6.1 For RT-PCR

Mouse myomesin	
mMy-ex15.fw	P1-TGACCGTCGTAGGGGACAAACT
mMy-ex18.rv	P2- TCAAGACAAGTGATGTCATAGG
Mouse M-protein	
mMp-ex4.fw	P3- CGGTCTCAAGCGGCTTCTTACG
mMp-ex7.rv	P4-CCACCGCAGCATTGGTAGACAC
Mouse myomesin 3	
mMy3-ex10.fw	P5- GCAGATACTCTACGCAGACCGC
mMy3-ex12.rv	P6- CCGTGACAACTGCTTCTGAGGC
Human myomesin	
hMy-ex15.fw	P9- TGACTGTGGTAGGGGACAAACT
hMy-ex18.rv	P10- AGAACCATTGAGTCACGAAAAC
hEH.rv	P11- GCGGTTAGTCCACCAGGCTCAT
Human M-protein	
hMp-ex3.fw	P12- CACAGAGAGCCTCCAGCCAGAC
hMp-ex5.rv	P13- CCGCTCTTCAAATGTGTGTCTC
Human myomesin 3	
hMy3-ex5.fw	P14- GCCGTCTGGGAGCACACCACGGT
hMy3-ex6.rv	P15- AGCAGCCCGTAGTTGTTGGTGAT
Human β-actin	
hbAct-ex4.fw	P7-GAAGAGCTACGAGCTGCCTGACG
hbAct-ex6.rv	P8-AGAAGCATTTGCGGTGGACGAT

8.6.2 For cloning

pETAvaI.fw	TATGCATCATCATCATCATCACGAAAAGCTCGGGTGCTGCTAAG
pETAvaI.rv	GATCCTTAGCAGCACCCGAGCTTTTCGTGATGATGATGATGATGCA
AvaIhMyFn6.fw	GAAGATCTCTCGGGAAACTTGATATCCCCAAGGC
hMyFn6AvaI.rv	ATGGTACCCGAGAATAGCAGCTTTGACTTCAATAG
hMyEHAvaI.rv	ATGGTACCCGAGTGGAGATGGTGGTGCTCTGTCTG
AvaIhMyIg10.fw	GAAGATCTCTCGGGCTCAGCCATGAACACAAGTTC
hMy10AvaI.rv	ATGGTACCCGAGTTCAACAAAGTGAGGACCTTG
XhoI_mMy3d1fw	CCGCTCGAGGCATGACTCTGCCCCACAGCCC
mMy3d1_EcoRI.rv	CCGGAATTCTTATTCCTTGGCCTCTCGGACC
mMy3Ig3_EcoRI.rv	CCGGAATTCTTACTTCTCAGCTGCAGCATCTC
EcoRI_mMy3Ig11.fw	CCGGAATTCCGCAAAGAGAAGAGACTGGAAG
EcoRI_mMy3Ig13.fw	CCGGAATTCTAAGGCCTTGGCTGTCATTGAG
mMy3Ig13_BamHI.rv	CGCGGATCCTTACTTCTTCTTCAGCTCCTTGG

8.6.3 For sequencing

EGFPCMV.fw	GGCGTGTACGGTGGGA
SV40AA.rv	CATTCATTTTATGTTTCAGGTTCAG

8.7 Media and solutions

8.7.1 DNA

0.5x TE

TrisCl	5 mM
EDTA	0.5 mM
pH 7.5	

0.5x TBE (for 10 liters)

Tris base	54 g
Boric acid	27.5 g
EDTA	4.6 g

Loading buffer I

Bromphenol blue	0.02 %
Xylene cyanole FF	0.004 %
Sucrose	13.3 %

Ethidium bromide stock (1:25000)

Ethidium bromide	10 mg/ml

8.7.2 Isolation of plasmid DNA

S1 buffer

Tris/Cl	50 mM
EDTA	10 mM
pH 8	
RNAse A	

S2 buffer

NaOH	200 mM
SDS	1%

S3 buffer

KAc	2.8 M
Acetic acid	60 %

N3 buffer

TrisCl	100 mM
Ethanol	15 %
KCl	1.15 M
H_3PO_4	66 %
pH 7.4	

N5 buffer

TrisCl	100 mM
Ethanol	15 %
KCl	1 M
H_3PO_4	66 %
pH 7.4	

8.7.3 Bacteria

SOB (per liter)

Bacto yeast extract	5 g
Bato tryptone	20 g
NaCl	0.5 g
KCl	250 mM
ph 7.0 with sodium hydroxide	
autoclave and cool to 60°C	
2 M $MgCl_2$ solution	5 ml (sterile)

TfbI

KAc	30mM
RbCl	100mM
$CaCl_2$	10mM
$MnCl_2$	50mM
Glycerol	15% v/v
pH 5.8 with diluted acetic acid	

TfbII

MOPS	10mM
$CaCl_2$	75mM
RbCl	10mM
Glycerol	15% v/v
pH 6.5 with diluted NaOH	

LB medium (for 5 liters)

Bacto yeast extract	25g
Bacto-tryptone	50g
NaCl	50g

LB-agar

Bacto agar	7.5g
per 500ml LB medium	

SOC medium (for 2 liters)

Bacto tryptone	40g
Yeast extract	10g
NaCl	1g
250mM KCl	20ml
pH 7.0 with NaOH	
1M glucose	40ml
(add after autoclaving)	

Ampicillin stock (1:1000)

Ampicillin	50mg/ml

Tetracycline stock (1:1000)

Tetracyclin (in 70% EtOH)	10mg/ml

Kanamycin stock (1:1000)

Kanamycin	30mg/ml

8.7.4 Immunofluorescence and specimen preparation

Gelatine coated slides

Gelatine	1 %
Potassium chromosulfate	0.1 %
(dissolve in water at 50-60°C)	

4% PFA in PBS (100 ml)

PFA	4 g
10N NaOH	7.5 µl
heat to 65°C and stir until dissolved	
filter	

PBS (10x)

NaCl	1.5 M
Na_2HPO_4	65 mM
KCl	27 mM
KH_2PO_4	15 mM
PH 7.4	

Embedding medium

0.1 M Tris pH 9.5	15 ml
Glycerol	35 ml
N-propyl-gallate	2.5 g

8.7.5 SDS gel electrophoresis and immunoblot analysis

Sample preparation buffer

Urea	3.7 M
Tris pH 6.8	134.6 mM
SDS	5.4 %
NP-40	2.3 %
β-mercaptoethanol	4.45 %
Glycerol	4 %
Bromphenol blue	6 mg/100ml

6 % SDS-PAGE gel

Separating gel:

Glycerol	3.0 ml
ddH_2O	2.5 ml
Lower buffer	2.5 ml
Acrylamide 30 % / Bisacrylamide 0.8 % (Applichem, Darmstadt, Germany)	2.0 ml
10 % Ammonium persulfate	50 µl
TEMED	5 µl

Stacking gel:

ddH_2O	3 ml
Upper buffer	1.3 ml
Acrylamide 30 % / Bisacrylamide 0.8 %	0.65 ml
Phenolred	3 µl
10 % Ammonium persulfate	25 µl
TEMED	5 µl

Lower buffer for SDS-page

For 0.5 liters:	
Tris base	1.5 M (91 g)
SDS	0.4 % (2 g)
1N HCl	62.5 ml
pH 8.8	

Upper buffer for SDS-page

For 0.5 liters:	
Tris base	0.5 M (30.3 g)
SDS	0.4 % (2 g)
1N HCl	48 ml
pH 6.8	

Running buffer (5x)

For 1 liter:	
Tris-Base (Sigma, Buchs, Switzerland)	15 g
Glycin (Fluka, Buchs, Switzerland)	14.4 g
SDS	5 g

Coomassie blue

MetOH	50 %
Acidic acid	10 %
Coomassie R-250	0.2 %

Blotting buffer

For 1 liter:	
Tris-Base (Sigma, Buchs, Switzerland)	3.03 g
Glycin (Fluka, Buchs, Switzerland)	14.4 g
SDS (BDH Laboratory Supplies Poole, England)	0.1 g
MetOH	200 ml

Low salt buffer

For 1 liter:	
NaCl	0.9 %
Tris-Base	10 mM
Tween 20	0.1 %

Enhanced chemoluminescence solution

ddH_2O	7.5 ml
Luminol stock solution	1 ml
Iodophenol stock solution	1 ml
1M Tris pH 7.5	0.5 ml
add 30% H_2O_2 shortly before use	5 µl

Luminol 10x stock (10 ml)

Luminol	25 mM (50 mg)
dissolve in H2O	

Iodophenol 10x stock (10 ml)

Iodophenol	5 nM (11 mg)
dissolve in DMSO	

8.7.6 Cell culture

Plating medium

Dulbecco's MEM (Amimed AG)	67 %
Medium M199	17 %
Horse serum (Gibco)	10 %
Fetal calf serum	5 %
Glutamine 4 mM	
Penicillin/Streptomycin (Animed)	1 %

NRC maintenance medium

Medium M199	20 %
DBSS-K	75 %
Horse serum (Gibco)	4 %
Glutamine	4 mM
Penicillin/Streptomycin (Animed)	1%
Phenylephrine	0.1 mM

DBSS-K

NaCl	6.8 g/l
NaH_2PO_4	0.14 mM
$CaCl_2$	0.2 mM
$MgSO_4$ x $7H_2O$	0.2 mM
Dextrose	1 mM
$NaHCO_3$	2.7 mM

NRC transfection medium

Medium M199	20 %
DBSS-K	75 %
Horse serum (Gibco)	4 %
Glutamine	4 mM

9 REFERENCES

Agarkova, I. (2000) Functional diversity of contractile isoproteins: Expression of actin and myomesin isoforms in striated muscle. Swiss Federal Institute of Technology, Zurich, Zurich.

Agarkova, I., Auerbach, D., Ehler, E. & Perriard, J.C. (2000) A novel marker for vertebrate embryonic heart, the EH-myomesin isoform. *J. Biol. Chem.*, 275, 10256-10264.

Agarkova, I., Ehler, E., Lange, S., Schoenauer, R. & Perriard, J.C. (2003) M-band: a safeguard for sarcomere stability? *J. Muscle Res. Cell Motil*, 24, 191-203.

Agarkova, I. & Perriard, J.C. (2005) The M-band: an elastic web that crosslinks thick filaments in the center of the sarcomere. *Trends Cell Biol.*, 15, 477-485.

Agarkova, I., Schoenauer, R., Ehler, E., Carlsson, L., Carlsson, E., Thornell, L.E. & Perriard, J.C. (2004) The molecular composition of the sarcomeric M-band correlates with muscle fiber type. *Eur. J. Cell Biol.*, 83, 193-204.

Aigner, S., Gohlsch, B., Hamalainen, N., Staron, R.S., Uber, A., Wehrle, U. & Pette, D. (1993) Fast myosin heavy chain diversity in skeletal muscles of the rabbit: heavy chain IId, not IIb predominates. *Eur. J. Biochem.*, 211, 367-372.

Allen, D.G. (2001) Eccentric muscle damage: mechanisms of early reduction of force. *Acta Physiol. Scand.*, 171, 311-319.

Allen, D.L. & Leinwand, L.A. (2001) Postnatal myosin heavy chain isoform expression in normal mice and mice null for IIb or IId myosin heavy chains. *Dev. Biol.*, 229, 383-395.

Amodeo, P., Castiglione Morelli, M.A., Strazzullo, G., Fucile, P., Gautel, M. & Motta, A. (2001) Kinase recognition by calmodulin: modeling the interaction with the autoinhibitory region of human cardiac titin kinase. *J. Mol. Biol.*, 306, 81-95.

Anan, R., Greve, G., Thierfelder, L., Watkins, H., McKenna, W.J., Solomon, S., Vecchio, C., Shono, H., Nakao, S., Tanaka, H. & et al. (1994) Prognostic implications of novel beta cardiac myosin heavy chain gene mutations that cause familial hypertrophic cardiomyopathy. *J. Clin. Invest.*, 93, 280-285.
Andrade, F.H., Merriam, A.P., Guo, W., Cheng, G., McMullen, C.A., Hayess, K., van der ven, P.F. & Porter, J.D. (2003) Paradoxical absence of M lines and downregulation of creatine kinase in mouse extraocular muscle. *J. Appl. Physiol.*, 95, 692-699.

Antos, C.L., Frey, N., Marx, S.O., Reiken, S., Gaburjakova, M., Richardson, J.A., Marks, A.R. & Olson, E.N. (2001) Dilated cardiomyopathy and sudden death resulting from constitutive activation of protein kinase a. *Circ. Res.*, 89, 997-1004.

Anversa, P., Olivetti, G., Bracchi, P.G. & Loud, A.V. (1981) Postnatal development of the M-band in rat cardiac myofibrils. *Circ. Res.*, 48, 561-568.

Arber, S. & Caroni, P. (1996) Specificity of single LIM motifs in targeting and LIM/LIM interactions in situ. *Genes Dev.*, 10, 289-300.

Arber, S., Halder, G. & Caroni, P. (1994) Muscle LIM protein, a novel essential regulator of myogenesis, promotes myogenic differentiation. *Cell*, 79, 221-231.

Arber, S., Hunter, J.J., Ross, J.J., Hongo, M., Sansig, G., Borg, J., Perriard, J.C., Chien, K.R. & Caroni, P. (1997) MLP-deficient mice exhibit a disruption of cardiac cytoarchitectural organization, dilated cardiomyopathy, and heart failure. *Cell,* 88, 393-403.

Auerbach, D., Bantle, S., Keller, S., Hinderling, V., Leu, M., Ehler, E. & Perriard, J.C. (1999) Different domains of the M-band protein myomesin are involved in myosin binding and M-band targeting. *Mol. Biol. Cell,* 10, 1297-1308.

Bantle, S., Keller, S., Haussmann, I., Auerbach, D., Perriard, E., Muhlebach, S. & Perriard, J.C. (1996) Tissue-specific isoforms of chicken myomesin are generated by alternative splicing. *J. Biol. Chem.,* 271, 19042-19052.

Bennett, P., Craig, R., Starr, R. & Offer, G. (1986) The ultrastructural location of C-protein, X-protein and H-protein in rabbit muscle. *J. Muscle Res. Cell Motil.,* 7, 550-567.

Bennett, P.M., Furst, D.O. & Gautel, M. (1999) The C-protein (myosin binding protein C) family: regulators of contraction and sarcomere formation? *Rev. Physiol. Biochem. Pharmacol.,* 138, 203-234.

Bergman, R.A. (1983) Ultrastructural configuration of sarcomeres in passive and contracted frog sartorius muscle. *Am. J. Anat.,* 166, 209-222.

Blair, E., Redwood, C., de Jesus Oliveira, M., Moolman-Smook, J.C., Brink, P., Corfield, V.A., Ostman-Smith, I. & Watkins, H. (2002) Mutations of the light meromyosin domain of the beta-myosin heavy chain rod in hypertrophic cardiomyopathy. *Circ. Res.,* 90, 263-269.

Bonne, G., Carrier, L., Bercovici, J., Cruaud, C., Richard, P., Hainque, B., Gautel, M., Labeit, S., James, M., Beckmann, J., Weissenbach, J., Vosberg, H.P., Fiszman, M., Komajda, M. & Schwartz, K. (1995) Cardiac myosin binding protein-C gene splice acceptor site mutation is associated with familial hypertrophic cardiomyopathy. *Nat. Genet.,* 11, 438-440.

Bottinelli, R. (2001) Functional heterogeneity of mammalian single muscle fibres: do myosin isoforms tell the whole story? *Pflugers Arch.,* 443, 6-17.

Bottinelli, R., Betto, R., Schiaffino, S. & Reggiani, C. (1994a) Maximum shortening velocity and coexistence of myosin heavy chain isoforms in single skinned fast fibres of rat skeletal muscle. *J. Muscle Res. Cell Motil.,* 15, 413-419.

Bottinelli, R., Betto, R., Schiaffino, S. & Reggiani, C. (1994b) Unloaded shortening velocity and myosin heavy chain and alkali light chain isoform composition in rat skeletal muscle fibres. *J. Physiol.,* 478, 341-349.

Bouchiat, C., Wang, M.D., Allemand, J., Strick, T., Block, S.M. & Croquette, V. (1999) Estimating the persistence length of a worm-like chain molecule from force-extension measurements. *Biophys. J.,* 76, 409-413.

Bustamante, C., Marko, J.F., Siggia, E.D. & Smith, S. (1994) Entropic elasticity of lambda-phage DNA. *Science,* 265, 1599-1600.

Carlsson, E., Grove, B.K., Wallimann, T., Eppenberger, H.M. & Thornell, L.E. (1990) Myofibrillar M-band proteins in rat skeletal muscles during development. *Histochemistry,* 95, 27-35.

Carlsson, E., Kjorell, U., Thornell, L.E., Lambertsson, A. & Strehler, E. (1982) Differentiation of the myofibrils and the intermediate filament system during postnatal development of the rat heart. *Eur. J. Cell Biol.,* 27, 62-73.

Carlsson, E. & Thornell, L.E. (1987) Diversification of the myofibrillar M-band in rat skeletal muscle during postnatal development. *Cell. Tissue Res.*, 248, 169-180.

Carrion-Vazquez, M., Marszalek, P.E., Oberhauser, A.F. & Fernandez, J.M. (1999a) Atomic force microscopy captures length phenotypes in single proteins. *Proc. Natl. Acad. Sci. USA*, 96, 11288-11292.

Carrion-Vazquez, M., Oberhauser, A.F., Fowler, S.B., Marszalek, P.E., Broedel, S.E., Clarke, J. & Fernandez, J.M. (1999b) Mechanical and chemical unfolding of a single protein: a comparison. *Proc. Natl. Acad. Sci. USA*, 96, 3694-3699.

Centner, T., Yano, J., Kimura, E., McElhinny, A.S., Pelin, K., Witt, C.C., Bang, M.L., Trombitas, K., Granzier, H., Gregorio, C.C., Sorimachi, H. & Labeit, S. (2001) Identification of muscle specific ring finger proteins as potential regulators of the titin kinase domain. *J. Mol. Biol.*, 306, 717-726.

Charron, P., Dubourg, O., Desnos, M., Bennaceur, M., Carrier, L., Camproux, A.C., Isnard, R., Hagege, A., Langlard, J.M., Bonne, G., Richard, P., Hainque, B., Bouhour, J.B., Schwartz, K. & Komajda, M. (1998) Clinical features and prognostic implications of familial hypertrophic cardiomyopathy related to the cardiac myosin-binding protein C gene. *Circulation*, 97, 2230-2236.

Chen, Y.W., Nader, G.A., Baar, K.R., Fedele, M.J., Hoffman, E.P. & Esser, K.A. (2002) Response of rat muscle to acute resistance exercise defined by transcriptional and translational profiling. *J. Physiol.*, 545, 27-41.

Chien, K.R. (1999) Stress pathways and heart failure. *Cell*, 98, 555-558.
Colbert, M.C., Hall, D.G., Kimball, T.R., Witt, S.A., Lorenz, J.N., Kirby, M.L., Hewett, T.E., Klevitsky, R. & Robbins, J. (1997) Cardiac compartment-specific overexpression of a modified retinoic acid receptor produces dilated cardiomyopathy and congestive heart failure in transgenic mice. *J. Clin. Invest.*, 100, 1958-1968.

Cooke, R. (2004) The sliding filament model: 1972-2004. *J. Gen. Physiol.*, 123, 643-656.
Daehmlow, S., Erdmann, J., Knueppel, T., Gille, C., Froemmel, C., Hummel, M., Hetzer, R. & Regitz-Zagrosek, V. (2002) Novel mutations in sarcomeric protein genes in dilated cardiomyopathy. *Biochem. Biophys. Res. Commun.*, 298, 116-120.

D'Angelo, D.D., Sakata, Y., Lorenz, J.N., Boivin, G.P., Walsh, R.A., Liggett, S.B. & Dorn, G.W., 2nd (1997) Transgenic Galphaq overexpression induces cardiac contractile failure in mice. *Proc. Natl. Acad. Sci. USA*, 94, 8121-8126.

Dunker, A.K., Brown, C.J. & Obradovic, Z. (2002) Identification and functions of usefully disordered proteins. *Adv. Protein Chem.*, 62, 25-49.

Durbeej, M. & Campbell, K.P. (2002) Muscular dystrophies involving the dystrophin-glycoprotein complex: an overview of current mouse models. *Curr. Opin. Genet. Dev.*, 12, 349-361.

Edman, A.C., Squire, J.M. & Sjostrom, M. (1988) Fine structure of the A-band in cryo-sections. Diversity of M-band structure in chicken breast muscle. *J. Ultrastruct. Mol. Struct. Res.*, 100, 1-12.

Ehler, E., Horowits, R., Zuppinger, C., Price, R.L., Perriard, E., Leu, M., Caroni, P., Sussman, M., Eppenberger, H.M. & Perriard, J.C. (2001) Alterations at the intercalated disk associated with the absence of muscle LIM protein. *J. Cell Biol.*, 153, 763-772.

Ehler, E., Rothen, B.M., Hammerle, S.P., Komiyama, M. & Perriard, J.C. (1999) Myofibrillogenesis in the developing chicken heart: assembly of Z-disk, M-line and the thick filaments. *J. Cell. Sci.*, 112, 1529-1539.

Eppenberger, H.M., Perriard, J.C., Rosenberg, U.B. & Strehler, E.E. (1981) The Mr 165,000 M-protein myomesin: a specific protein of cross-striated muscle cells. *J. Cell Biol.*, 89, 185-193.

Farah, C.S. & Reinach, F.C. (1995) The troponin complex and regulation of muscle contraction. *Faseb J.*, 9, 755-767.

Fatkin, D., Christe, M.E., Aristizabal, O., McConnell, B.K., Srinivasan, S., Schoen, F.J., Seidman, C.E., Turnbull, D.H. & Seidman, J.G. (1999) Neonatal cardiomyopathy in mice homozygous for the Arg403Gln mutation in the alpha cardiac myosin heavy chain gene. *J. Clin. Invest.*, 103, 147-153.

Fentzke, R.C., Korcarz, C.E., Lang, R.M., Lin, H. & Leiden, J.M. (1998) Dilated cardiomyopathy in transgenic mice expressing a dominant-negative CREB transcription factor in the heart. *J. Clin. Invest.*, 101, 2415-2426.

Flashman, E., Redwood, C., Moolman-Smook, J. & Watkins, H. (2004) Cardiac myosin binding protein C: its role in physiology and disease. *Circ. Res.*, 94, 1279-1289.

Flick, M.J. & Konieczny, S.F. (2000) The muscle regulatory and structural protein MLP is a cytoskeletal binding partner of betal-spectrin. *J. Cell Sci.*, 113 (Pt 9), 1553-1564.

Forsgren, S., Strehler, E. & Thornell, L.E. (1982) Differentiation of Purkinje fibres and ordinary ventricular and atrial myocytes in the bovine heart: an immuno- and enzyme histochemical study. *Histochem J.*, 14, 929-942.

Freeman, K., Lerman, I., Kranias, E.G., Bohlmeyer, T., Bristow, M.R., Lefkowitz, R.J., Iaccarino, G., Koch, W.J. & Leinwand, L.A. (2001) Alterations in cardiac adrenergic signaling and calcium cycling differentially affect the progression of cardiomyopathy. *J. Clin. Invest.*, 107, 967-974.

Freiburg, A. & Gautel, M. (1996) A molecular map of the interactions between titin and myosin-binding protein C. Implications for sarcomeric assembly in familial hypertrophic cardiomyopathy. *Eur. J. Biochem.*, 235, 317-323.

Freiburg, A., Trombitas, K., Hell, W., Cazorla, O., Fougerousse, F., Centner, T., Kolmerer, B., Witt, C., Beckmann, J.S., Gregorio, C.C., Granzier, H. & Labeit, S. (2000) Series of exon-skipping events in the elastic spring region of titin as the structural basis for myofibrillar elastic diversity. *Circ. Res.*, 86, 1114-1121.

Frey, N. & Olson, E.N. (2003) Cardiac hypertrophy: the good, the bad, and the ugly. *Annu. Rev. Physiol.*, 65, 45-79.

Fürst, D.O., Osborn, M., Nave, R. & Weber, K. (1988) The organization of titin filaments in the half-sarcomere revealed by monoclonal antibodies in immunoelectron microscopy: a map of ten nonrepetitive epitopes starting at the Z line extends close to the M line. *J. Cell Biol.*, 106, 1563-1572.
Garrels, J.I. & Gibson, W. (1976) Identification and characterization of multiple forms of actin. *Cell*, 9, 793-805.
Geier, C., Perrot, A., Ozcelik, C., Binner, P., Counsell, D., Hoffmann, K., Pilz, B., Martiniak, Y., Gehmlich, K., van der Ven, P.F., Furst, D.O., Vornwald, A., von Hodenberg, E., Nurnberg, P., Scheffold, T., Dietz, R. & Osterziel, K.J. (2003) Mutations in the human muscle LIM protein gene in families with hypertrophic cardiomyopathy. *Circulation*, 107, 1390-1395.

Geisterfer-Lowrance, A.A., Christe, M., Conner, D.A., Ingwall, J.S., Schoen, F.J., Seidman, C.E. & Seidman, J.G. (1996) A mouse model of familial hypertrophic cardiomyopathy. *Science*, 272, 731-734.

Geisterfer-Lowrance, A.A., Kass, S., Tanigawa, G., Vosberg, H.P., McKenna, W., Seidman, C.E. & Seidman, J.G. (1990) A molecular basis for familial hypertrophic cardiomyopathy: a beta cardiac myosin heavy chain gene missense mutation. *Cell,* 62, 999-1006.

Gillis, J.M. (1996) The mdx mouse: why diaphragm? *Muscle Nerve,* 19, 1230.

Gomes, A.V. & Potter, J.D. (2004) Molecular and cellular aspects of troponin cardiomyopathies. *Ann. N. Y. Acad. Sci.,* 1015, 214-224.

Gotthardt, M., Hammer, R.E., Hubner, N., Monti, J., Witt, C.C., McNabb, M., Richardson, J.A., Granzier, H., Labeit, S. & Herz, J. (2003) Conditional expression of mutant M-line titins results in cardiomyopathy with altered sarcomere structure. *J. Biol. Chem.,* 278, 6059-6065.

Granzier, H.L. & Labeit, S. (2004) The giant protein titin: a major player in myocardial mechanics, signaling, and disease. *Circ. Res.,* 94, 284-295.

Granzier, H.L. & Labeit, S. (2005) Titin and its associated proteins: the third myofilament system of the sarcomere. *Adv. Protein Chem.,* 71, 89-119.

Grater, F., Shen, J., Jiang, H., Gautel, M. & Grubmuller, H. (2005) Mechanically induced titin kinase activation studied by force-probe molecular dynamics simulations. *Biophys. J.,* 88, 790-804.

Gregorio, C.C., Granzier, H., Sorimachi, H. & Labeit, S. (1999) Muscle assembly: a titanic achievement? *Curr. Opin. Cell Biol.,* 11, 18-25.

Gregorio, C.C., Trombitas, K., Centner, T., Kolmerer, B., Stier, G., Kunke, K., Suzuki, K., Obermayr, F., Herrmann, B., Granzier, H., Sorimachi, H. & Labeit, S. (1998) The NH2 terminus of titin spans the Z-disc: its interaction with a novel 19-kD ligand (T-cap) is required for sarcomeric integrity. *J. Cell Biol.,* 143, 1013-1027.

Gregorio, C.C., Weber, A., Bondad, M., Pennise, C.R. & Fowler, V.M. (1995) Requirement of pointed-end capping by tropomodulin to maintain actin filament length in embryonic chick cardiac myocytes. *Nature,* 377, 83-86.

Grove, B.K., Cerny, L., Perriard, J.C. & Eppenberger, H.M. (1985) Myomesin and M-protein: expression of two M-band proteins in pectoral muscle and heart during development. *J. Cell Biol.,* 101, 1413-1421.

Grove, B.K., Cerny, L., Perriard, J.-C., Eppenberger, H.M. & Thornell, L.-E. (1989) Fiber type-specific distribution of M-band proteins in chicken muscle. *J. Histochem. Cytochem.,* 37, 447-454.

Grove, B.K., Holmbom, B. & Thornell, L.E. (1987) Myomesin and M protein: differential expression in embryonic fibers during pectoral muscle development. *Differentiation,* 34, 106-114.

Grove, B.K., Kurer, V., Lehner, C., Doetschman, T.C., Perriard, J.C. & Eppenberger, H.M. (1984) A new 185,000-dalton skeletal muscle protein detected by monoclonal antibodies. *J. Cell Biol.,* 98, 518-524.

Hamalainen, N. & Pette, D. (1995) Patterns of myosin isoforms in mammalian skeletal muscle fibres. *Microsc. Res. Tech.,* 30, 381-389.

Harris, S.P., Bartley, C.R., Hacker, T.A., McDonald, K.S., Douglas, P.S., Greaser, M.L., Powers, P.A. & Moss, R.L. (2002) Hypertrophic cardiomyopathy in cardiac myosin binding protein-C knockout mice. *Circ. Res.,* 90, 594-601.

Hartley, J.L. & Gregori, T.J. (1981) Cloning multiple copies of a DNA segment. *Gene,* 13, 347-353.

Hilber, K. & Galler, S. (1997) Mechanical properties and myosin heavy chain isoform composition of skinned skeletal muscle fibres from a human biopsy sample. *Pflugers Arch.*, 434, 551-558.

Hodge, T. & Cope, M.J. (2000) A myosin family tree. *J. Cell Sci.*, 113 Pt 19, 3353-3354.

Hornemann, T., Kempa, S., Himmel, M., Hayess, K., Fürst, D.O. & Wallimann, T. (2003) Muscle-type creatine kinase interacts with central domains of the M-band proteins myomesin and M-protein. *J. Mol. Biol.*, 332, 877-887.

Horowits, R., Maruyama, K. & Podolsky, R.J. (1989) Elastic behavior of connectin filaments during thick filament movement in activated skeletal muscle. *J. Cell Biol.*, 109, 2169-2176.

Horowits, R. & Podolsky, R.J. (1987) The positional stability of thick filaments in activated skeletal muscle depends on sarcomere length: evidence for the role of titin filaments. *J. Cell Biol.*, 105, 2217-2223.

Horowits, R. & Podolsky, R.J. (1988) Thick filament movement and isometric tension in activated skeletal muscle. *Biophys. J.*, 54, 165-171.

Hoshijima, M., Pashmforoush, M., Knoll, R. & Chien, K.R. (2002) The MLP family of cytoskeletal Z disc proteins and dilated cardiomyopathy: a stress pathway model for heart failure progression. *Cold Spring Harb. Symp. Quant. Biol.*, 67, 399-408.

Hutter, J.L. & Bechhoefer, J. (1993) Calibration of atomic-force microscope tips. *Rev. Sci. Instrum.*, 64, 3342-3342.

Huxley, H. & Hanson, J. (1954) Changes in the cross-striations of muscle during contraction and stretch and their structural interpretation. *Nature*, 173, 973-976.

Huxley, H.E. (1963) Electron Microscope Studies on the Structure of Natural and Synthetic Protein Filaments from Striated Muscle. *J. Mol. Biol.*, 16, 281-308.

Kabsch, W., Mannherz, H.G., Suck, D., Pai, E.F. & Holmes, K.C. (1990) Atomic structure of the actin:DNase I complex. *Nature*, 347, 37-44.

Kamisago, M., Sharma, S.D., DePalma, S.R., Solomon, S., Sharma, P., McDonough, B., Smoot, L., Mullen, M.P., Woolf, P.K., Wigle, E.D., Seidman, J.G. & Seidman, C.E. (2000) Mutations in sarcomere protein genes as a cause of dilated cardiomyopathy. *N. Engl. J. Med.*, 343, 1688-1696.

Kellermayer, M.S., Smith, S.B., Bustamante, C. & Granzier, H.L. (1998) Complete unfolding of the titin molecule under external force. *J. Struct. Biol.*, 122, 197-205.

Kenny, P.A., Liston, E.M. & Higgins, D.G. (1999) Molecular evolution of immunoglobulin and fibronectin domains in titin and related muscle proteins. *Gene*, 232, 11-23.

Kinbara, K., Sorimachi, H., Ishiura, S. & Suzuki, K. (1997) Muscle-specific calpain, p94, interacts with the extreme C-terminal region of connectin, a unique region flanked by two immunoglobulin C2 motifs. *Arch. Biochem. Biophys.*, 342, 99-107.

Knappeis, G.G. & Carlsen, F. (1968) The ultrastructure of the M line in skeletal muscle. *J. Cell Biol.*, 38, 202-211.

Knöll, R., Hoshijima, M., Hoffman, H.M., Person, V., Lorenzen-Schmidt, I., Bang, M.L., Hayashi, T., Shiga, N., Yasukawa, H., Schaper, W., McKenna, W., Yokoyama, M., Schork, N.J., Omens, J.H., McCulloch, A.D., Kimura, A., Gregorio, C.C., Poller, W., Schaper, J., Schultheiss, H.P. & Chien,

K.R. (2002) The cardiac mechanical stretch sensor machinery involves a Z disc complex that is defective in a subset of human dilated cardiomyopathy. *Cell,* 111, 943-955.

Knudsen, K.A., Soler, A.P., Johnson, K.R. & Wheelock, M.J. (1995) Interaction of alpha-actinin with the cadherin/catenin cell-cell adhesion complex via alpha-catenin. *J. Cell Biol.,* 130, 67-77.

Kolmerer, B., Olivieri, N., Witt, C.C., Herrmann, B.G. & Labeit, S. (1996) Genomic organization of M-line titin and its tissue-specific expression in two distinct isoforms. *J. Mol. Biol.,* 256, 556-563.
Kudej, R.K., Iwase, M., Uechi, M., Vatner, D.E., Oka, N., Ishikawa, Y., Shannon, R.P., Bishop, S.P. & Vatner, S.F. (1997) Effects of chronic beta-adrenergic receptor stimulation in mice. *J. Mol. Cell. Cardiol.,* 29, 2735-2746.

Kulke, M., Fujita-Becker, S., Rostkova, E., Neagoe, C., Labeit, D., Manstein, D.J., Gautel, M. & Linke, W.A. (2001) Interaction between PEVK-titin and actin filaments: origin of a viscous force component in cardiac myofibrils. *Circ. Res.,* 89, 874-881.

Labeit, S. & Kolmerer, B. (1995) Titins: giant proteins in charge of muscle ultrastructure and elasticity. *Science,* 270, 293-296.

Lahmers, S., Wu, Y., Call, D.R., Labeit, S. & Granzier, H. (2004) Developmental control of titin isoform expression and passive stiffness in fetal and neonatal myocardium. *Circ. Res.,* 94, 505-513.

Lange, S. (2005) Structural and signalling functions of sarcomeric proteins. Swiss Federal Institute of Technology, Zurich, Zurich.

Lange, S., Agarkova, I., Perriard, J.C. & Ehler, E. (2005a) The sarcomeric M-band during development and in disease. *J. Muscle Res. Cell Motil.,* 26, 375-379.

Lange, S., Auerbach, D., McLoughlin, P., Perriard, E., Schafer, B.W., Perriard, J.C. & Ehler, E. (2002) Subcellular targeting of metabolic enzymes to titin in heart muscle may be mediated by DRAL/FHL-2. *J. Cell Sci.,* 115, 4925-4936.

Lange, S., Himmel, M., Auerbach, D., Agarkova, I., Hayess, K., Fürst, D.O., Perriard, J.C. & Ehler, E. (2005b) Dimerisation of myomesin: implications for the structure of the sarcomeric M-band. *J. Mol. Biol.,* 345, 289-298.

Leake, M.C., Wilson, D., Gautel, M. & Simmons, R.M. (2004) The elasticity of single titin molecules using a two-bead optical tweezers assay. *Biophys. J.,* 87, 1112-1135.

Leinwand, L.A., Saez, L., McNally, E. & Nadal-Ginard, B. (1983) Isolation and characterization of human myosin heavy chain genes. *Proc. Natl. Acad. Sci. U S A,* 80, 3716-3720.
Li, H., Linke, W.A., Oberhauser, A.F., Carrion-Vazquez, M., Kerkvliet, J.G., Lu, H., Marszalek, P.E. & Fernandez, J.M. (2002) Reverse engineering of the giant muscle protein titin. *Nature,* 418, 998-1002.

Li, H., Oberhauser, A.F., Redick, S.D., Carrion-Vazquez, M., Erickson, H.P. & Fernandez, J.M. (2001) Multiple conformations of PEVK proteins detected by single-molecule techniques. *Proc. Natl. Acad. Sci. USA,* 98, 10682-10686.

Li, T.B., Liu, X.H., Feng, S., Hu, Y., Yang, W.X., Han, Y., Wang, Y.G. & Gong, L.M. (2004) Characterization of MR-1, a novel myofibrillogenesis regulator in human muscle. *Acta Biochim. Biophys Sin.,* 36, 412-418.

Linke, W.A., Kulke, M., Li, H., Fujita-Becker, S., Neagoe, C., Manstein, D.J., Gautel, M. & Fernandez, J.M. (2002) PEVK domain of titin: an entropic spring with actin-binding properties. *J. Struct. Biol.,* 137, 194-205.

Lowey, S. & Steiner, L.A. (1972) An immunochemical approach to the structure of myosin and the thick filament. *J. Mol. Biol.*, 65, 111-126.

Luther, P. & Squire, J. (1978) Three-dimensional structure of the vertebrate muscle M-region. *J. Mol. Biol.*, 125, 313-324.

Luther, P.K., Munro, P.M. & Squire, J.M. (1981) Three-dimensional structure of the vertebrate muscle A-band. III. M-region structure and myosin filament symmetry. *J. Mol. Biol.*, 151, 703-730.
Ma, K. & Wang, K. (2003) Malleable conformation of the elastic PEVK segment of titin: non-co-operative interconversion of polyproline II helix, beta-turn and unordered structures. *Biochem. J.*, 374, 687-695.

Macpherson, P.C., Schork, M.A. & Faulkner, J.A. (1996) Contraction-induced injury to single fiber segments from fast and slow muscles of rats by single stretches. *Am. J. Physiol.*, 271, C1438-1446.
Maggs, A.M., Taylor-Harris, P., Peckham, M. & Hughes, S.M. (2000) Evidence for differential post-translational modifications of slow myosin heavy chain during murine skeletal muscle development. *J. Muscle Res. Cell Motil.*, 21, 101-113.

Makarenko, I., Opitz, C.A., Leake, M.C., Neagoe, C., Kulke, M., Gwathmey, J.K., del Monte, F., Hajjar, R.J. & Linke, W.A. (2004) Passive stiffness changes caused by upregulation of compliant titin isoforms in human dilated cardiomyopathy hearts. *Circ. Res.*, 95, 708-716.

Marko, J.F. & Siggia, E.D. (1995) Statistical mechanics of supercoiled DNA. *Physical Review. E. Statistical Physics, Plasmas, Fluids, and Related Interdisciplinary Topics*, 52, 2912-2938.

Maruyama, K. (1994) Connectin, an elastic protein of striated muscle. *Biophys. Chem.*, 50, 73-85.

Masaki, T. & Takaiti, O. (1974) M-protein. *J. Biochem. Tokyo*, 75, 367-380.

Mayans, O., van der Ven, P.F., Wilm, M., Mues, A., Young, P., Furst, D.O., Wilmanns, M. & Gautel, M. (1998) Structural basis for activation of the titin kinase domain during myofibrillogenesis. *Nature*, 395, 863-869.

Mazzolai, L., Pedrazzini, T., Nicoud, F., Gabbiani, G., Brunner, H.R. & Nussberger, J. (2000) Increased cardiac angiotensin II levels induce right and left ventricular hypertrophy in normotensive mice. *Hypertension*, 35, 985-991.

McConnell, B.K., Jones, K.A., Fatkin, D., Arroyo, L.H., Lee, R.T., Aristizabal, O., Turnbull, D.H., Georgakopoulos, D., Kass, D., Bond, M., Niimura, H., Schoen, F.J., Conner, D., Fischman, D.A., Seidman, C.E. & Seidman, J.G. (1999) Dilated cardiomyopathy in homozygous myosin-binding protein-C mutant mice. *J. Clin. Invest.*, 104, 1235-1244.

Megeney, L.A., Kablar, B., Perry, R.L., Ying, C., May, L. & Rudnicki, M.A. (1999) Severe cardiomyopathy in mice lacking dystrophin and MyoD. *Proc. Natl. Acad. Sci. USA*, 96, 220-225.

Miller, M.K., Bang, M.L., Witt, C.C., Labeit, D., Trombitas, C., Watanabe, K., Granzier, H., McElhinny, A.S., Gregorio, C.C. & Labeit, S. (2003) The muscle ankyrin repeat proteins: CARP, ankrd2/Arpp and DARP as a family of titin filament-based stress response molecules. *J. Mol. Biol.*, 333, 951-964.

Millevoi, S., Trombitas, K., Kolmerer, B., Kostin, S., Schaper, J., Pelin, K., Granzier, H. & Labeit, S. (1998) Characterization of nebulette and nebulin and emerging concepts of their roles for vertebrate Z-discs. *J. Mol. Biol.*, 282, 111-123.

Milner, D.J., Weitzer, G., Tran, D., Bradley, A. & Capetanaki, Y. (1996) Disruption of muscle architecture and myocardial degeneration in mice lacking desmin. *J. Cell Biol.,* 134, 1255-1270.

Minamisawa, S., Hoshijima, M., Chu, G., Ward, C.A., Frank, K., Gu, Y., Martone, M.E., Wang, Y., Ross, J., Jr., Kranias, E.G., Giles, W.R. & Chien, K.R. (1999) Chronic phospholamban-sarcoplasmic reticulum calcium ATPase interaction is the critical calcium cycling defect in dilated cardiomyopathy. *Cell,* 99, 313-322.

Moolman, J.C., Corfield, V.A., Posen, B., Ngumbela, K., Seidman, C., Brink, P.A. & Watkins, H. (1997) Sudden death due to troponin T mutations. *J. Am. Coll. Cardiol.,* 29, 549-555.

Nave, R., Fürst, D.O. & Weber, K. (1989) Visualization of the polarity of isolated titin molecules: a single globular head on a long thin rod as the M band anchoring domain? *J. Cell Biol.,* 109, 2177-2187.

Nieset, J.E., Redfield, A.R., Jin, F., Knudsen, K.A., Johnson, K.R. & Wheelock, M.J. (1997) Characterization of the interactions of alpha-catenin with alpha-actinin and beta-catenin/plakoglobin. *J. Cell Sci.,* 110 (Pt 8), 1013-1022.

Oberhauser, A.F., Badilla-Fernandez, C., Carrion-Vazquez, M. & Fernandez, J.M. (2002) The mechanical hierarchies of fibronectin observed with single-molecule AFM. *J. Mol. Biol.,* 319, 433-447.

Obermann, W.M., Plessmann, U., Weber, K. & Fürst, D.O. (1995) Purification and biochemical characterization of myomesin, a myosin- binding and titin-binding protein, from bovine skeletal muscle. *Eur. J. Biochem.,* 233, 110-115.

Obermann, W.M.J., Gautel, M., Steiner, F., Vanderven, P.F.M., Weber, K. & Fürst, D.O. (1996) The structure of the sarcomeric M band: localization of defined domains of myomesin, M-protein, and the 250-kD carboxy-terminal region of titin by immunoelectron microscopy. *J. Cell Biol.,* 134, 1441-1453.

Obermann, W.M.J., Gautel, M., Weber, K. & Fürst, D.O. (1997) Molecular structure of the sarcomeric M band: mapping of titin and myosin binding domains in myomesin and the identification of a potential regulatory phosphorylation site in myomesin. *Embo J.,* 16, 211-220.

Obermann, W.M.J., van der Ven, P.F.M., Steiner, F., Weber, K. & Fürst, D.O. (1998) Mapping of a myosin-binding domain and a regulatory phosphorylation site in M-protein, a structural protein of the sarcomeric M band. *Mol. Biol. Cell,* 9, 829-840.

Ogilvie, R.W., Armstrong, R.B., Baird, K.E. & Bottoms, C.L. (1988) Lesions in the rat soleus muscle following eccentrically biased exercise. *Am. J. Anat.,* 182, 335-346.

Opitz, C.A., Leake, M.C., Makarenko, I., Benes, V. & Linke, W.A. (2004) Developmentally regulated switching of titin size alters myofibrillar stiffness in the perinatal heart. *Circ. Res.,* 94, 967-975.

Page, S.G. & Huxley, H.E. (1963) Filament lengths in striated muscle. *J. Cell Biol.,* 19, 369-390.

Pask, H.T., Jones, K.L., Luther, P.K. & Squire, J.M. (1994) M-band structure, M-bridge interactions and contraction speed in vertebrate cardiac muscles. *J. Muscle Res. Cell Motil.,* 15, 633-645.

Perriard, J.C. & Eppenberger, H.M. (1978) Demonstration of the presence of M-creatine kinase in mammalian myogenic cell lines. *Experientia,* 34, 1149-1151.

Pette, D. & Spamer, C. (1986) Metabolic properties of muscle fibers. *Fed. Proc.,* 45, 2910-2914.

Pette, D. & Staron, R.S. (1990) Cellular and molecular diversities of mammalian skeletal muscle fibers. *Rev. Physiol. Biochem. Pharmacol.*, 116, 1-76.

Pette, D. & Staron, R.S. (2000) Myosin isoforms, muscle fiber types, and transitions. *Microsc. Res. Tech.*, 50, 500-509.

Pinotsis, N., Petoukhov, M., Lange, S., Svergun, D., Zou, P., Gautel, M. & Wilmanns, M. (2006) Evidence for a dimeric assembly of two titin/telethonin complexes induced by the telethonin C-terminus. *J. Struct. Biol.*

Politou, A.S., Thomas, D.J. & Pastore, A. (1995) The folding and stability of titin immunoglobulin-like modules, with implications for the mechanism of elasticity. *Biophys. J.*, 69, 2601-2610.

Pollard, T.D. (1990) Actin. *Curr. Opin. Cell Biol.*, 2, 33-40.

Porter, J.D., Merriam, A.P., Gong, B., Kasturi, S., Zhou, X., Hauser, K.F., Andrade, F.H. & Cheng, G. (2003) Postnatal suppression of myomesin, muscle creatine kinase and the M-line in rat extraocular muscle. *J. Exp. Biol.*, 206, 3101-3112.

Price, M.G. (1987) Skelemins: cytoskeletal proteins located at the periphery of M-discs in mammalian striated muscle. *J. Cell Biol.*, 104, 1325-1336.

Price, M.G. & Gomer, R.H. (1993) Skelemin, a cytoskeletal M-disc periphery protein, contains motifs of adhesion/recognition and intermediate filament proteins. *J. Biol. Chem.*, 268, 21800-21810.

Quinlan, J.G., Hahn, H.S., Wong, B.L., Lorenz, J.N., Wenisch, A.S. & Levin, L.S. (2004) Evolution of the mdx mouse cardiomyopathy: physiological and morphological findings. *Neuromuscul. Disord.*, 14, 491-496.

Rayment, I., Rypniewski, W.R., Schmidt-Base, K., Smith, R., Tomchick, D.R., Benning, M.M., Winkelmann, D.A., Wesenberg, G. & Holden, H.M. (1993) Three-dimensional structure of myosin subfragment-1: a molecular motor. *Science,* 261, 50-58.

Redfern, C.H., Degtyarev, M.Y., Kwa, A.T., Salomonis, N., Cotte, N., Nanevicz, T., Fidelman, N., Desai, K., Vranizan, K., Lee, E.K., Coward, P., Shah, N., Warrington, J.A., Fishman, G.I., Bernstein, D., Baker, A.J. & Conklin, B.R. (2000) Conditional expression of a Gi-coupled receptor causes ventricular conduction delay and a lethal cardiomyopathy. *Proc. Natl. Acad. Sci. USA,* 97, 4826-4831.

Rief, M., Gautel, M., Oesterhelt, F., Fernandez, J.M. & Gaub, H.E. (1997) Reversible unfolding of individual titin immunoglobulin domains by AFM. *Science,* 276, 1109-1112.

Rief, M., Gautel, M., Schemmel, A. & Gaub, H.E. (1998) The mechanical stability of immunoglobulin and fibronectin III domains in the muscle protein titin measured by atomic force microscopy. *Biophys. J.*, 75, 3008-3014.

Roopnarine, O. & Leinwand, L.A. (1998) Functional analysis of myosin mutations that cause familial hypertrophic cardiomyopathy. *Biophys. J.*, 75, 3023-3030.

Sah, V.P., Minamisawa, S., Tam, S.P., Wu, T.H., Dorn, G.W., 2nd, Ross, J., Jr., Chien, K.R. & Brown, J.H. (1999) Cardiac-specific overexpression of RhoA results in sinus and atrioventricular nodal dysfunction and contractile failure. *J. Clin. Invest.*, 103, 1627-1634.

Sande, J.B., Sjaastad, I., Hoen, I.B., Bokenes, J., Tonnessen, T., Holt, E., Lunde, P.K. & Christensen, G. (2002) Reduced level of serine(16) phosphorylated phospholamban in the failing rat myocardium: a major contributor to reduced SERCA2 activity. *Cardiovasc. Res.*, 53, 382-391.

Sato, Y., Kiriazis, H., Yatani, A., Schmidt, A.G., Hahn, H., Ferguson, D.G., Sako, H., Mitarai, S., Honda, R., Mesnard-Rouiller, L., Frank, K.F., Beyermann, B., Wu, G., Fujimori, K., Dorn, G.W., 2nd & Kranias, E.G. (2001) Rescue of contractile parameters and myocyte hypertrophy in calsequestrin overexpressing myocardium by phospholamban ablation. *J. Biol. Chem.*, 276, 9392-9399.

Schäfer, B.W. & Perriard, J.C. (1988) Intracellular targeting of isoproteins in muscle cytoarchitecture. *J. Cell Biol.*, 106, 1161-1170.

Schiaffino, S. & Reggiani, C. (1996) Molecular diversity of myofibrillar proteins: gene regulation and functional significance. *Physiol. Rev.*, 76, 371-423.

Schmitt, J.P., Kamisago, M., Asahi, M., Li, G.H., Ahmad, F., Mende, U., Kranias, E.G., MacLennan, D.H., Seidman, J.G. & Seidman, C.E. (2003) Dilated cardiomyopathy and heart failure caused by a mutation in phospholamban. *Science,* 299, 1410-1413.

Schneider, A.G., Sultan, K.R. & Pette, D. (1999) Muscle LIM protein: expressed in slow muscle and induced in fast muscle by enhanced contractile activity. *Am. J. Physiol.*, 276, C900-906.

Schoenauer, R. (2002) Regulation of EH-myomesin expression in mouse skeletal muscle. Swiss Federal Institute of Technology, Zurich.

Schoenauer, R., Bertoncini, P., Machaidze, G., Aebi, U., Perriard, J.C., Hegner, M. & Agarkova, I. (2005) Myomesin is a molecular spring with adaptable elasticity. *J. Mol. Biol.*, 349, 367-379.

Sellers, J.R., Goodson, H.V. & Wang, F. (1996) A myosin family reunion. *J. Muscle Res. Cell Motil.*, 17, 7-22.

Shou, W., Aghdasi, B., Armstrong, D.L., Guo, Q., Bao, S., Charng, M.J., Mathews, L.M., Schneider, M.D., Hamilton, S.L. & Matzuk, M.M. (1998) Cardiac defects and altered ryanodine receptor function in mice lacking FKBP12. *Nature,* 391, 489-492.

Sjostrom, M. & Squire, J.M. (1977) Fine structure of the A-band in cryo-sections. The structure of the A-band of human skeletal muscle fibres from ultra-thin cryo-sections negatively stained. *J. Mol. Biol.*, 109, 49-68.

Smolich, J.J. (1995) Ultrastructural and functional features of the developing mammalian heart: a brief overview. *Reprod. Fertil. Dev.*, 7, 451-461.

Soteriou, A., Clarke, A., Martin, S. & Trinick, J. (1993) Titin folding energy and elasticity. *Proc. R. Soc. Lond. B. Biol. Sci.*, 254, 83-86.

Spinale, F.G., Coker, M.L., Heung, L.J., Bond, B.R., Gunasinghe, H.R., Etoh, T., Goldberg, A.T., Zellner, J.L. & Crumbley, A.J. (2000) A matrix metalloproteinase induction/activation system exists in the human left ventricular myocardium and is upregulated in heart failure. *Circulation,* 102, 1944-1949.

Squire, J. (1981) *The structural basis of muscular contraction,* Plenum Press, New York ; London.

Steiner, F., Weber, K. & Furst, D.O. (1998) Structure and expression of the gene encoding murine M-protein, a sarcomere-specific member of the immunoglobulin superfamily. *Genomics,* 49, 83-95.

Steiner, F., Weber, K. & Fürst, D.O. (1999) M-band proteins myomesin and skelemin are encoded by the same gene: analysis of its organization and expression. *Genomics,* 56, 78-89.

Stolz, M., Kraft, T. & Wallimann, T. (1998) The isoenzyme-diagnostic regions of muscle-type creatine kinase, the M-260 and M-300 box, are not responsible for its binding to the myofibrillar M-band. *Eur. J. Cell Biol.*, 77, 1-9.

Strehler, E.E., Carlsson, E., Eppenberger, H.M. & Thornell, L.E. (1983) Ultrastructural localization of M-band proteins in chicken breast muscle as revealed by combined immunocytochemistry and ultramicrotomy. *J. Mol. Biol.*, 166, 141-158.

Strehler, E.E., Pelloni, G., Heizmann, C.W. & Eppenberger, H.M. (1980) Biochemical and ultrastructural aspects of Mr 165,000 M-protein in cross-striated chicken muscle. *J. Cell Biol.*, 86, 775-783.

Sussman, M.A., Welch, S., Cambon, N., Klevitsky, R., Hewett, T.E., Price, R., Witt, S.A. & Kimball, T.R. (1998) Myofibril degeneration caused by tropomodulin overexpression leads to dilated cardiomyopathy in juvenile mice. *J. Clin. Invest.*, 101, 51-61.

Sweeney, H.L., Rosenfeld, S.S., Brown, F., Faust, L., Smith, J., Xing, J., Stein, L.A. & Sellers, J.R. (1998) Kinetic tuning of myosin via a flexible loop adjacent to the nucleotide binding pocket. *J. Biol. Chem.*, 273, 6262-6270.

Tada, M., Yabuki, M. & Toyofuku, T. (1998) Molecular regulation of phospholamban function and gene expression. *Ann. N. Y. Acad. Sci.*, 853, 116-129.

Thornell, L.E., Carlsson, E., Kugelberg, E. & Grove, B.K. (1987) Myofibrillar M-band structure and composition of physiologically defined rat motor units. *Am. J. Physiol.*, 253, C456-468.

Thornell, L.-E., Carlsson, E. & Perdrosa, F. (1990) M-band structure and composition in relation to fiber types. In *The dynamic state of muscle fibers.* (D., P. ed.), pp. 370-383. Walter de Gruyter & Co, Berlin. New York.

Tompa, P. (2002) Intrinsically unstructured proteins. *Trends Biochem. Sci.*, 27, 527-533.
Toyoshima, Y.Y., Kron, S.J., McNally, E.M., Niebling, K.R., Toyoshima, C. & Spudich, J.A. (1987) Myosin subfragment-1 is sufficient to move actin filaments in vitro. *Nature*, 328, 536-539.

Trinick, J. (1994) Titin and nebulin: protein rulers in muscle? *Trends Biochem. Sci.*, 19, 405-409.

Trinick, J. (1996) Titin as a scaffold and spring. Cytoskeleton. *Curr. Biol.*, 6, 258-260.

Trinick, J., Knight, P. & Whiting, A. (1984) Purification and properties of native titin. *J. Mol. Biol.*, 180, 331-356.

Trombitas, K., Freiburg, A., Centner, T., Labeit, S. & Granzier, H. (1999) Molecular dissection of N2B cardiac titin's extensibility. *Biophys. J.*, 77, 3189-3196.

Trombitas, K., Greaser, M., Labeit, S., Jin, J.P., Kellermayer, M., Helmes, M. & Granzier, H. (1998) Titin extensibility in situ: entropic elasticity of permanently folded and permanently unfolded molecular segments. *J Cell Biol*, 140, 853-859.

Tskhovrebova, L. & Trinick, J. (2003) Titin: properties and family relationships. *Nat. Rev. Mol. Cell. Biol.*, 4, 679-689.

Tskhovrebova, L. & Trinick, J. (2004) Properties of titin immunoglobulin and fibronectin-3 domains. *J. Biol. Chem.*, 279, 46351-46354.

Tskhovrebova, L., Trinick, J., Sleep, J.A. & Simmons, R.M. (1997) Elasticity and unfolding of single molecules of the giant muscle protein titin. *Nature*, 387, 308-312.

Turner, D.C., Maier, V. & Eppenberger, H.M. (1974) Creatine kinase and aldolase isoenzyme transitions in cultures of chick skeletal muscle cells. *Dev. Biol.*, 37, 63-89.

Tyska, M.J., Hayes, E., Giewat, M., Seidman, C.E., Seidman, J.G. & Warshaw, D.M. (2000) Single-molecule mechanics of R403Q cardiac myosin isolated from the mouse model of familial hypertrophic cardiomyopathy. *Circ. Res.*, 86, 737-744.

van Deursen, J., Heerschap, A., Oerlemans, F., Ruitenbeek, W., Jap, P., ter Laak, H. & Wieringa, B. (1993) Skeletal muscles of mice deficient in muscle creatine kinase lack burst activity. *Cell*, 74, 621-631.

Vandekerckhove, J. & Weber, K. (1981) Actin typing on total cellular extracts: a highly sensitive protein-chemical procedure able to distinguish different actins. *Eur. J. Biochem.*, 113, 595-603.

Venkatraman, G., Gomes, A.V., Kerrick, W.G. & Potter, J.D. (2005) Characterization of troponin T dilated cardiomyopathy mutations in the fetal troponin isoform. *J. Biol. Chem.*, 280, 17584-17592.

Vinkemeier, U., Obermann, W., Weber, K. & Fürst, D.O. (1993) The globular head domain of titin extends into the center of the sarcomeric M band. cDNA cloning, epitope mapping and immunoelectron microscopy of two titin-associated proteins. *J. Cell Sci.*, 106, 319-330.

Wallimann, T., Doetschman, T.C. & Eppenberger, H.M. (1983) Novel staining pattern of skeletal muscle M-lines upon incubation with antibodies against MM-creatine kinase. *J. Cell Biol.*, 96, 1772-1779.

Wallimann, T., Schlosser, T. & Eppenberger, H.M. (1984) Function of M-line-bound creatine kinase as intramyofibrillar ATP regenerator at the receiving end of the phosphorylcreatine shuttle in muscle. *J. Biol. Chem.*, 259, 5238-5246.

Wallimann, T., Wyss, M., Brdiczka, D., Nicolay, K. & Eppenberger, H.M. (1992) Intracellular compartmentation, structure and function of creatine kinase isoenzymes in tissues with high and fluctuating energy demands: the 'phosphocreatine circuit' for cellular energy homeostasis. *Biochem. J.*, 281 (Pt 1), 21-40.

Walmsley, B., Hodgson, J.A. & Burke, R.E. (1978) Forces produced by medial gastrocnemius and soleus muscles during locomotion in freely moving cats. *J. Neurophysiol.*, 41, 1203-1216.

Wang, K., McClure, J. & Tu, A. (1979) Titin: major myofibrillar components of striated muscle. *Proc. Natl. Acad. Sci. U S A*, 76, 3698-3702.

Wang, S.M., Lo, M.C., Shang, C., Kao, S.C. & Tseng, Y.Z. (1998) Role of M-line proteins in sarcomeric titin assembly during cardiac myofibrillogenesis. *J. Cell. Biochem.*, 71, 82-95.

Watanabe, K., Muhle-Goll, C., Kellermayer, M.S., Labeit, S. & Granzier, H. (2002a) Different molecular mechanics displayed by titin's constitutively and differentially expressed tandem Ig segments. *J. Struct. Biol.*, 137, 248-258.

Watanabe, K., Nair, P., Labeit, D., Kellermayer, M.S., Greaser, M., Labeit, S. & Granzier, H. (2002b) Molecular mechanics of cardiac titin's PEVK and N2B spring elements. *J. Biol. Chem.*, 277, 11549-11558.

Weiss, A., Schiaffino, S. & Leinwand, L.A. (1999) Comparative sequence analysis of the complete human sarcomeric myosin heavy chain family: implications for functional diversity. *J. Mol. Biol.*, 290, 61-75.

Widrick, J.J., Romatowski, J.G., Karhanek, M. & Fitts, R.H. (1997) Contractile properties of rat, rhesus monkey, and human type I muscle fibers. *Am. J. Physiol.*, 272, R34-42.

Wiesel, P., Mazzolai, L., Nussberger, J. & Pedrazzini, T. (1997) Two-kidney, one clip and one-kidney, one clip hypertension in mice. *Hypertension,* 29, 1025-1030.

Witt, C.C., Olivieri, N., Centner, T., Kolmerer, B., Millevoi, S., Morell, J., Labeit, D., Labeit, S., Jockusch, H. & Pastore, A. (1998) A survey of the primary structure and the interspecies conservation of I-band titin's elastic elements in vertebrates. *J. Struct. Biol.*, 122, 206-215.

Young, P., Ehler, E. & Gautel, M. (2001) Obscurin, a giant sarcomeric Rho guanine nucleotide exchange factor protein involved in sarcomere assembly. *J. Cell Biol.*, 154, 123-136.

Young, P., Ferguson, C., Banuelos, S. & Gautel, M. (1998) Molecular structure of the sarcomeric Z-disk: two types of titin interactions lead to an asymmetrical sorting of alpha-actinin. *Embo J.*, 17, 1614-1624.

Zhang, B. & Evans, J.S. (2001) Modeling AFM-induced PEVK extension and the reversible unfolding of Ig/FNIII domains in single and multiple titin molecules. *Biophys. J.*, 80, 597-605.

Zhang, T., Johnson, E.N., Gu, Y., Morissette, M.R., Sah, V.P., Gigena, M.S., Belke, D.D., Dillmann, W.H., Rogers, T.B., Schulman, H., Ross, J., Jr. & Brown, J.H. (2002) The cardiac-specific nuclear delta(B) isoform of Ca2+/calmodulin-dependent protein kinase II induces hypertrophy and dilated cardiomyopathy associated with increased protein phosphatase 2A activity. *J. Biol. Chem.*, 277, 1261-1267.

Zhou, Q., Chu, P.H., Huang, C., Cheng, C.F., Martone, M.E., Knoll, G., Shelton, G.D., Evans, S. & Chen, J. (2001) Ablation of Cypher, a PDZ-LIM domain Z-line protein, causes a severe form of congenital myopathy. *J. Cell Biol.*, 155, 605-612.

Zou, P., Pinotsis, N., Lange, S., Song, Y.H., Popov, A., Mavridis, I., Mayans, O.M., Gautel, M. & Wilmanns, M. (2006) Palindromic assembly of the giant muscle protein titin in the sarcomeric Z-disk. *Nature,* 439, 229-233.

10 CURRICULUM VITAE

Personal data

Name:	Schönauer Roman
Date of birth:	10 April 1978
Place of birth:	Aarau, CH
Address:	Talweg 9, 5024 Küttigen
Citizenship:	Kirchberg BE, Switzerland

Education

2003-2006	PhD thesis: "Myomesin family members – implications for the M-band function"; Institute of Cell Biology, Prof. J.-C. Perriard
2003:	Diploma in biology (Dipl. Natw. ETH)
2002:	Diploma work: "Regulation of EH-myomesin expression in mouse skeletal muscle"; Institute of Cell Biology, Prof. J.-C. Perriard
2001:	Semester work: "Characterization of polyclonal rabbit antisera against mouse EH-myomesin and protein D"; Institute of Cell Biology, Prof. J.-C. Perriard
1998-2003:	Diploma student in biology, Swiss Federal Institute of Technology, Zurich
1994-1998:	Kantonsschule (Type B), Aarau
1990-1994:	Bezirksschule, Aarau
1985-1990:	Primary School, Küttigen

Publications

Schoenauer, R., Bertoncini, P., Machaidze, G., Aebi, U., Perriard, J.-C., Hegner, M., and Agarkova, I. 2005. Myomesin is a molecular spring with adaptable elasticity. *J Mol Biol.* 349(2), 367-379.

Bertoncini, P., Schoenauer, R., Agarkova, I., Hegner, M., Perriard, J.-C., and Güntherodt, H.-J. 2005. Study of the mechanical properties of myomesin proteins using dynamic force spectroscopy. *J Mol Biol.* 348(5):1127-1137.

Agarkova, I., Schoenauer, R., Ehler, E., Carlsson, L., Carlsson, E., Thornell, L.-E., and Perriard, J.-C. 2004. The molecular composition of the sarcomeric M-band correlates with muscle fiber type. *Eur J Cell Biol.* 83: 1-12.

Agarkova, I., Ehler, E., Lange, S., Schoenauer, R., and Perriard, J.-C. 2003. M-band: a safeguard for sarcomere stability? *J Muscle Res Cell Motil.* 24(2-3):191-203.

Talks

Schoenauer, R., Hirschy, A., Perriard, J.-C., and Agarkova., I. Characterization of myomesin 3 – a novel component of striated muscle. *XXXIVth European Muscle Conference, Hortobagy, Hungary,* 17-21 September 2005.

Schoenauer, R., Bertoncini, P., Machaidze, G., Aebi, U., Perriard, J.-C., Hegner, M., and Agarkova. EH-myomesin function in striated muscle. *Institute of Physiology, University Zurich-Irchel, Zurich,* 18 May 2004.

Poster presentations

Schoenauer, R., Perriard, J.-C., and Agarkova, I. Myomesin 3 – a novel component of striated muscle. *6th D-BIOL Symposium ETH Zurich, Davos.* 24-26 May 2006.

Schoenauer, R., Perriard, J.-C., and Agarkova, I. Myomesin 3 – a novel component of striated muscle. *Fifth International Ascona Workshop on Cardiomyocyte Cell Biology, Ascona.* 2-6 April 2006.

Schoenauer, R., Hirschy, A., Perriard, J.-C., and Agarkova, I. Myomesin 3 – a novel component of striated muscle. *SCRTN Annual Meeting, Bern,* 27 January 2006.

Schoenauer, R., Hirschy, A., Perriard, J.-C., and Agarkova, I. Characterization of myomesin 3 – a novel component of striated muscle. *11th Cardiovascular Biology and Clinical Implications Meeting, Thun,* 6-8 October 2005.

Schoenauer, R., Bertoncini, P., Hegner, M., Agarkova, I., Machaidze, G., Aebi, U., and Perriard, J.-C. Mechanical portrait of myomesin: Implications for sarcomeric M-band function. *USGEB, Zurich,* 17-19 February 2005.

Schoenauer, R., Bertoncini, P., Hegner, M., Perriard, J.-C., and Agarkova, I. Mechanical portrait of myomesin: Implications for sarcomeric M-band function. *5th Swiss Meeting on Muscle Research 2004, Magglingen,* 28-30 November 2004.

Schoenauer, R., Bertoncini, P., Hegner, M., Perriard, J.-C., and Agarkova, I. Mechanical portrait of myomesin: Implications for sarcomeric M-band function. *33rd European Muscle Conference, Elba (It),* 19-23 September 2004.

Schoenauer, R., Bertoncini, P., Agarkova, I., Hegner, M., and Perriard, J.-C. Molecular dissection of M-band component myomesin by atomic force microscopy. *SCRTN Annual Meeting, Bern,* 12 December 2003.

Schoenauer, R., Agarkova, I., Ehler, E., and Perriard, J.-C. Expression of the EH-myomesin isoform in slow skeletal muscle of mouse. *32nd European Muscle Conference, Montpellier (F),* 07-10 September 2003.

Schoenauer, R., Agarkova, I., Ehler, E., and Perriard, J.-C. Differential expression of the EH-myomesin isoform in skeletal muscle of adult mouse. *USGEB, Lugano,* 07-08 March 2002.

11 ACKNOWLEDGEMENTS

First of all I would like to thank Prof. Jean-Claude Perriard for giving me the opportunity to do my thesis in his lab, for his continous support and for providing an ideal atmosphere for creative research. I specially thank Irina Agarkova for being a good supervisor, for her practical advice, useful suggestions and for her coreviewing of this thesis. I would also like to thank Prof. Urs Boutellier for his supervision of this work and useful comments. In addition, I thank our collaborators in Basel, Dr. Martin Hegner and Prof. Ueli Aebi, for interesting inputs into my scientific work

A special thank to all the (past) members of the Perriard group for providing a good atmosphere in the lab, especially to Alain Hirschy, Stephan Lange and Elisabeth Ehler for stimulating discussions and technical help. A separate thank goes to Evelyne Perriard for the preparation of the primary cultures of neonatal rat cardiomyocytes. In addition, I thank Prof. Dieter O. Fürst and Prof. Mathias Gautel for providing the antibodies.

Finally, I would like to thank my parents for their continuous support and my best friends for their encouragement during my thesis.